Transient spiral arms and galaxy rotation curves

Francesco Sylos Labini

- Institute for Complex Systems, CNR (Rome, Italy)
- Enrico Fermi Center (Rome, Italy)

- New dynamical mechanism of formation of a disk, bar and spiral galaxies
- Velocity-shape degeneracy for line-of-sight velocity maps of external galaxies
- *Qualitative* predictions for velocity fields in our galaxy

Spiral galaxies

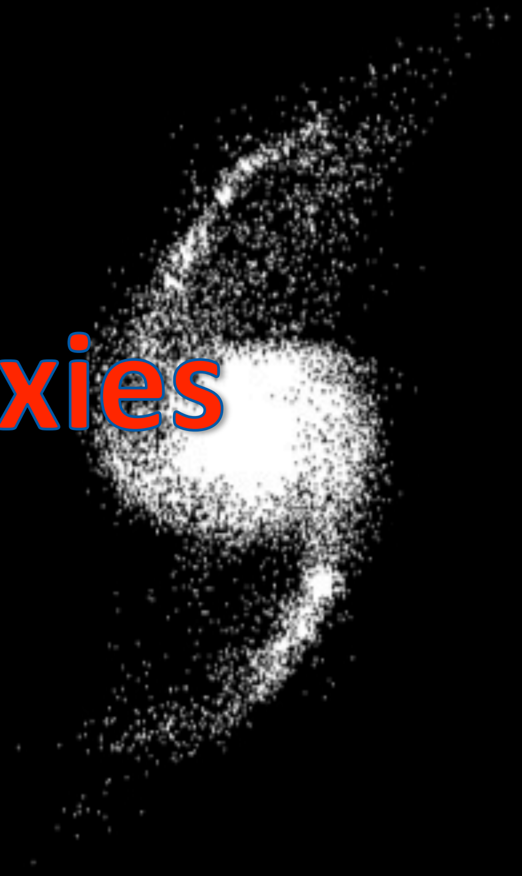




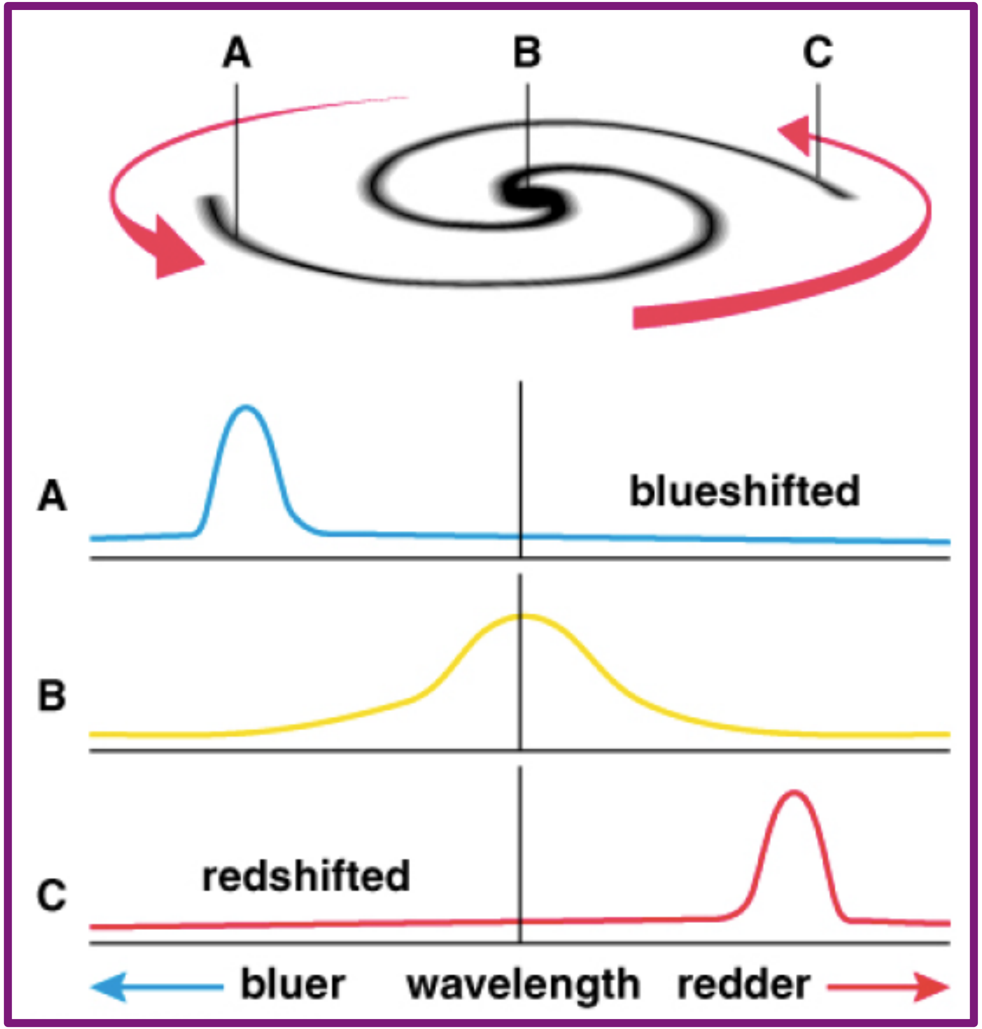
A
B
C
A
blueshifted
B
C
redshifted
bluer
wavelength
redder

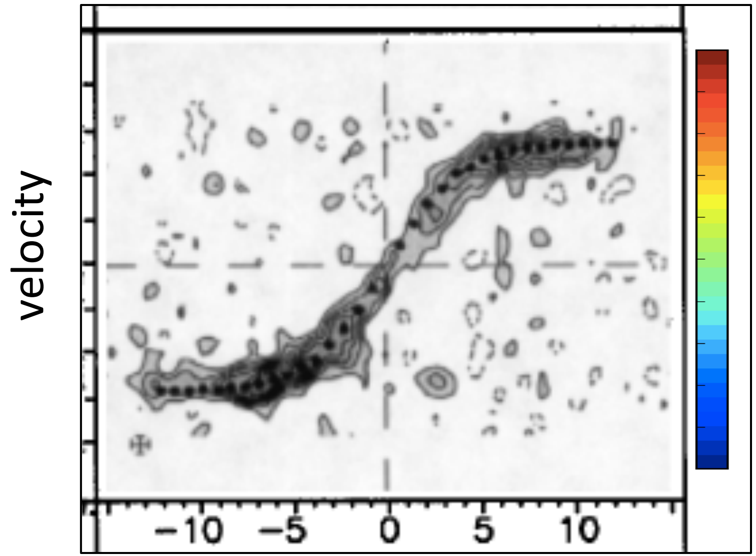
velocity
−10
−5
0
5
10

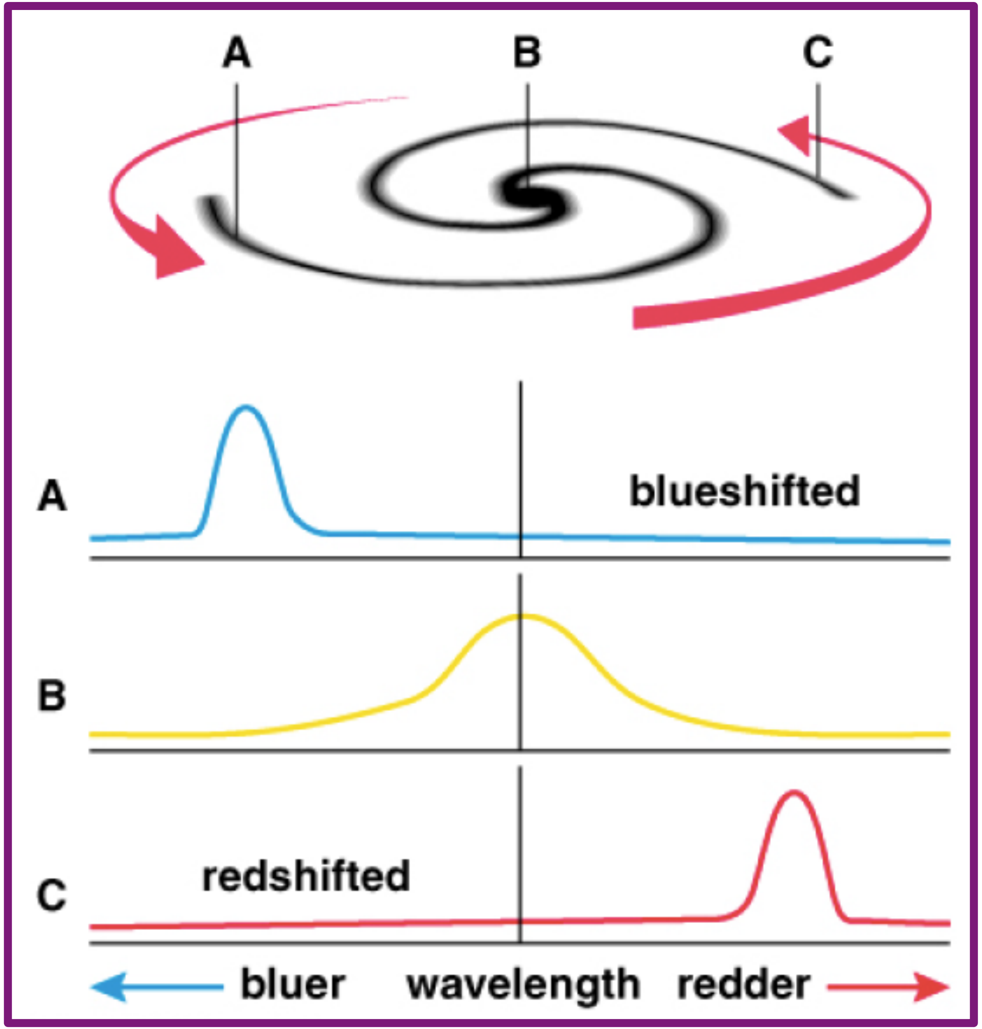
A
B
C
A
blueshifted
B
C
redshifted
bluer
wavelength
redder

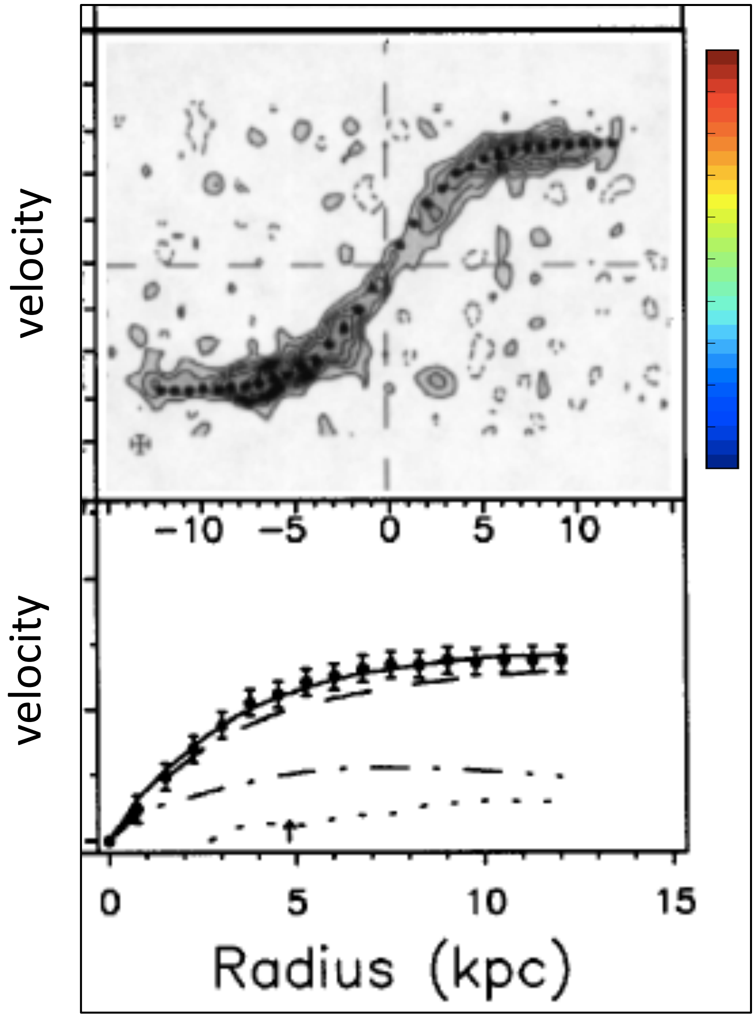
velocity
−10
−5
0
5
10
velocity
0
5
10
15
Radius (kpc)

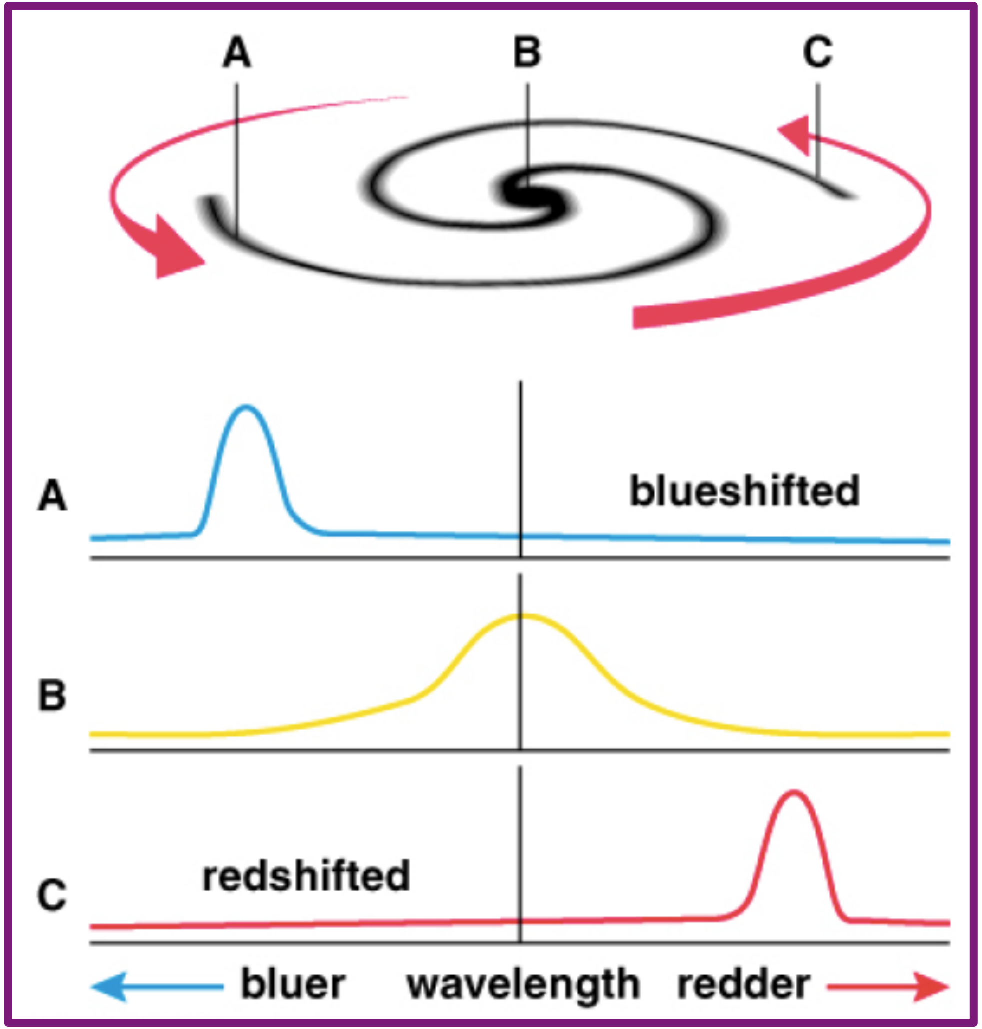
A
B
C
A
blueshifted
B
C
redshifted
bluer
wavelength
redder

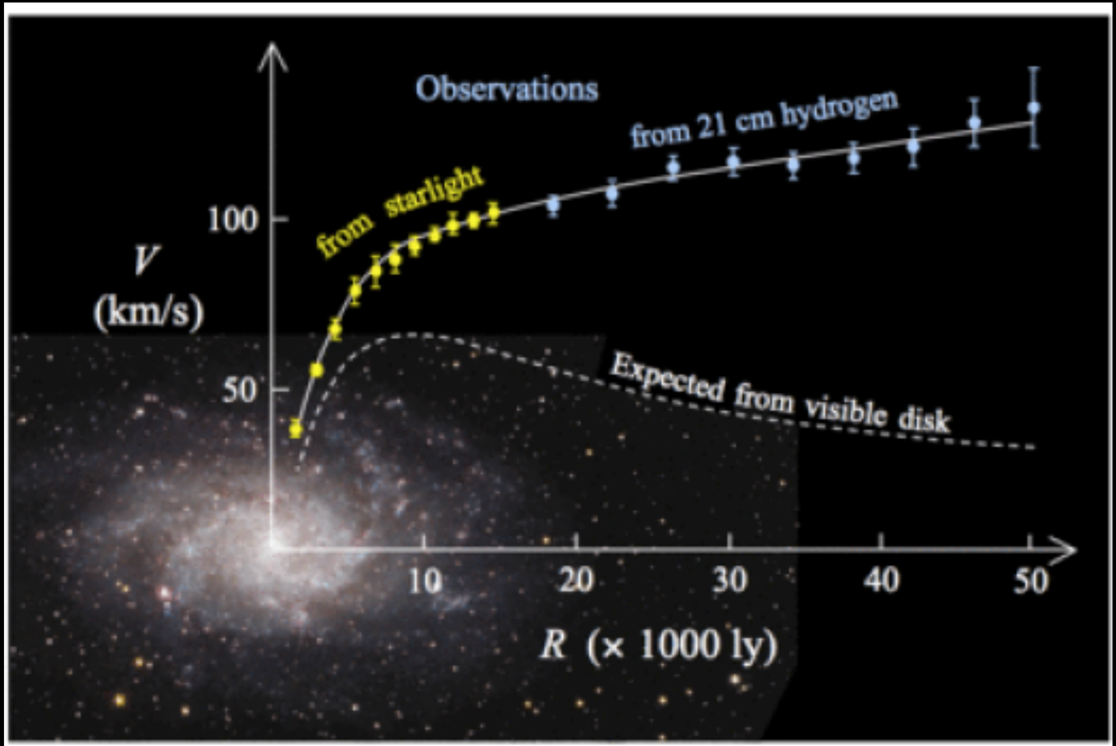
Observations
from 21 cm hydrogen
from starlight
100
V
(km/s)
50
Expected from visible disk
10
20
30
40
50
R (× 1000 ly)

$$F_N = ma$$

24 June 1983, Volume 220, Number 4604

SCIENCE

The Rotation of Spiral Galaxies

Vera C. Rubin

the galaxy carries the stars toward the observer, spectral lines are shifted toward the blue region of the spectrum with respect to the central velocity. On the opposite side, where rotation carries the stars away from the observer, lines are shifted toward the red spectral region.

Several years later, Pease (*8*) convinc-

$$F_N = ma$$

$$ma = m\frac{v_c^2(r)}{r} = \frac{GmM(r)}{r^2}$$

Spheroidal mass distribution

24 June 1983, Volume 220, Number 4604 SCIENCE

The Rotation of Spiral Galaxies

Vera C. Rubin

the galaxy carries the stars toward the observer, spectral lines are shifted toward the blue region of the spectrum with respect to the central velocity. On the opposite side, where rotation carries the stars away from the observer, lines are shifted toward the red spectral region.

Several years later, Pease (8) convinc-

$$F_N = ma$$

$$ma = m\frac{v_c^2(r)}{r} = \frac{GmM(r)}{r^2}$$ **Spheroidal mass distribution**

$$\boxed{M(r) \propto v_c^2(r) \cdot r \sim r^{1+\alpha} \quad \alpha \geq 0 \ \ (\text{but also} \ \ \alpha < 0)}$$

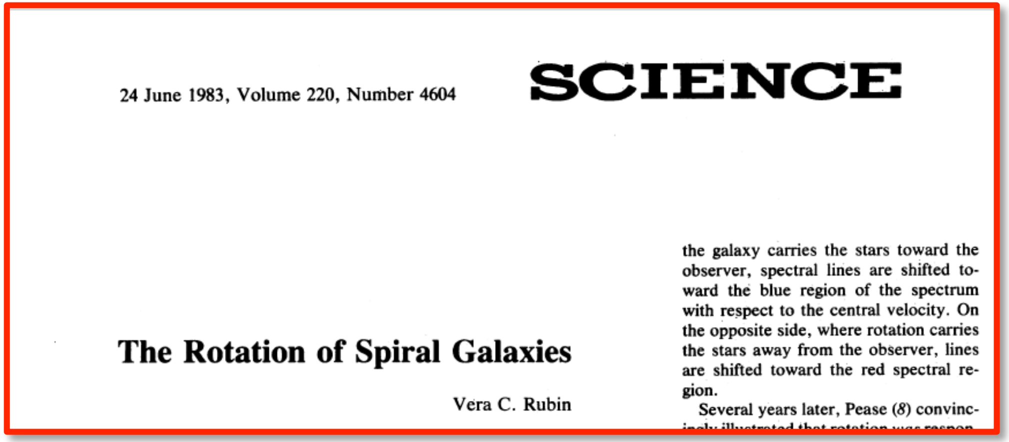

24 June 1983, Volume 220, Number 4604

SCIENCE

The Rotation of Spiral Galaxies

Vera C. Rubin

the galaxy carries the stars toward the observer, spectral lines are shifted toward the blue region of the spectrum with respect to the central velocity. On the opposite side, where rotation carries the stars away from the observer, lines are shifted toward the red spectral region.

Several years later, Pease (8) convinc-

$$F_N = ma$$

$$ma = m\frac{v_c^2(r)}{r} = \frac{GmM(r)}{r^2}$$ **Spheroidal mass distribution**

$$\boxed{M(r) \propto v_c^2(r) \cdot r \sim r^{1+\alpha} \quad \alpha \geq 0 \ \ (\text{but also} \ \ \alpha < 0)}$$

24 June 1983, Volume 220, Number 4604 **SCIENCE**

The Rotation of Spiral Galaxies

Vera C. Rubin

the galaxy carries the stars toward the observer, spectral lines are shifted toward the blue region of the spectrum with respect to the central velocity. On the opposite side, where rotation carries the stars away from the observer, lines are shifted toward the red spectral region.

Several years later, Pease (8) convinc-

- ➢ Newton's dynamics
- ➢ Newton's gravity
- ➢ *Equilibrium*

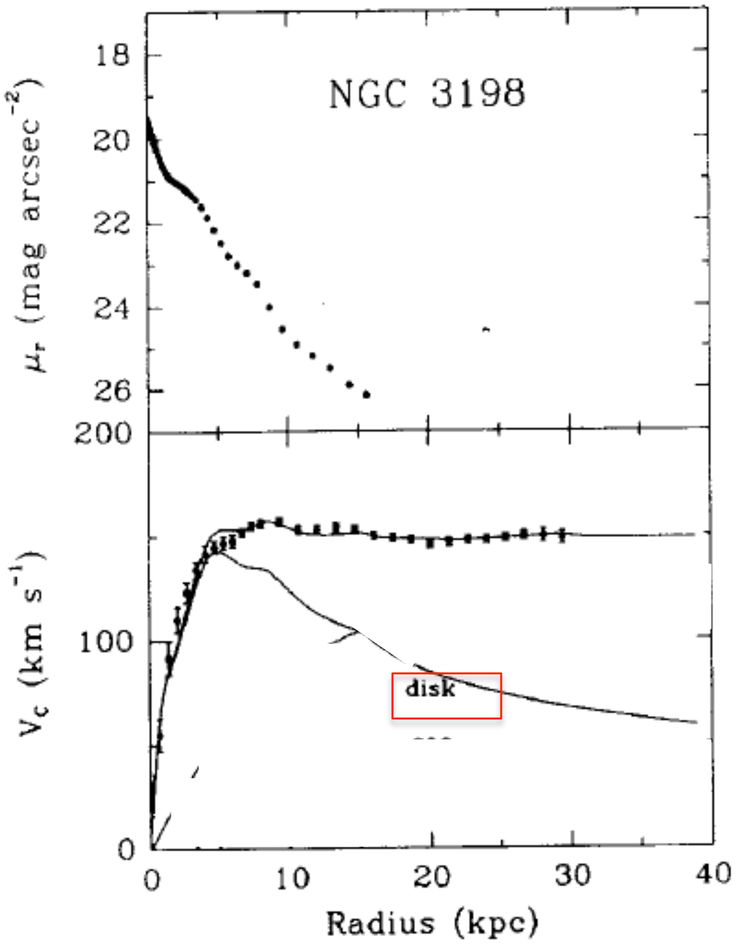
NGC 3198
μ_r (mag arcsec^{-2})
18
20
22
24
26
200
100
0
V_c (km s^{-1})
disk
0
10
20
30
40
Radius (kpc)

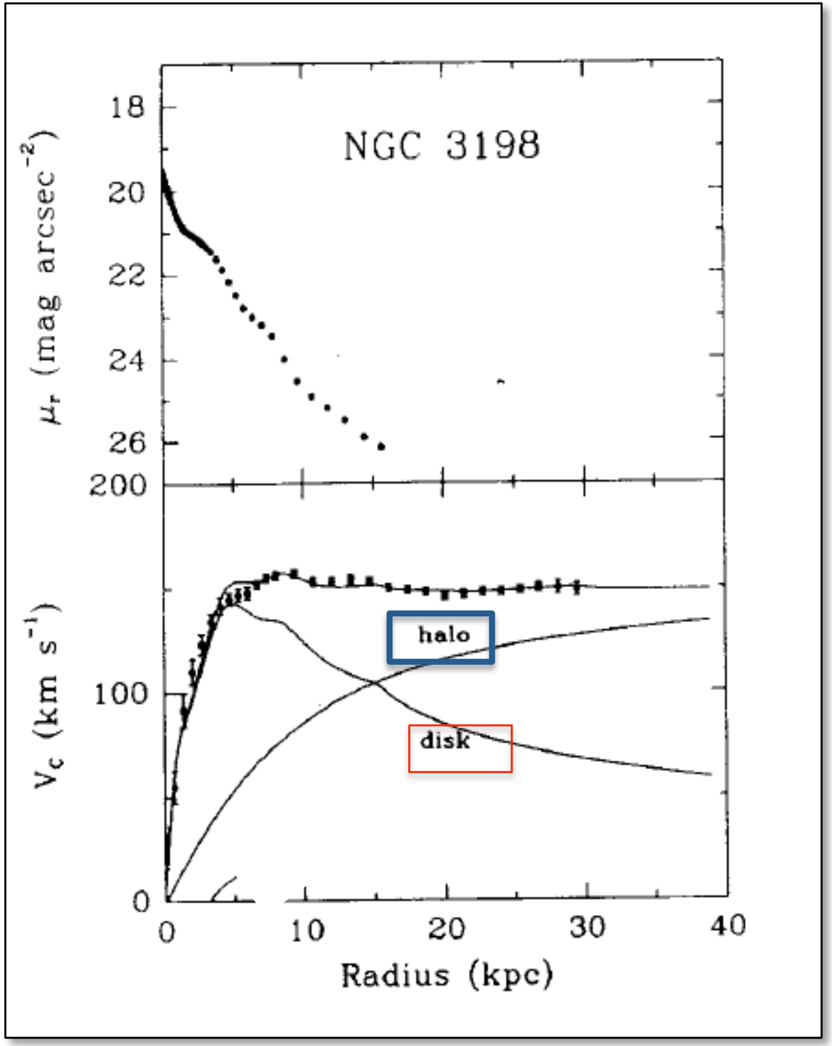

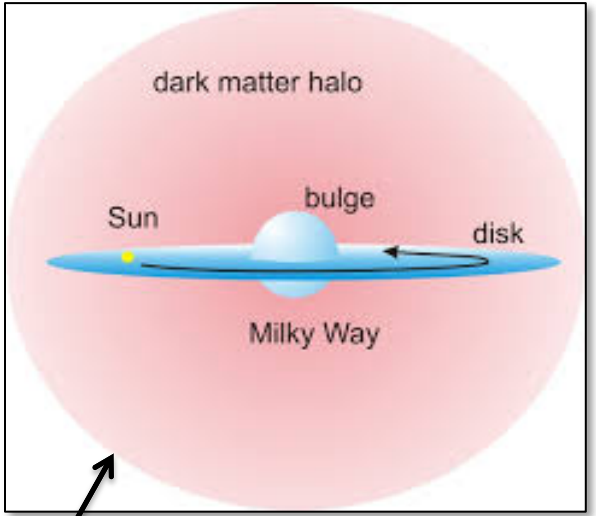

$$P(v) \approx \quad \text{isotropic}$$

$$F_N = m\mu\left(\frac{a}{a_0}\right)a$$

$$\mu(x) \rightarrow 1 \quad for \quad x \gg 1$$

$$\mu(x) \rightarrow x \quad for \quad x \ll 1$$

A MODIFICATION OF THE NEWTONIAN DYNAMICS AS A POSSIBLE ALTERNATIVE TO THE HIDDEN MASS HYPOTHESIS[1]

M. MILGROM
Department of Physics, The Weizmann Institute of Science, Rehovot, Israel; and
The Institute for Advanced Study

Received 1982 February 4; accepted 1982 December 28

$$F_N = m\mu\left(\frac{a}{a_0}\right)a$$

$$\mu(x) \to 1 \quad for \quad x \gg 1$$

$$\mu(x) \to x \quad for \quad x \ll 1$$

$$F_N = m\frac{a^2}{a_0} \quad for \quad a < a_0$$

A MODIFICATION OF THE NEWTONIAN DYNAMICS AS A POSSIBLE ALTERNATIVE TO THE HIDDEN MASS HYPOTHESIS[1]

M. MILGROM
Department of Physics, The Weizmann Institute of Science, Rehovot, Israel; and
The Institute for Advanced Study

Received 1982 February 4; accepted 1982 December 28

$$F_N = m\mu\left(\frac{a}{a_0}\right)a$$

$$\mu(x) \to 1 \quad for \quad x \gg 1$$

$$\mu(x) \to x \quad for \quad x \ll 1$$

$$F_N = m\frac{a^2}{a_0} \quad for \quad a < a_0$$

$$m\frac{a^2}{a_0} = m\frac{(v^2/r)^2}{a_0} = \frac{GMm}{r^2} \to \boxed{v^4 = GMa_0}$$

A MODIFICATION OF THE NEWTONIAN DYNAMICS AS A POSSIBLE ALTERNATIVE TO THE HIDDEN MASS HYPOTHESIS[1]

M. MILGROM
Department of Physics, The Weizmann Institute of Science, Rehovot, Israel; and The Institute for Advanced Study

Received 1982 February 4; accepted 1982 December 28

- Modified Newton dynamics
- Newton gravity
- *Equilibrium*

$$v_G = 200\beta \text{ km sec}^{-1}$$

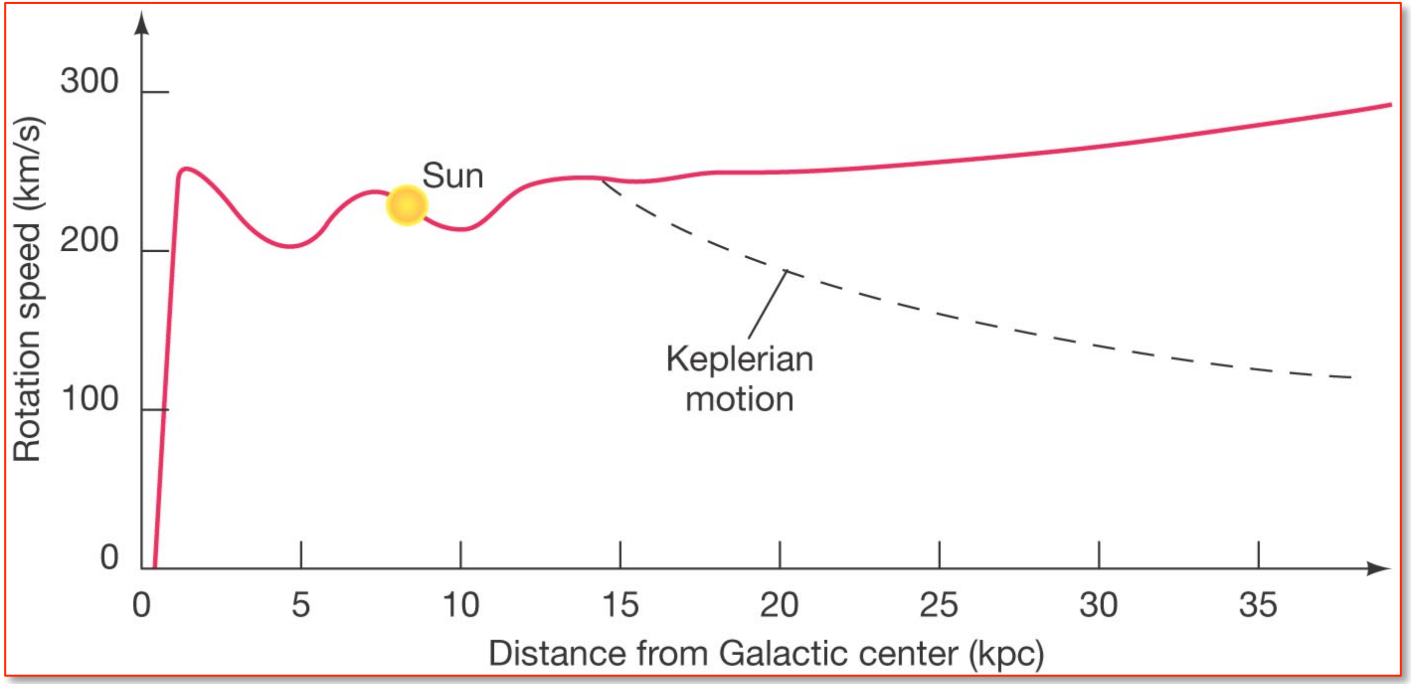

$$v_G = 200\beta \text{ km sec}^{-1}$$

$$T_G = 10 \cdot \Delta \text{ Gyr}$$

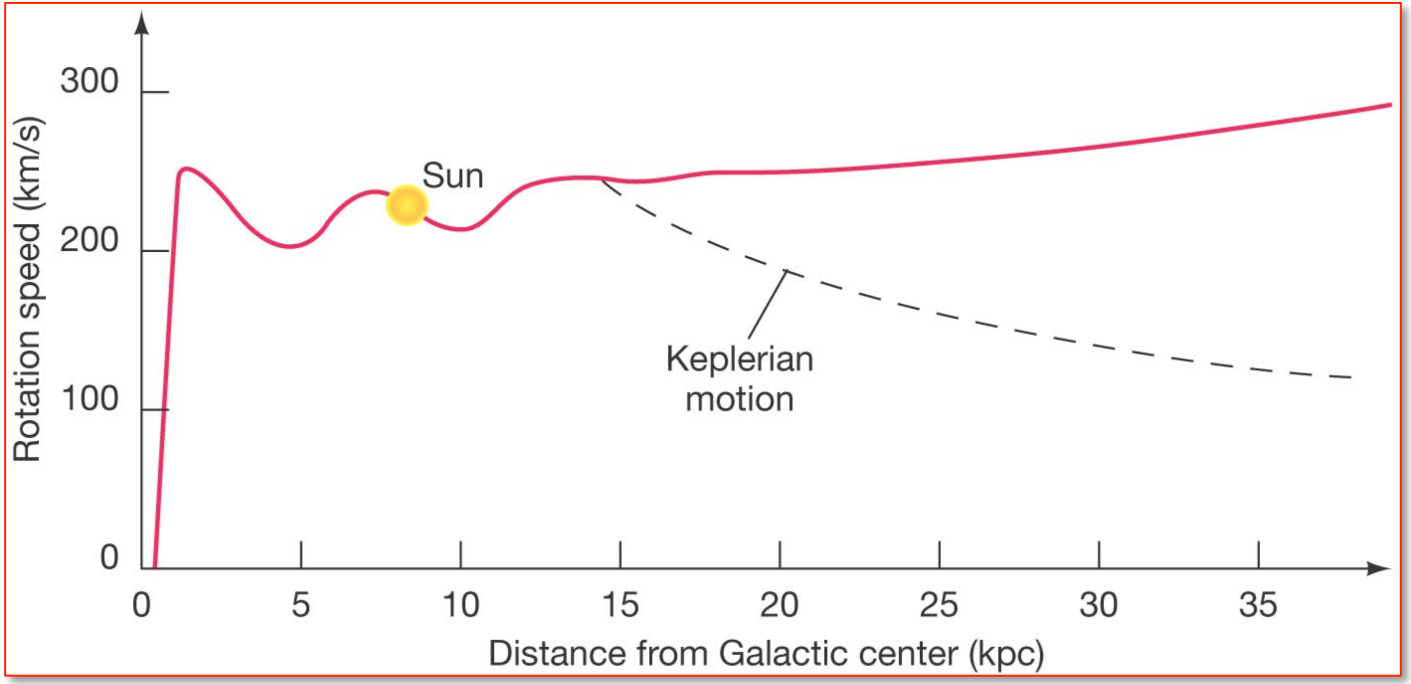

$$v_G = 200\beta \text{ km sec}^{-1}$$

$$T_G = 10 \cdot \Delta \text{ Gyr}$$

$$\boxed{n_{Rev}(R) = \frac{T_{age}}{\tau_{Rev}(R)} = \frac{T_{age} v_c(R)}{2\pi R} \approx \frac{30\Delta\beta}{R/10\text{Kpc}}}$$

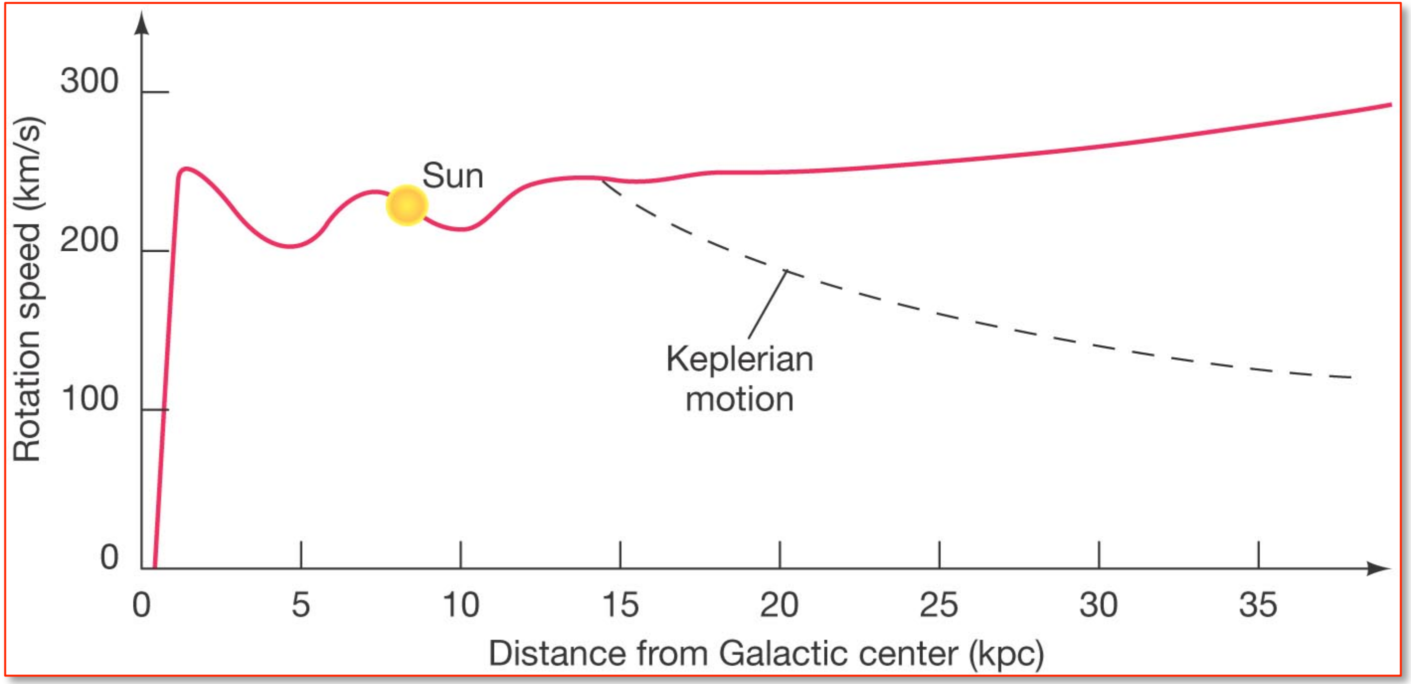

$$v_G = 200\beta \text{ km sec}^{-1}$$

$$T_G = 10 \cdot \Delta \text{ Gyr}$$

$$\boxed{n_{Rev}(R) = \frac{T_{age}}{\tau_{Rev}(R)} = \frac{T_{age} v_c(R)}{2\pi R} \approx \frac{30\Delta\beta}{R/10\text{Kpc}}}$$

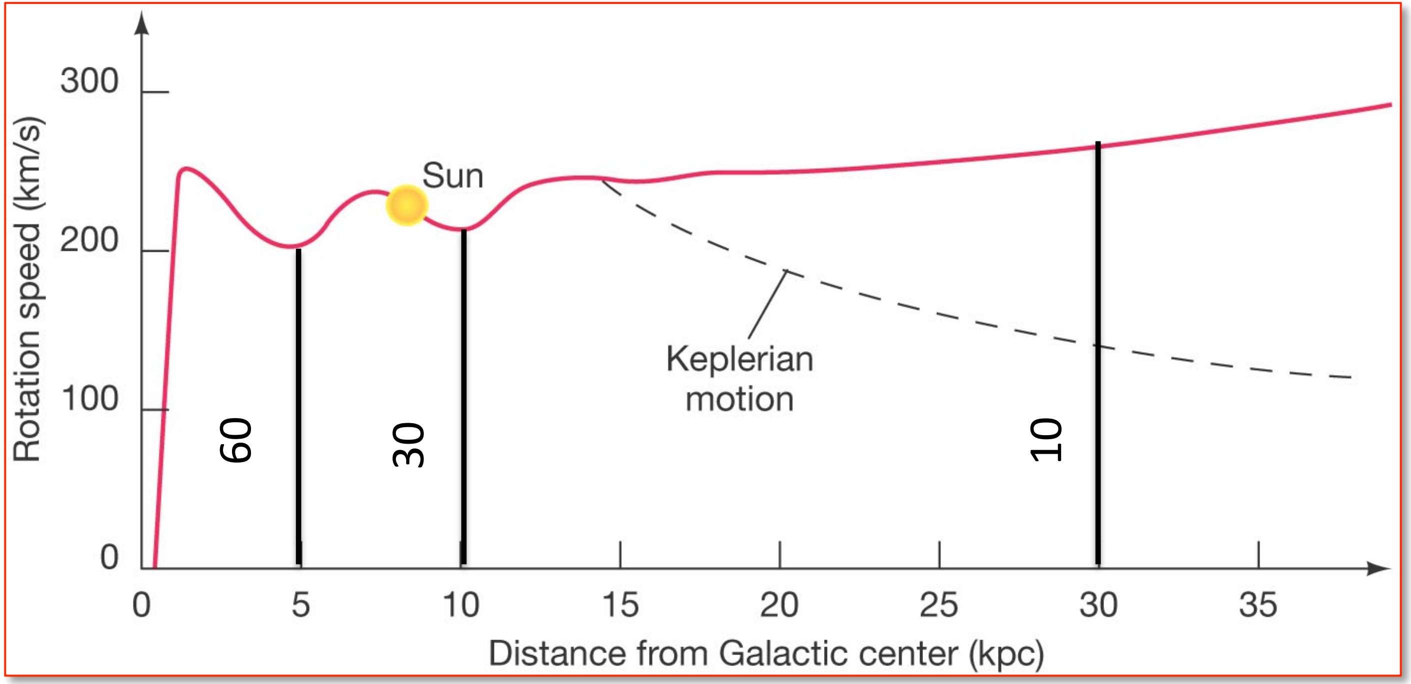

$$\boxed{a = a_c = \frac{v^2}{r}} \Longleftrightarrow \text{Stationary equilibrium}$$

$$\boxed{a = a_c = \frac{v^2}{r}} \Longleftrightarrow \text{Stationary equilibrium}$$

- Not a trivial assumption!

$$\boxed{a = a_c = \frac{v^2}{r}} \Longleftrightarrow \text{Stationary equilibrium}$$

- Not a trivial assumption!
- But used both by DM and MOND

$$\boxed{a = a_c = \frac{v^2}{r}} \Longleftrightarrow \text{Stationary equilibrium}$$

- Not a trivial assumption!
- But used both by DM and MOND
- How long to relax ? Transients? Which QSS?

$$\boxed{a = a_c = \frac{v^2}{r}} \Longleftrightarrow \text{Stationary equilibrium}$$

- Not a trivial assumption!
- But used both by DM and MOND
- How long to relax ? Transients? Which QSS?

Gravity is long-range !

$$\boxed{a = a_c = \frac{v^2}{r}} \Longleftrightarrow \text{Stationary equilibrium}$$

- Not a trivial assumption!
- But used both by DM and MOND
- How long to relax ? Transients? Which QSS?

Gravity is long-range !

- **Dynamics of spiral galaxy formation**

Dynamics of spiral arms formation

Dawes Review 4: Spiral Structures in Disc Galaxies

Clare Dobbs[1], and Junichi Baba[2]
[1]School of Physics and Astronomy, University of Exeter, Stocker Road, Exeter, EX4 4QL, UK
[2]Earth-Life Science Institute, Tokyo Institute of Technology 2-12-1-I2-44 Ookayama, Meguro, Tokyo 152–8551, Japan

Abstract

The majority of astrophysics involves the study of spiral galaxies, and stars and planets within them, but how spiral arms in galaxies form and evolve is still a fundamental problem. Major progress in this field was made primarily in the 1960s, and early 1970s, but since then there has been no comprehensive update on the

Three **main mechanisms** hypothesised to produce spiral arms

- Quasi-stationary density wave theory
- Local instabilities, perturbations, or noise which are swing amplified into spiral arms
- Tidal interactions

- **The strength and number of arms**: The dominance of two-armed patterns in grand-design spirals is a striking observational fact that **demands explanation** in a successful theory of spiral structure.

Trailing nature of arms

In all cases in which the answer is unambiguous, the spiral arms trail.

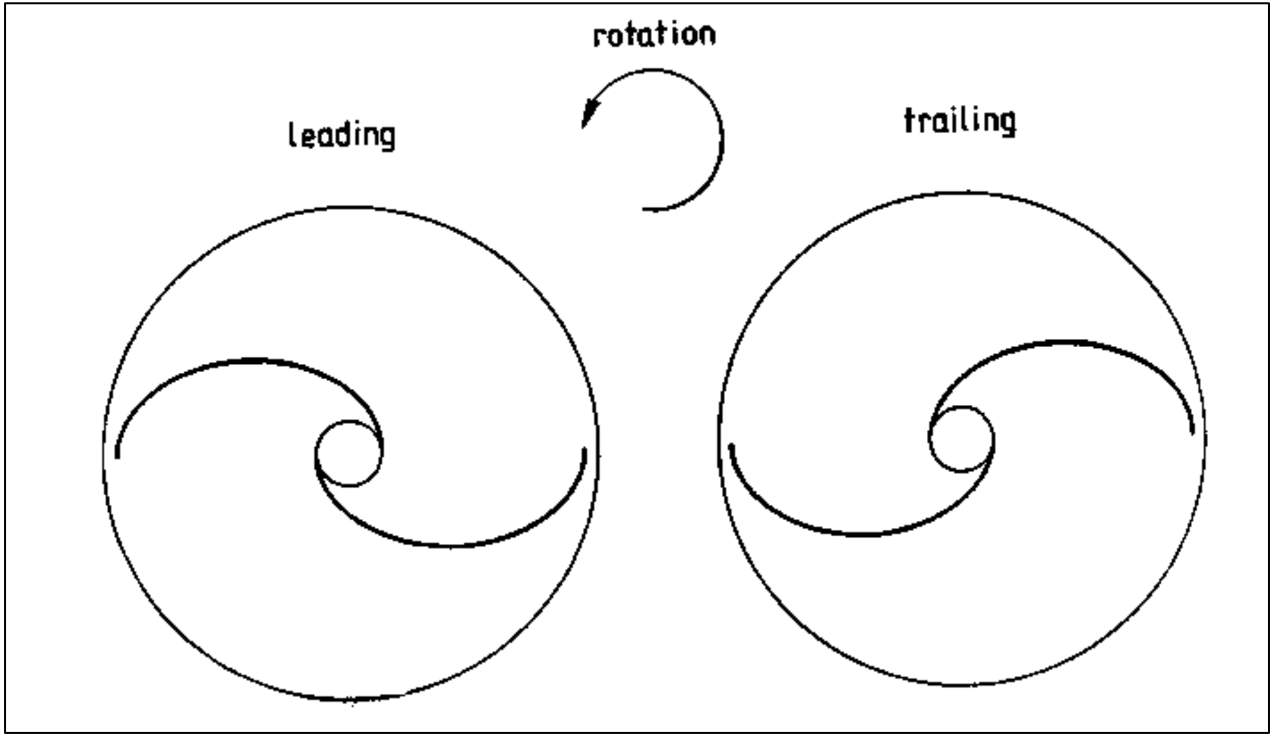

Winding Problem

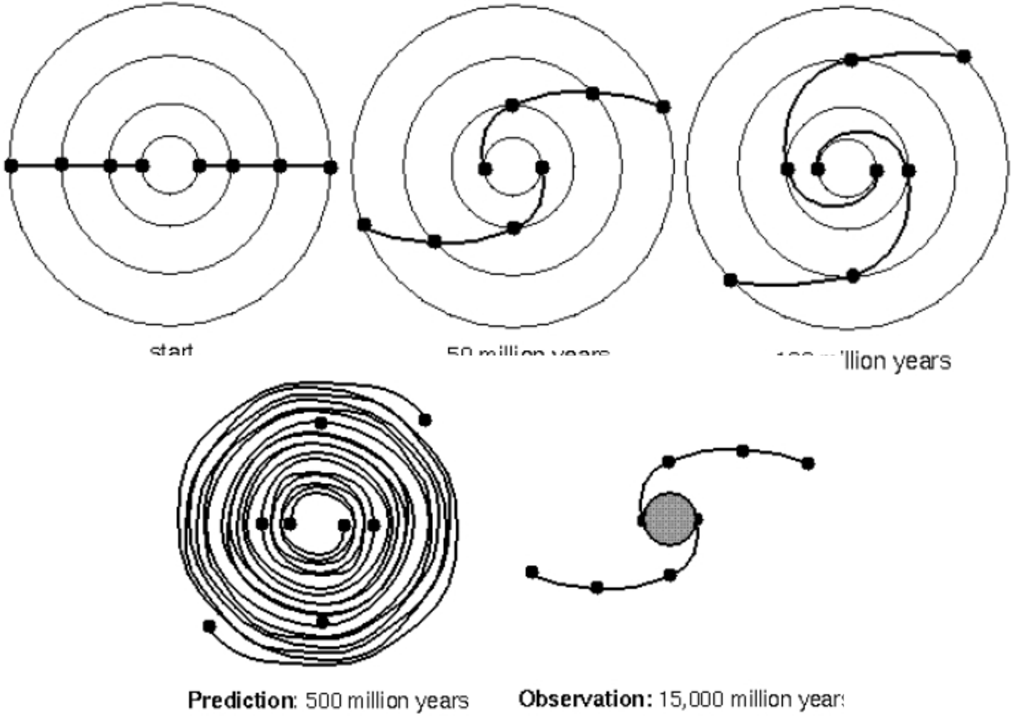

Differential rotation rotation creates a spiral pattern in a short time

Long Range

Long Range Interacting Systems

$$\lim_{r\to\infty}\phi(r)\sim\frac{1}{r^{\alpha}}\Rightarrow W(R,\epsilon)\sim\int_{\epsilon}^{R}\phi(r)r^{d-1}dr\propto\left[r^{d-\alpha}\right]_{\epsilon}^{R}$$

Long Range Interacting Systems

$$\boxed{\lim_{r\to\infty}\phi(r)\sim\frac{1}{r^{\alpha}}\Rightarrow W(R,\epsilon)\sim\int_{\epsilon}^{R}\phi(r)r^{d-1}dr\propto\left[r^{d-\alpha}\right]_{\epsilon}^{R}}$$

SRIS: $$\boxed{\lim_{R\to\infty}W(R)\sim\frac{1}{R^{|d-\alpha|}}<\infty \quad \text{for} \quad \alpha>d}$$

Long Range Interacting Systems

$$\boxed{\lim_{r\to\infty}\phi(r)\sim\frac{1}{r^\alpha}\Rightarrow W(R,\epsilon)\sim\int_\epsilon^R\phi(r)r^{d-1}dr\propto[r^{d-\alpha}]_\epsilon^R}$$

SRIS: $\boxed{\lim_{R\to\infty}W(R)\sim\frac{1}{R^{|d-\alpha|}}<\infty\quad\text{for}\quad\alpha>d}$

LRIS: $\boxed{\lim_{R\to\infty}W(R)\sim R^{|d-\alpha|}\to\infty\quad\text{for}\quad\alpha\le d}$

Long Range Interacting Systems (LRIS)

$$\boxed{E_{tot} = E_1 + E_2 + E_{int}}$$

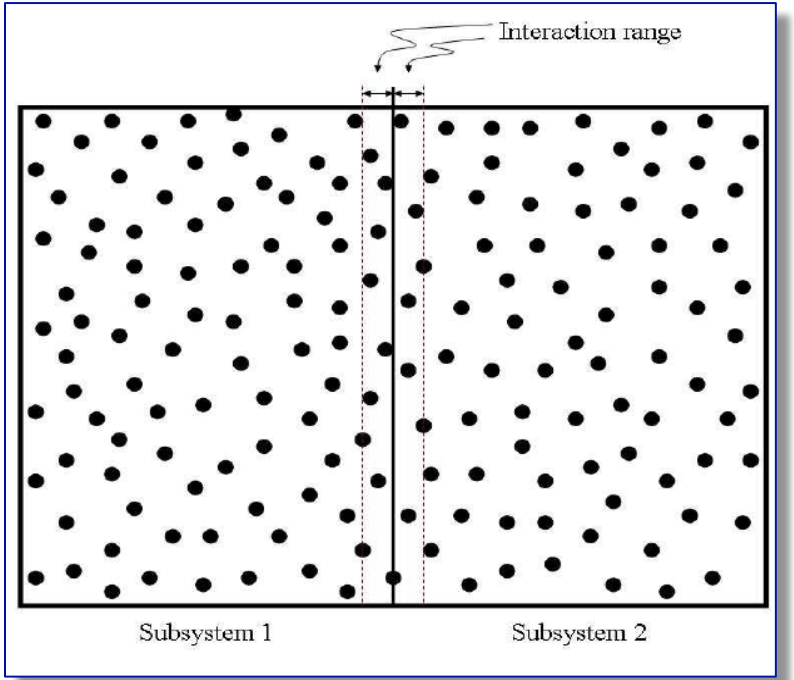

$$\lim_{N\to\infty} \frac{E_{int}}{E_{tot}}$$

$$N^{-1/3} \to 0$$

SRIS

$$O(1)$$

LRIS

Long Range Interacting Systems

- SRIS: **equilibrium**, thermodynamical properties from microscopic interactions (ensemble equivalence).
- SRIS: an out of equilibrium state is driven by **local interactions** towards a TDE state characterized by the maximum value of the **entropy** compatible with the conditions imposed

Long Range Interacting Systems

- SRIS: **equilibrium**, thermodynamical properties from microscopic interactions (ensemble equivalence).
- SRIS: an out of equilibrium state is driven by **local interactions** towards a TDE state characterized by the maximum value of the **entropy** compatible with the conditions imposed

- LRIS: energy **not additive**→ Virial theorem, negative specific heat
- LRIS **long-lived** dynamical states not in TDE → QSS
- LRIS: very different time scales in the **relaxation** process

Long Range Interacting Systems

If the system is isolated and confined in space and momentum:

$$I = \sum_{i=1}^{N} m_i r_i^2 \Rightarrow \frac{1}{2}\ddot{I} = 2K(t) + W(t) - E_s - E_{tidal}$$

Long Range Interacting Systems

If the system is isolated and confined in space and momentum:

$$I = \sum_{i=1}^{N} m_i r_i^2 \Rightarrow \frac{1}{2}\ddot{I} = 2K(t) + W(t) - E_s - E_{tidal}$$

$$\boxed{\frac{1}{2}\langle \ddot{I} \rangle = 2\langle K \rangle + \langle W \rangle = 0}$$

Self Gravitating systems

$$\begin{cases} \partial_t f + \vec{v} \cdot \nabla_{\vec{x}} f + \dfrac{1}{m} \vec{F} \cdot \nabla_{\vec{v}} f = 0 & \text{Collisionless Boltzmann equation} \\ \nabla^2 \Phi(\vec{x}) = 4\pi G m \displaystyle\int f(\vec{x}, \vec{v}, t) d\vec{v} & \text{Poisson equation} \end{cases}$$

Self Gravitating systems

$$\begin{cases} \partial_t f + \vec{v} \cdot \nabla_{\vec{x}} f + \dfrac{1}{m} \vec{F} \cdot \nabla_{\vec{v}} f = 0 \\ \nabla^2 \Phi(\vec{x}) = 4\pi G m \displaystyle\int f(\vec{x}, \vec{v}, t) d\vec{v} \end{cases}$$

$$\frac{1}{2} \langle \ddot{I} \rangle = 2\langle K \rangle + \langle W \rangle = 0$$

Self Gravitating systems

$$
\begin{cases}
\partial_t f + \vec{v} \cdot \nabla_{\vec{x}} f + \dfrac{1}{m} \vec{F} \cdot \nabla_{\vec{v}} f = 0 \\
\nabla^2 \Phi(\vec{x}) = 4\pi G m \displaystyle\int f(\vec{x}, \vec{v}, t) d\vec{v}
\end{cases}
$$

$$\frac{1}{2}\langle \ddot{I} \rangle = 2\langle K \rangle + \langle W \rangle = 0$$

Stationary solution

$$f(\vec{x}, \vec{v}, t) \rightarrow f(\vec{x}, \vec{v})$$

Collapse of an isolated cloud

Dynamics of a **spherical** isolated cold cloud

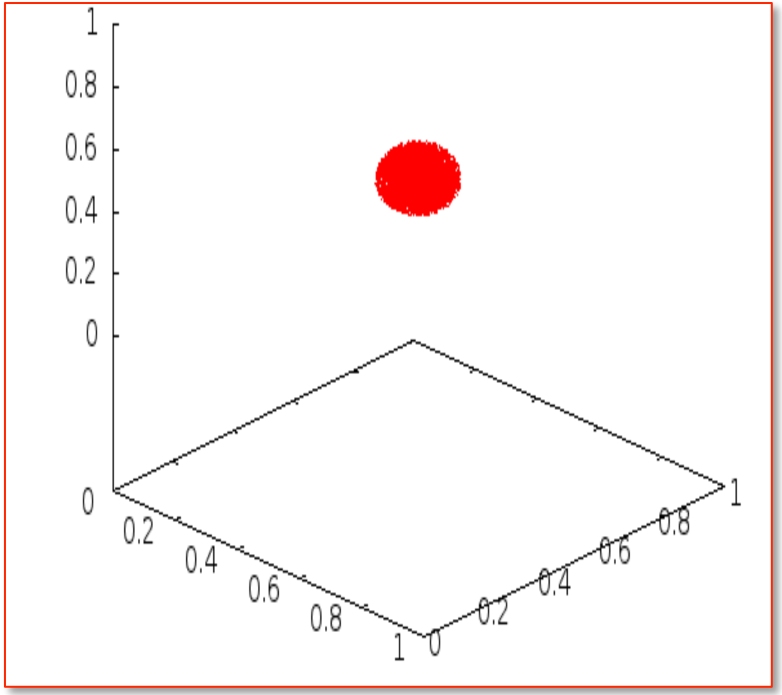

$$\begin{cases} E_{tot} = const \\ \vec{L}_{tot} = const \\ \vec{P}_{tot} = const \end{cases}$$

$$\boxed{\frac{d^2\vec{r}_i}{dt^2} = -Gm \sum_{j \neq i}^{j=1,N} \frac{\vec{r}_i - \vec{r}_j}{|\vec{r}_i - \vec{r}_j|^3}}$$

Joyce M., Marcos B., Sylos Labini F., MNRAS, **397**, 2, 775-792 (2009) Sylos Labini, F. 2013, Astron.Astrophys, **552A**, 36

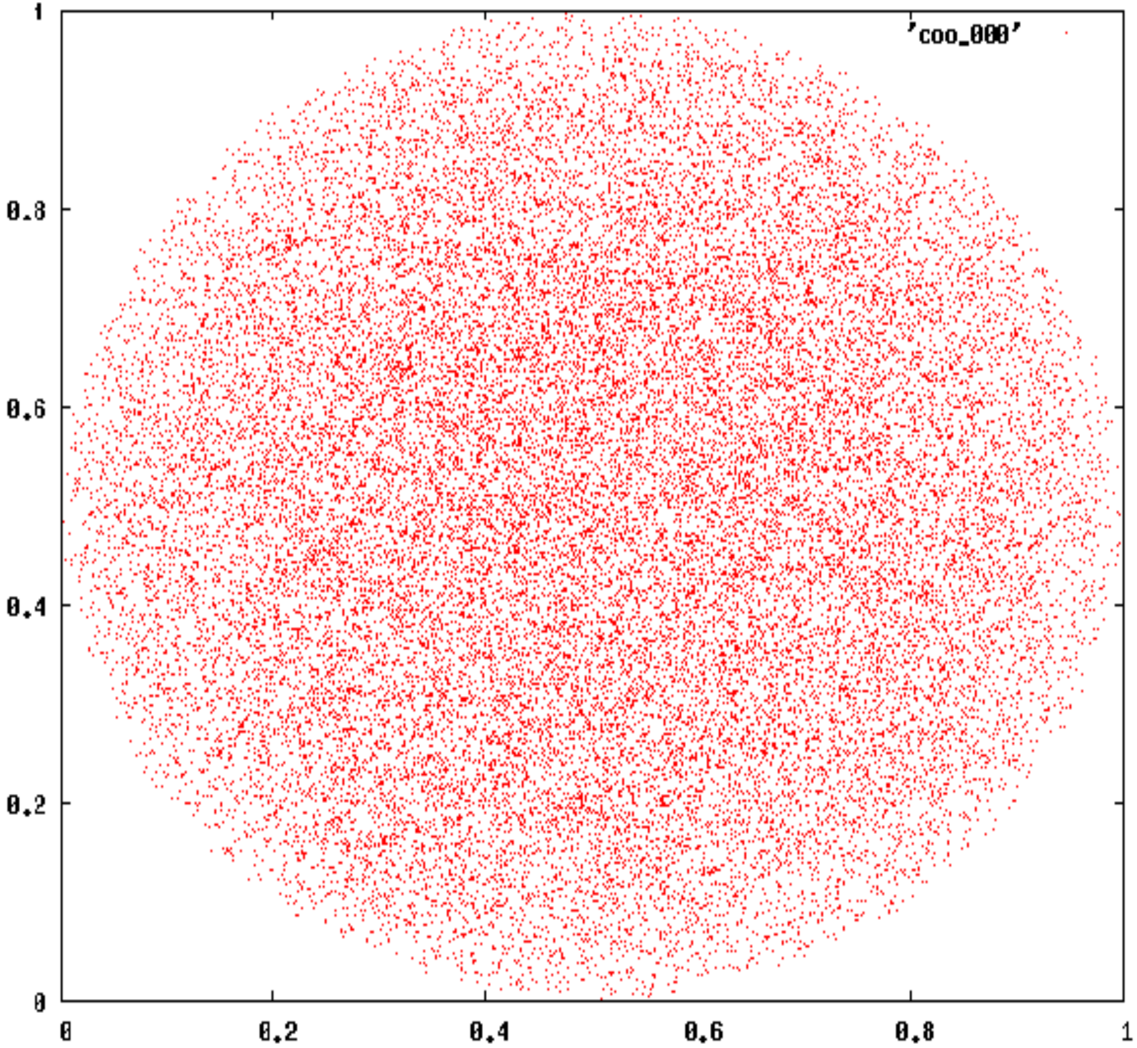

'coo_000'
0
0.2
0.4
0.6
0.8
1

Particles motion in a **rapidly varying** gravitational field

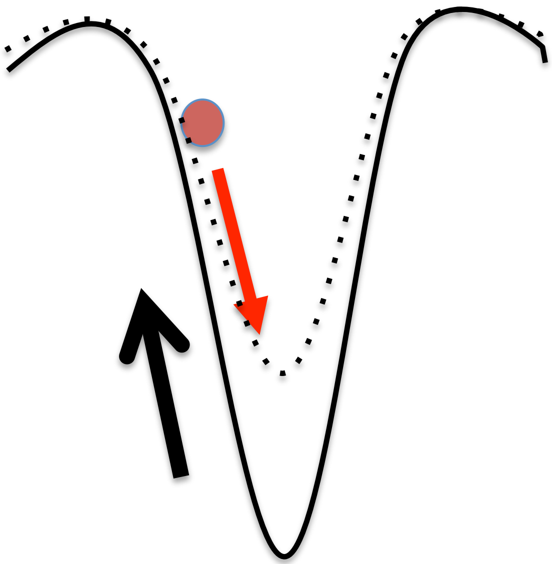

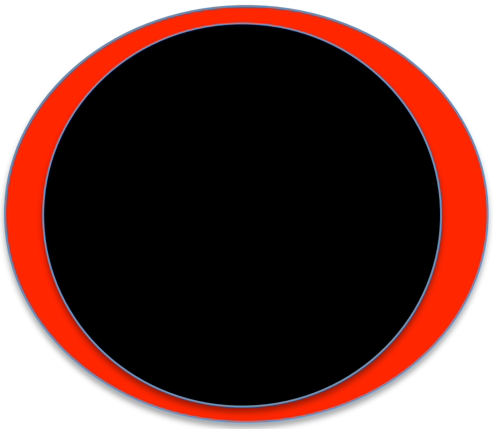

$$\boxed{\epsilon(t) \neq const}$$

Probability of being ejected

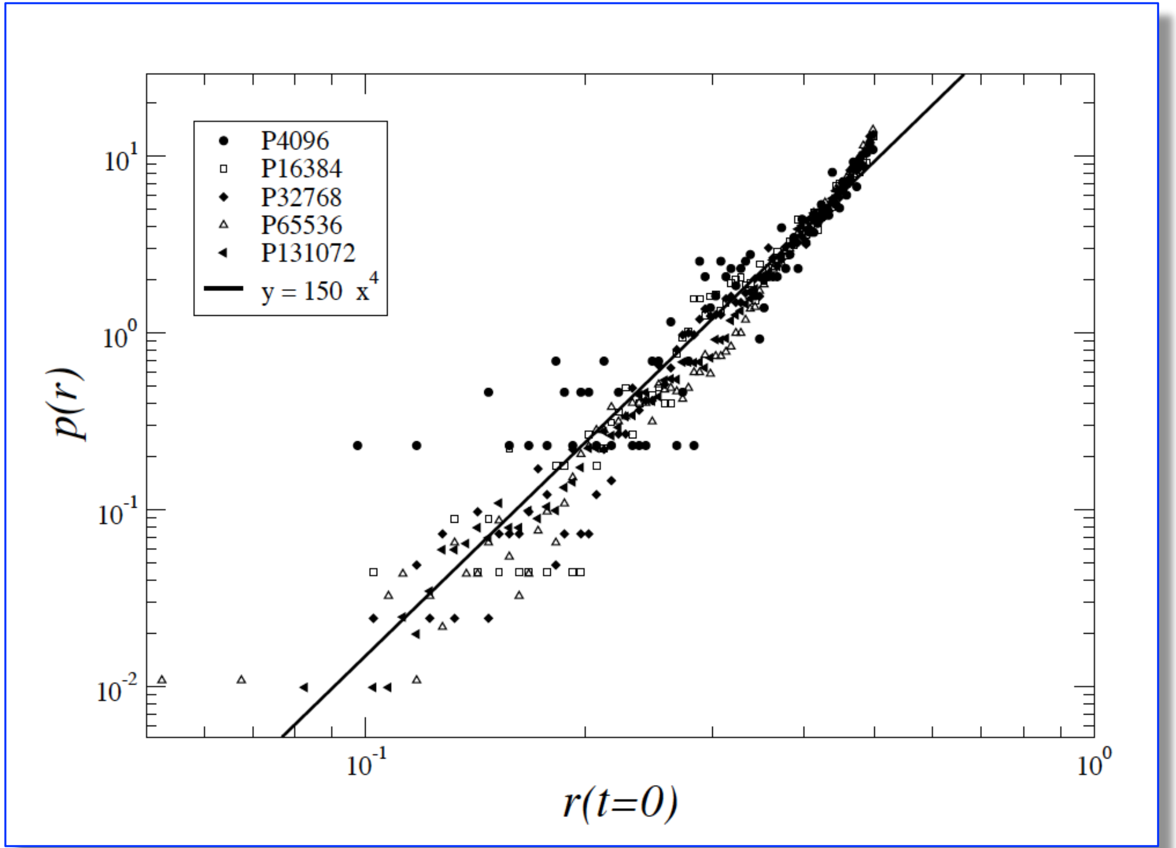

From cold to warm clouds

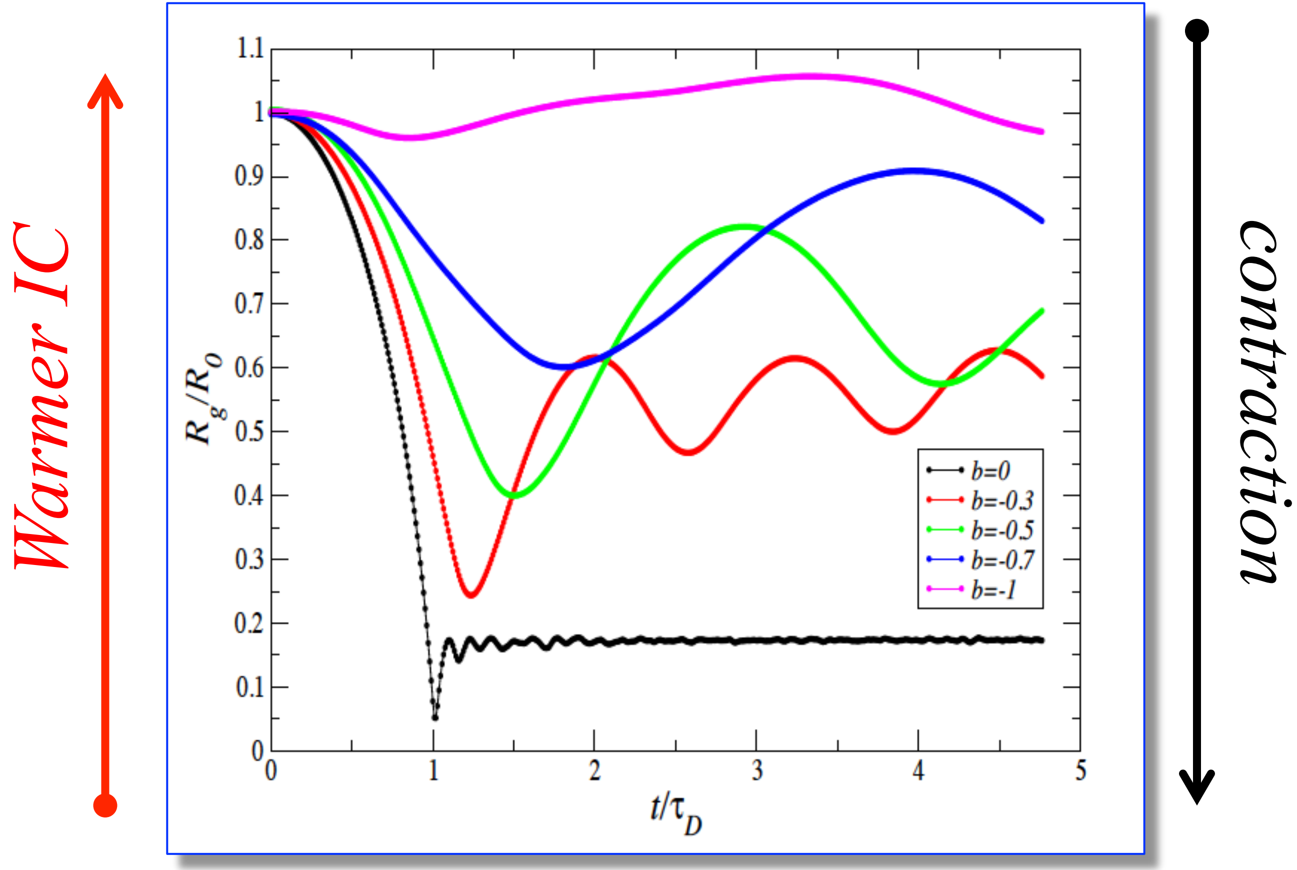

Sylos Labini, F, Mon.Not.R.Acad.Soc, **429**, 679, 2013

From cold to warm clouds

$$\boxed{b = \frac{2K}{W}}$$

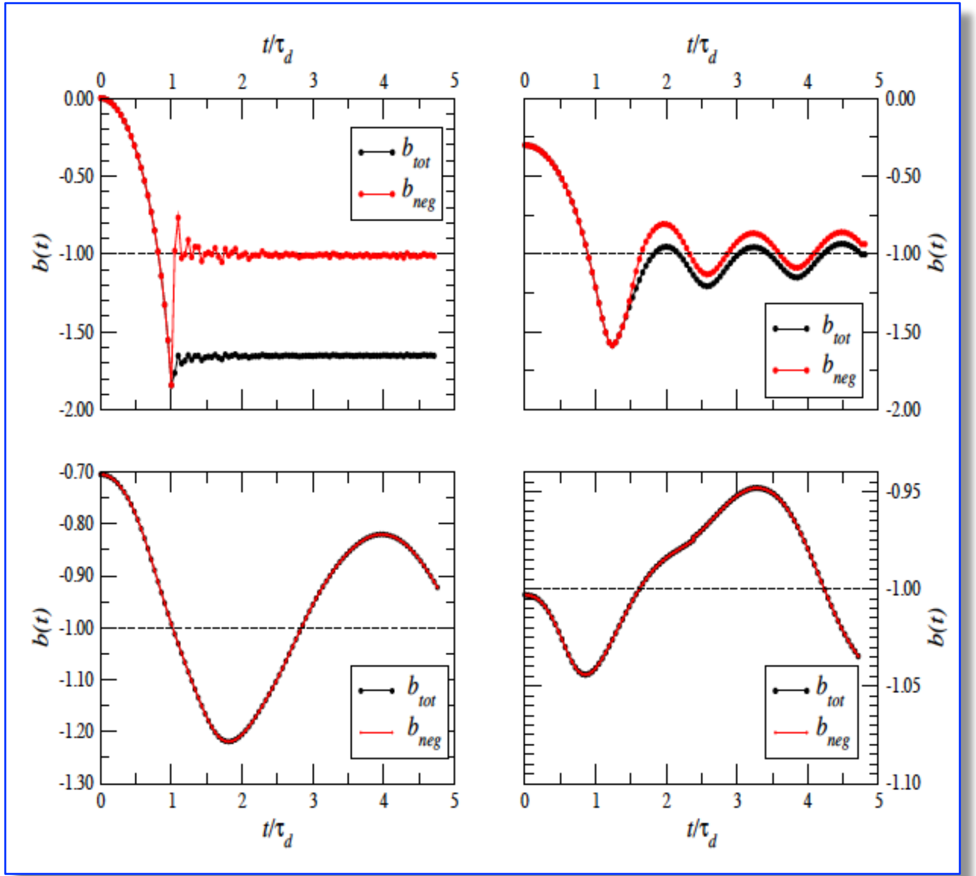

Sylos Labini, F, 2012, Mon.Not.R.Acad.Soc., **423**, 1610S

Breaking of spherical symmetry

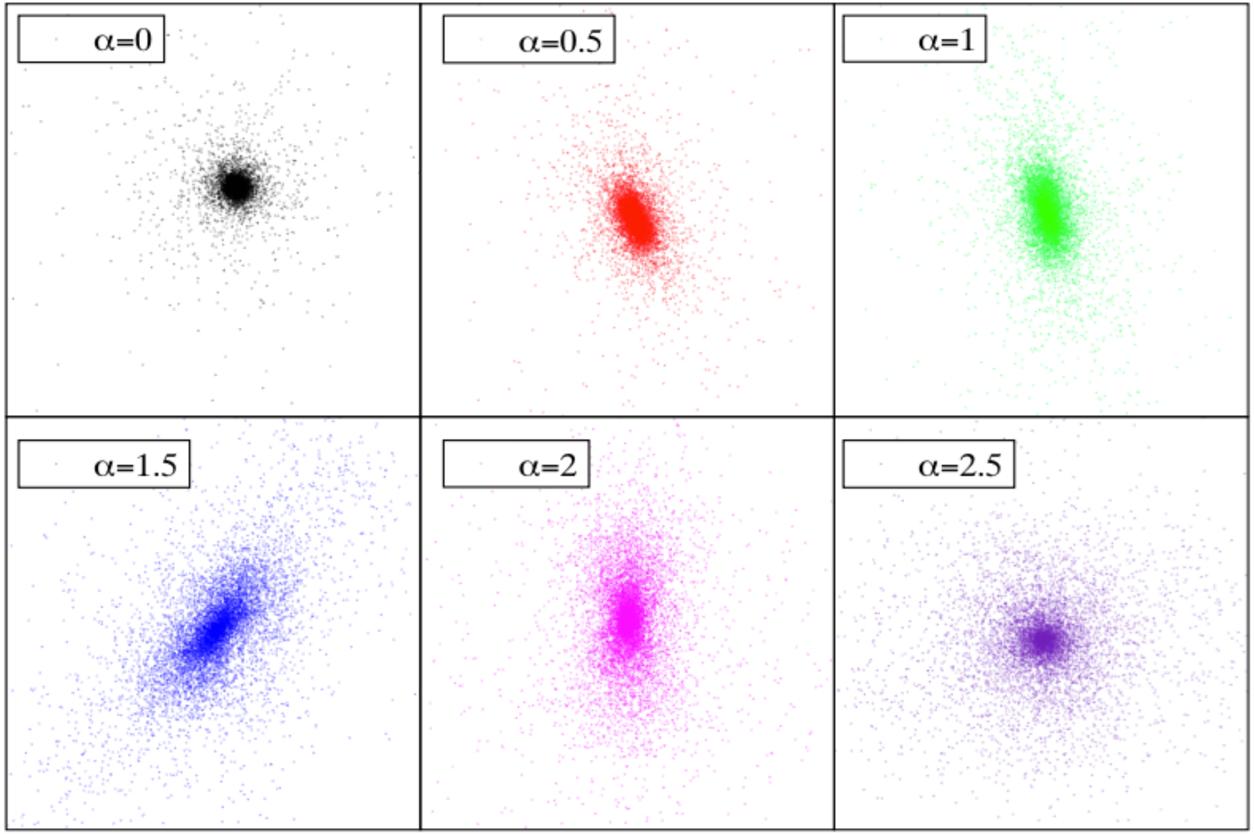

Benhaiem D. Joyce M., Sylos Labini F., Worrakiponpon, T. A&A, **585**, A139, 2016

Generation of Angular Momentum

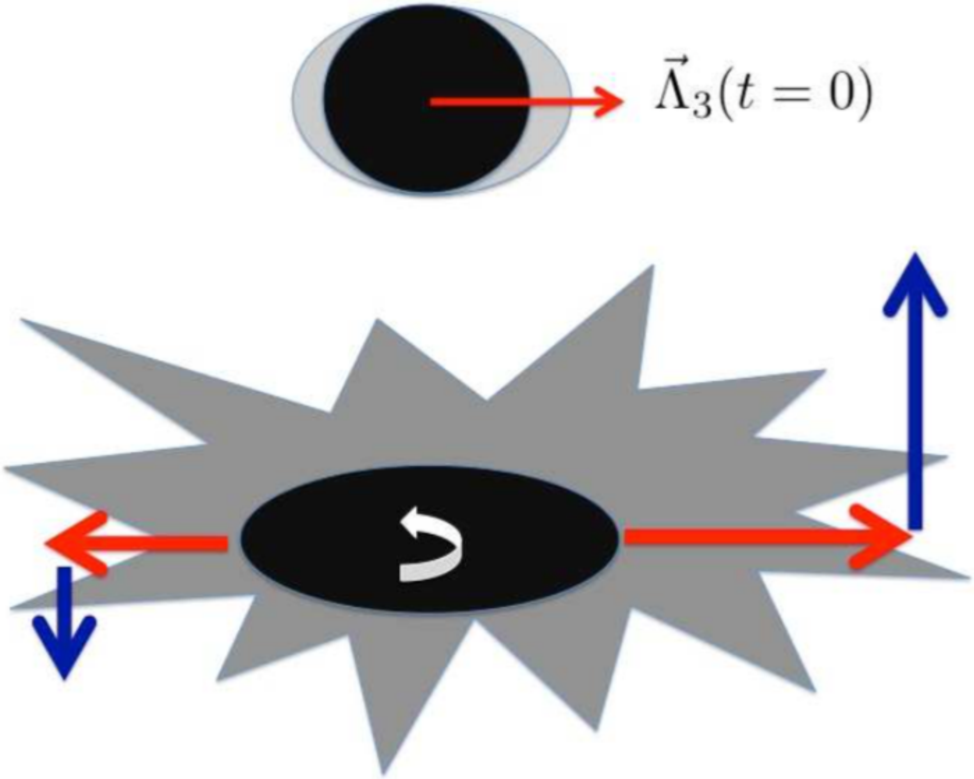

Benhaiem D. Joyce M., Sylos Labini F., Worrakiponpon, T. A&A, **585**, A139, 2016

Collapse of an **ellipsoidal** isolated cloud

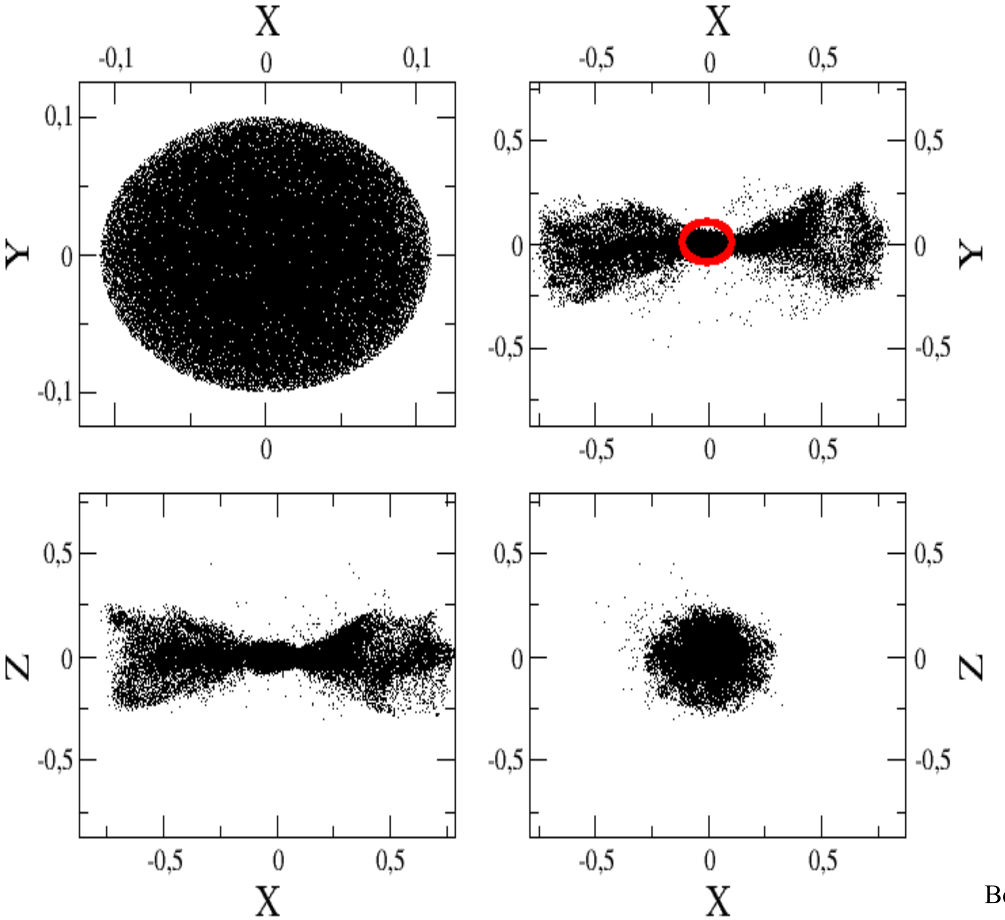

$$\boxed{a_x \geq a_y \geq a_z}$$

$$\begin{cases} \iota_x = \dfrac{a_x}{a_z} - 1 \\ \iota_y = \dfrac{a_y}{a_z} - 1 \end{cases}$$

Benhaiem & Sylos Labini Mon.Not.R. Astron. Soc 448, 2634-2643 (2015)

Collapse of an **ellipsoidal** isolated cloud

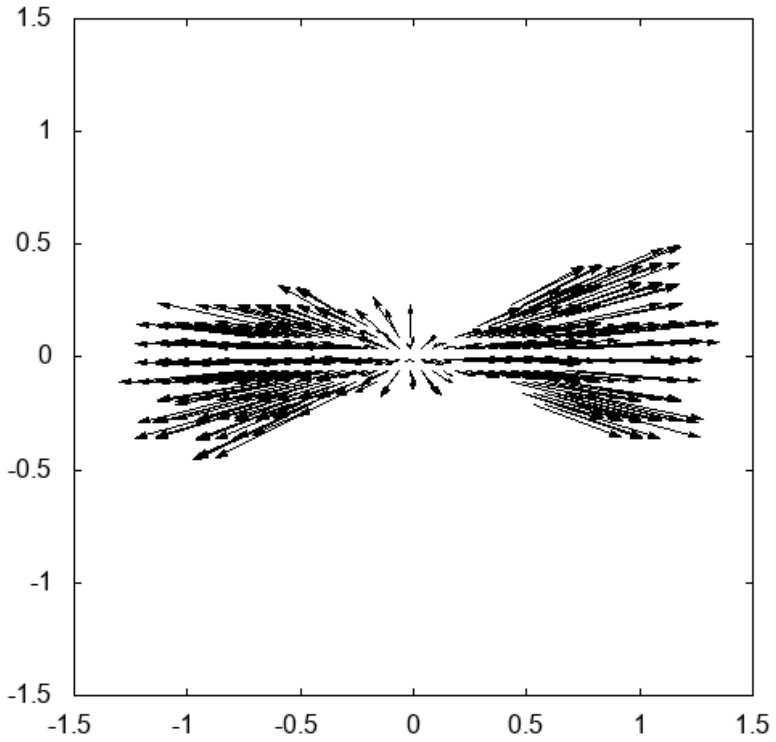

Collapse of irregular inhomogeneous clouds

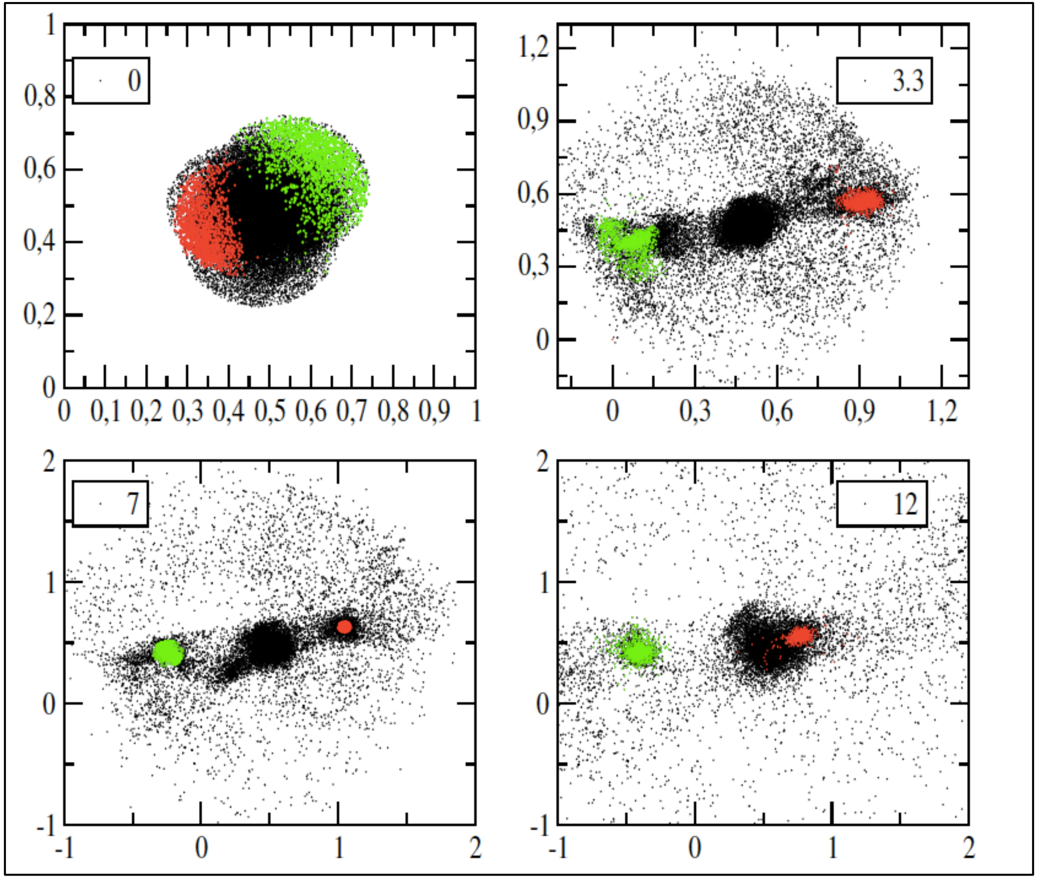

Benhaiem & Sylos Labini, Astron.Astrophys. 598, A95 (2017)

Collapse of **rotating ellipsoidal** clouds

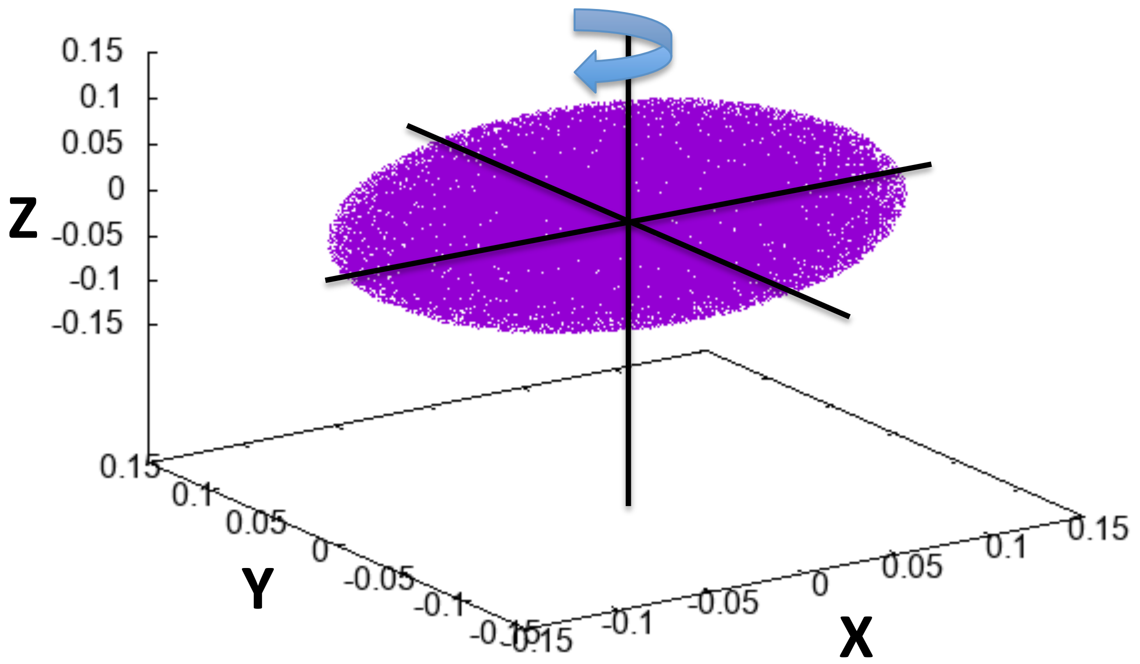

$$\begin{cases} \vec{v} = \vec{\Omega} \times \vec{r} \\ \vec{\Omega} = [0, 0, \Omega] \end{cases}$$

$$\boxed{\tau_d = \sqrt{\frac{\pi^2 a_3^3}{8GM}}}$$

D. Benhaiem, M. Joyce, F. Sylos Labini, Astrophys.J in the press (2017)

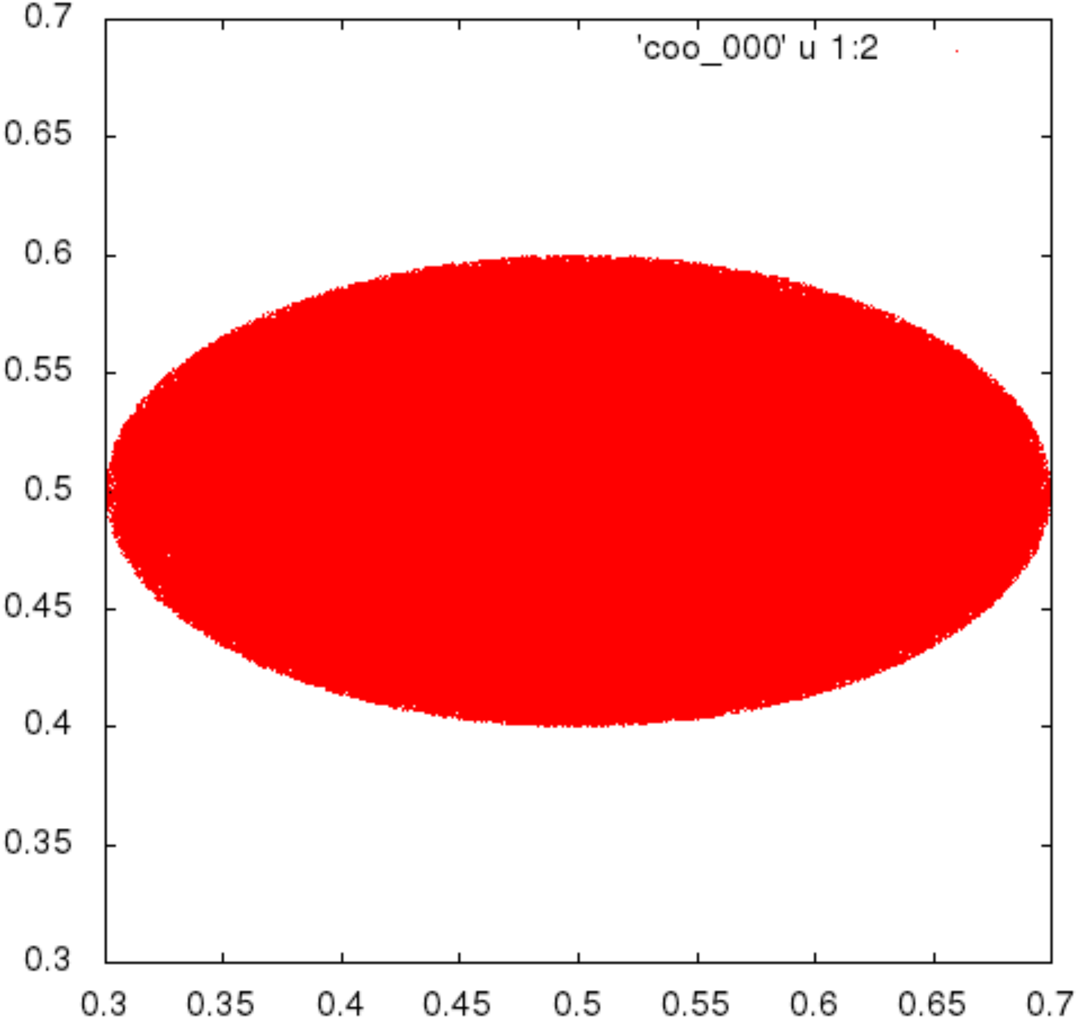

'coo_000' u 1:2
0.7
0.65
0.6
0.55
0.5
0.45
0.4
0.35
0.3
0.3
0.35
0.4
0.45
0.5
0.55
0.6
0.65
0.7

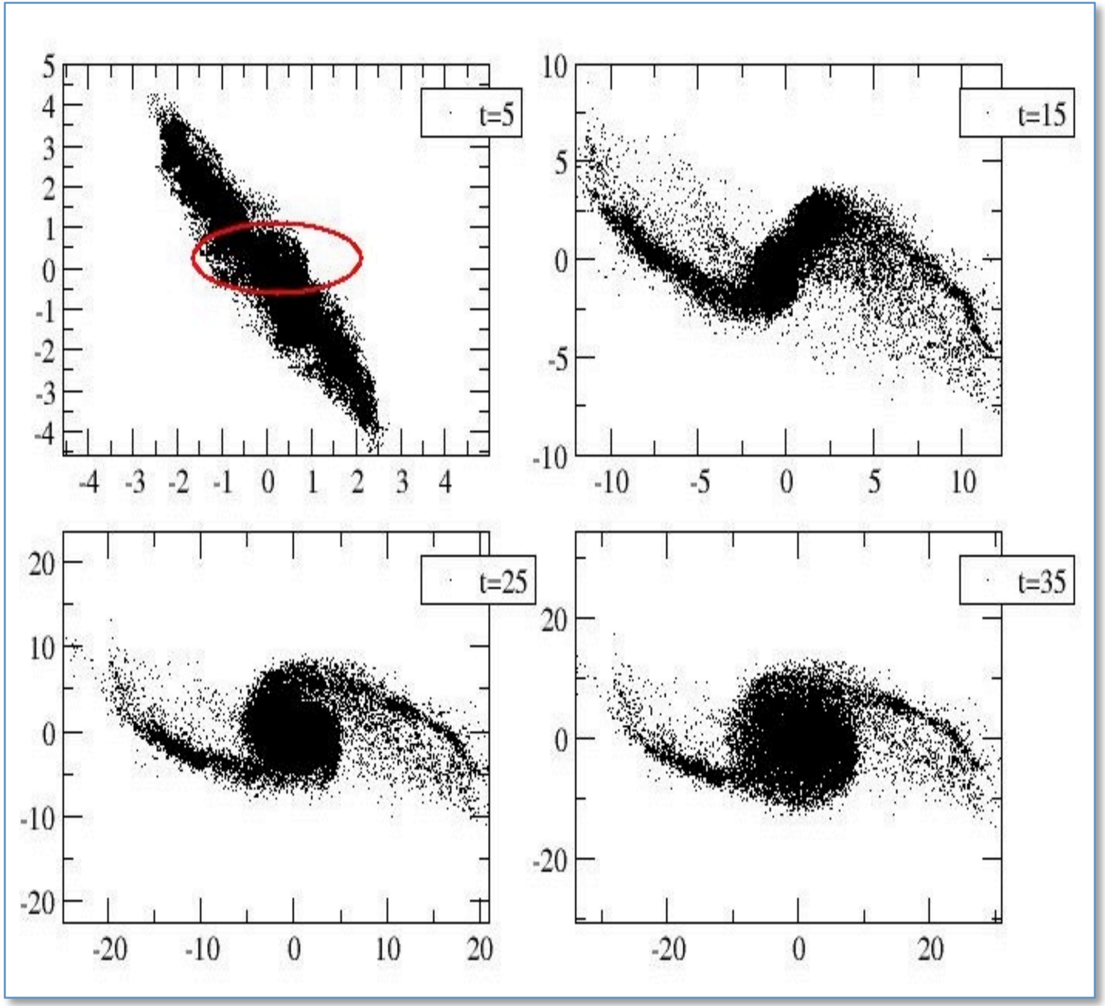

t=5
t=15
t=25
t=35

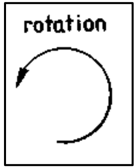

rotation

$\epsilon \leq 0$ $\longrightarrow$ Long return times **(long lasting transients)**

$$\epsilon \leq 0 \longrightarrow \text{Long return times}$$

$$\Phi(r) \sim \frac{GM_c}{r} \longrightarrow \text{Spherically symmetric potential}$$

$$\epsilon \leq 0 \Longrightarrow \text{Long return times}$$

$$\Phi(r) \sim \frac{GM_c}{r} \Longrightarrow \text{Spherically symmetric potential}$$

$$\epsilon(t) \approx const. \Longrightarrow \text{Energy conservation}$$

$$\vec{\ell}(t) \approx const. \Longrightarrow \text{Angular momentum conservation}$$

Angular momentum conservation

$$\vec{\ell} = \vec{r} \times m\vec{v} = (r^2 m)\vec{\omega} \approx const.$$

$$|\vec{\omega}| = \frac{|\vec{v}_\perp|}{r}$$

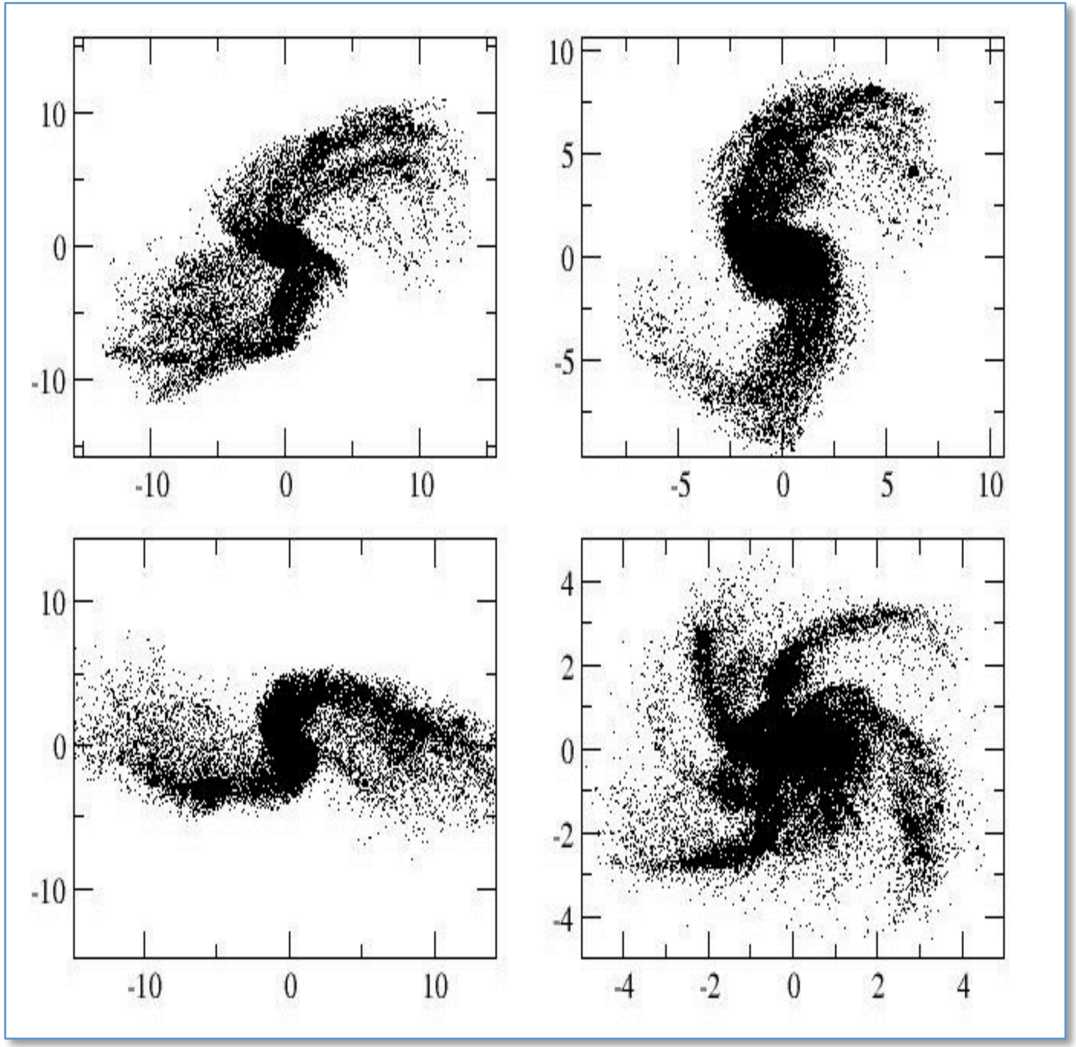
10
0
-10
-10
0
10
10
5
0
-5
-5
0
5
10
10
0
-10
-10
0
10
4
2
0
-2
-4
-4
-2
0
2
4

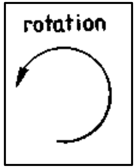
rotation

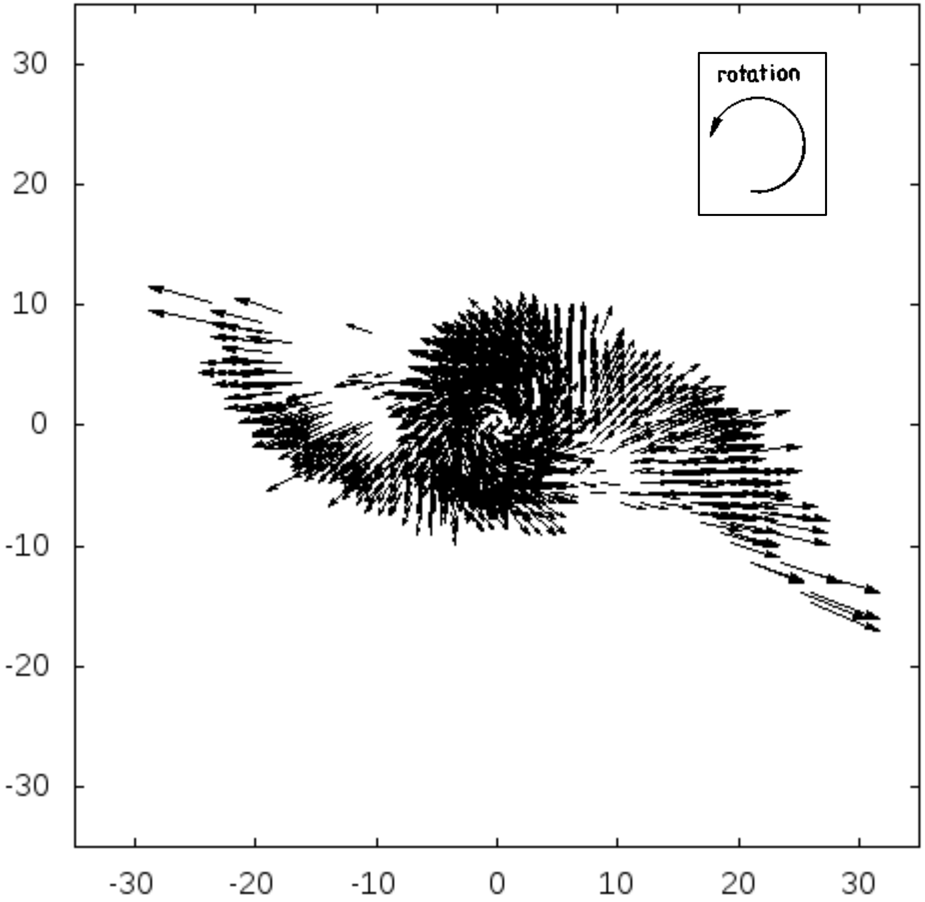
rotation
30
20
10
0
-10
-20
-30
-30
-20
-10
0
10
20
30

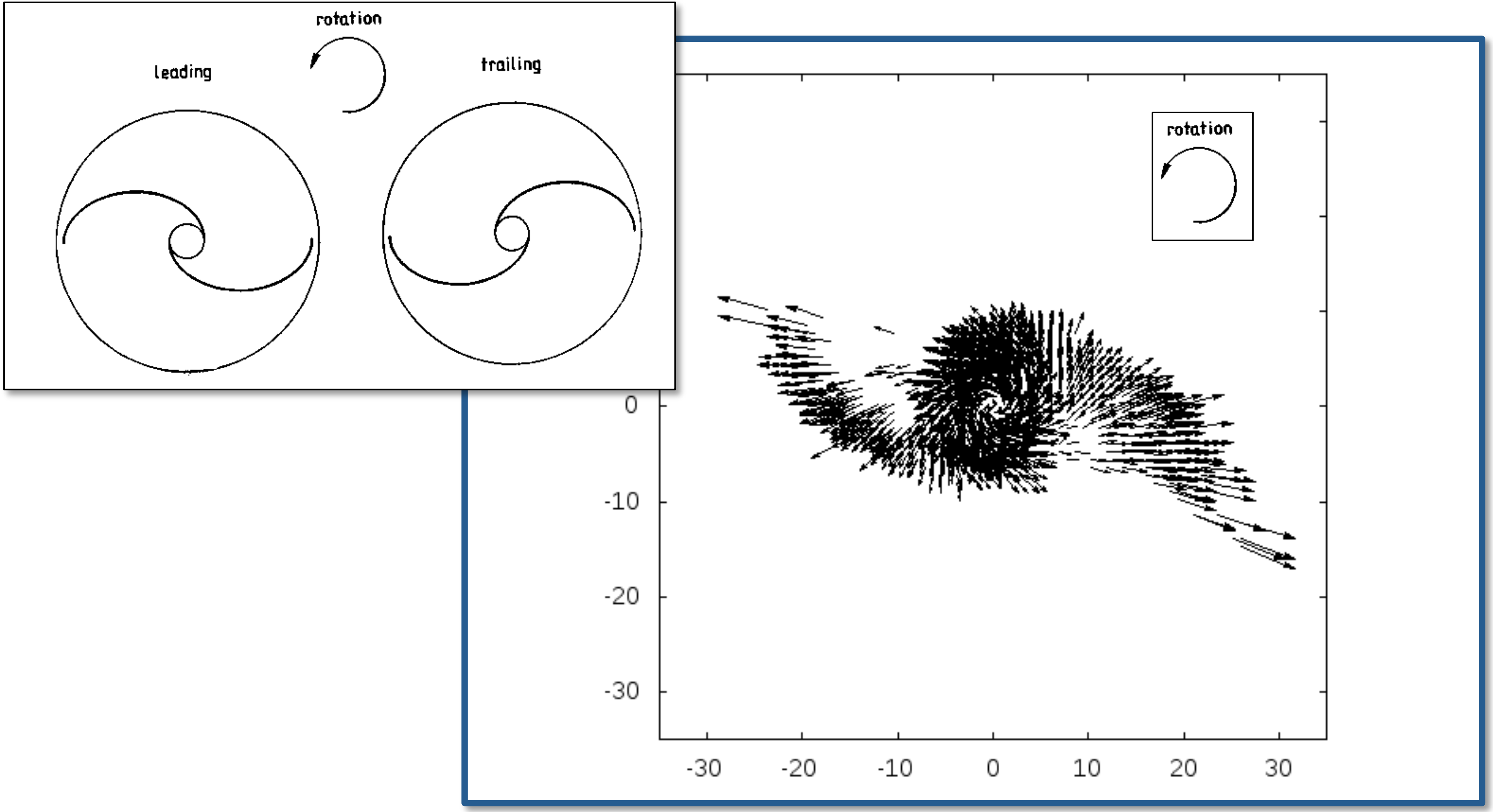

rotation
leading
trailing
rotation
0
-10
-20
-30
-30
-20
-10
0
10
20
30

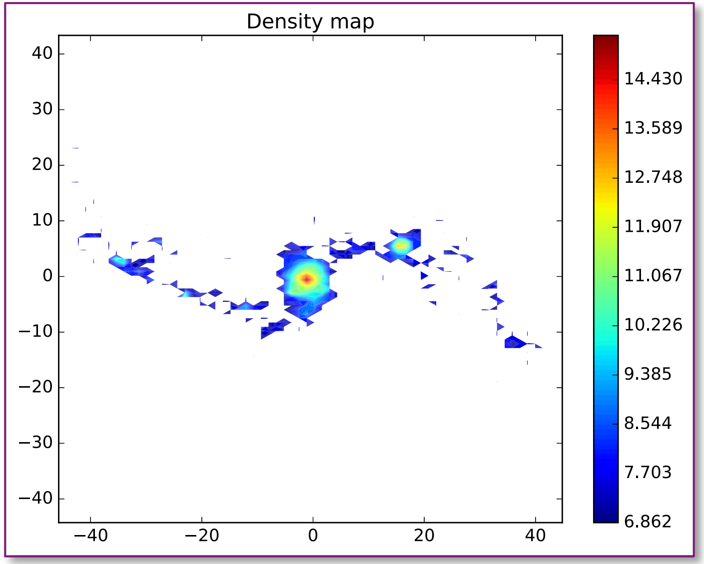

Density map
40
30
20
10
0
−10
−20
−30
−40
−40
−20
0
20
40
14.430
13.589
12.748
11.907
11.067
10.226
9.385
8.544
7.703
6.862

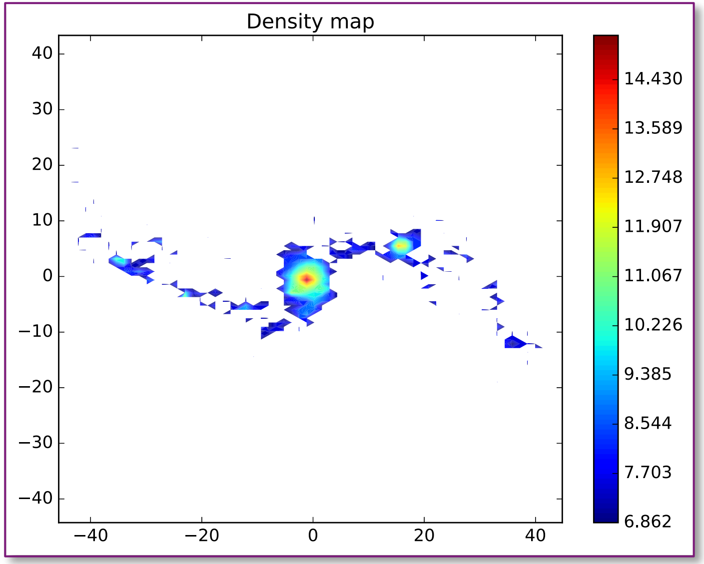
Density map
40
30
20
10
0
−10
−20
−30
−40
−40
−20
0
20
40
14.430
13.589
12.748
11.907
11.067
10.226
9.385
8.544
7.703
6.862

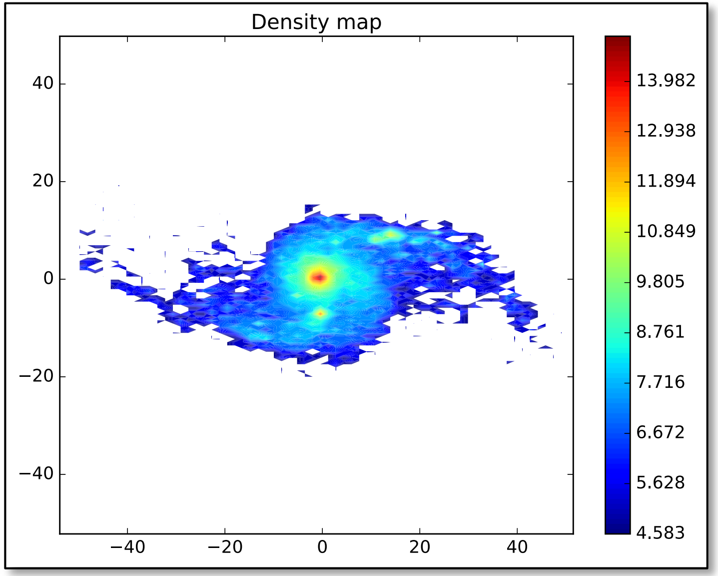
Density map
40
20
0
−20
−40
−40
−20
0
20
40
13.982
12.938
11.894
10.849
9.805
8.761
7.716
6.672
5.628
4.583

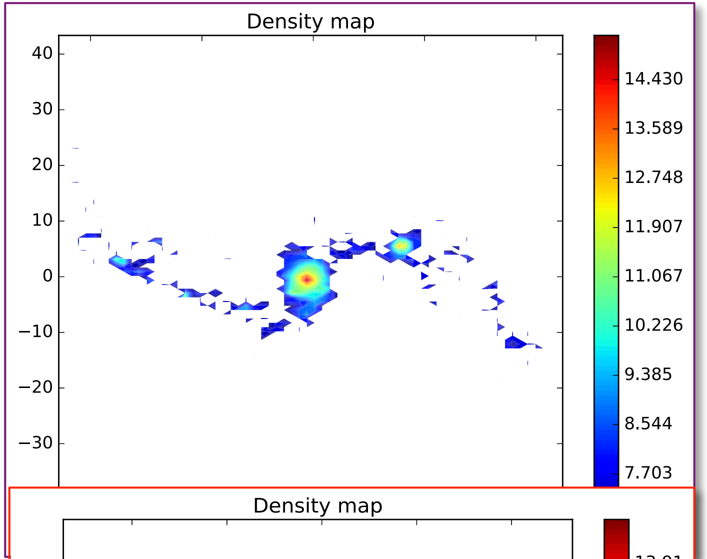
Density map
40
30
20
10
0
−10
−20
−30
14.430
13.589
12.748
11.907
11.067
10.226
9.385
8.544
7.703

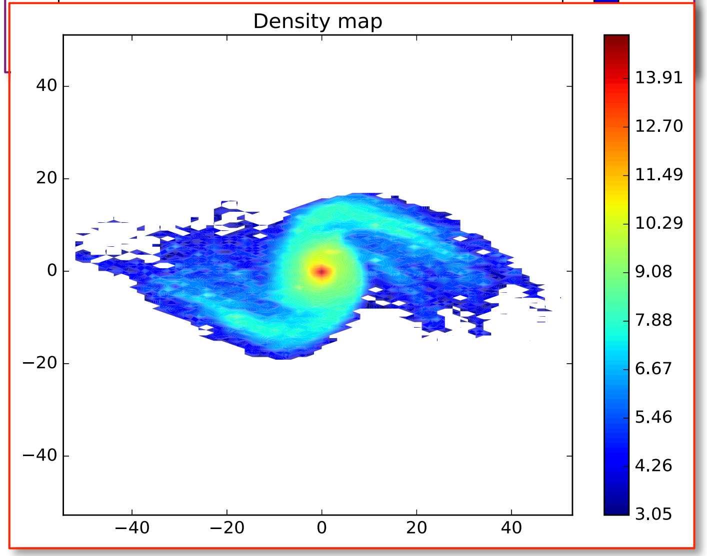
Density map
40
20
0
−20
−40
−40
−20
0
20
40
13.91
12.70
11.49
10.29
9.08
7.88
6.67
5.46
4.26
3.05

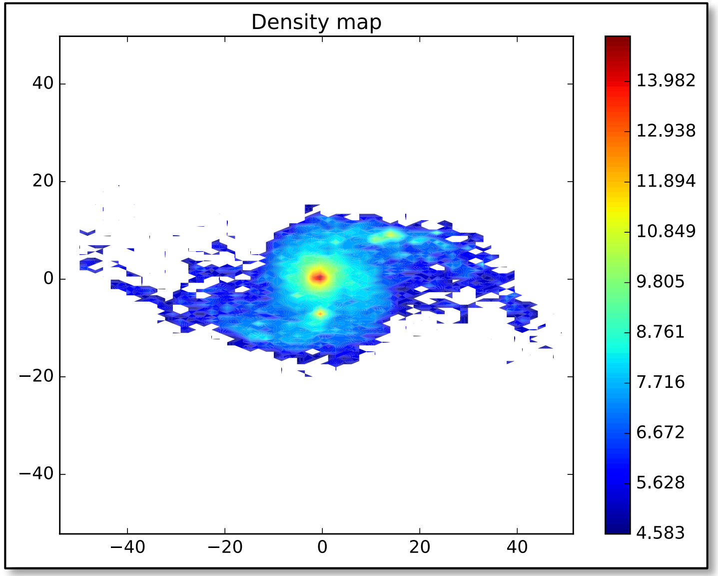
Density map
40
20
0
−20
−40
−40
−20
0
20
40
13.982
12.938
11.894
10.849
9.805
8.761
7.716
6.672
5.628
4.583

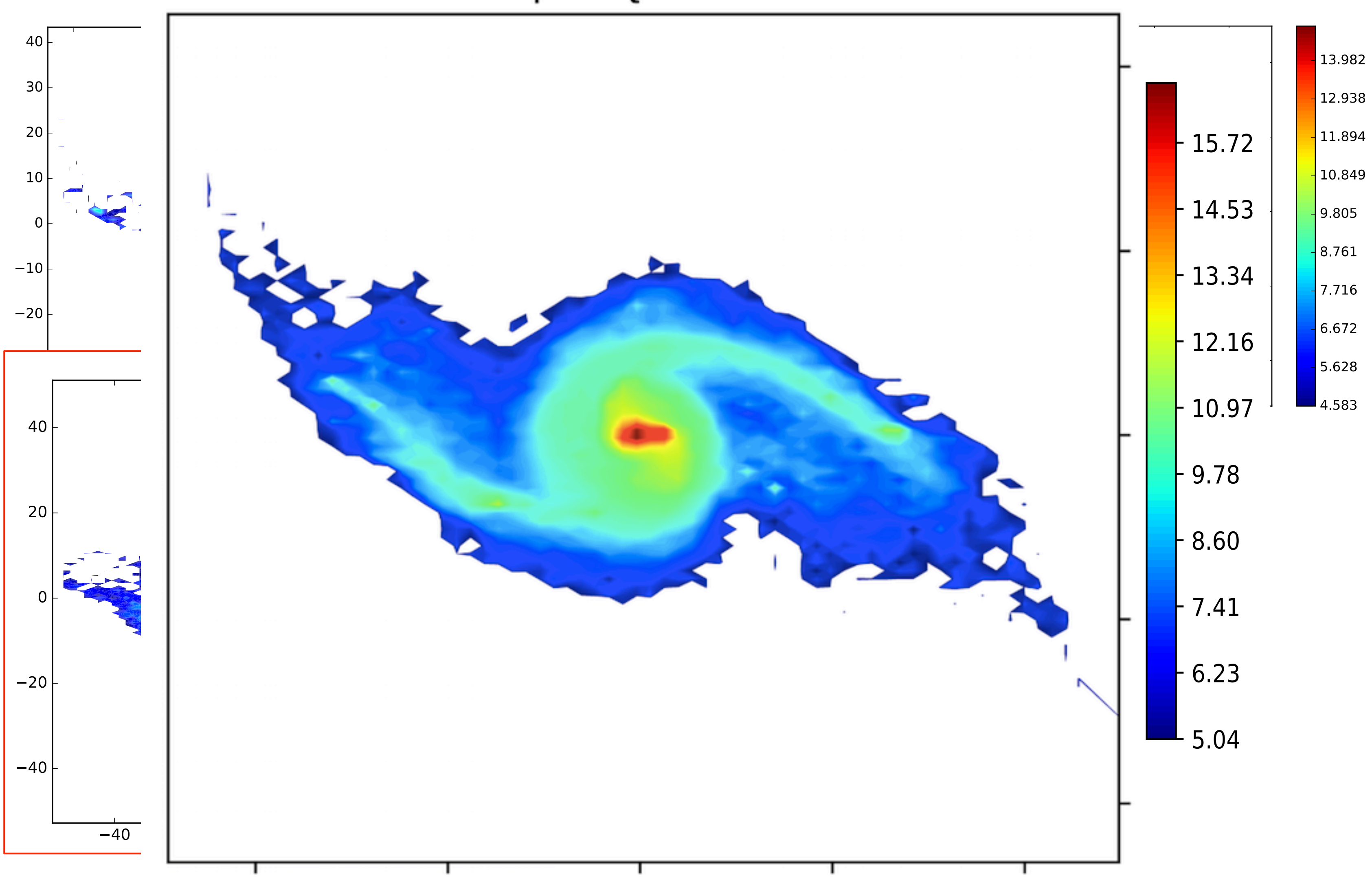

40
30
20
10
0
−10
−20
40
20
0
−20
−40
−40
15.72
14.53
13.34
12.16
10.97
9.78
8.60
7.41
6.23
5.04
13.982
12.938
11.894
10.849
9.805
8.761
7.716
6.672
5.628
4.583

- Two arms (mainly)
- Trailing arms
- No winding problem
- Pitch angle some tens degrees

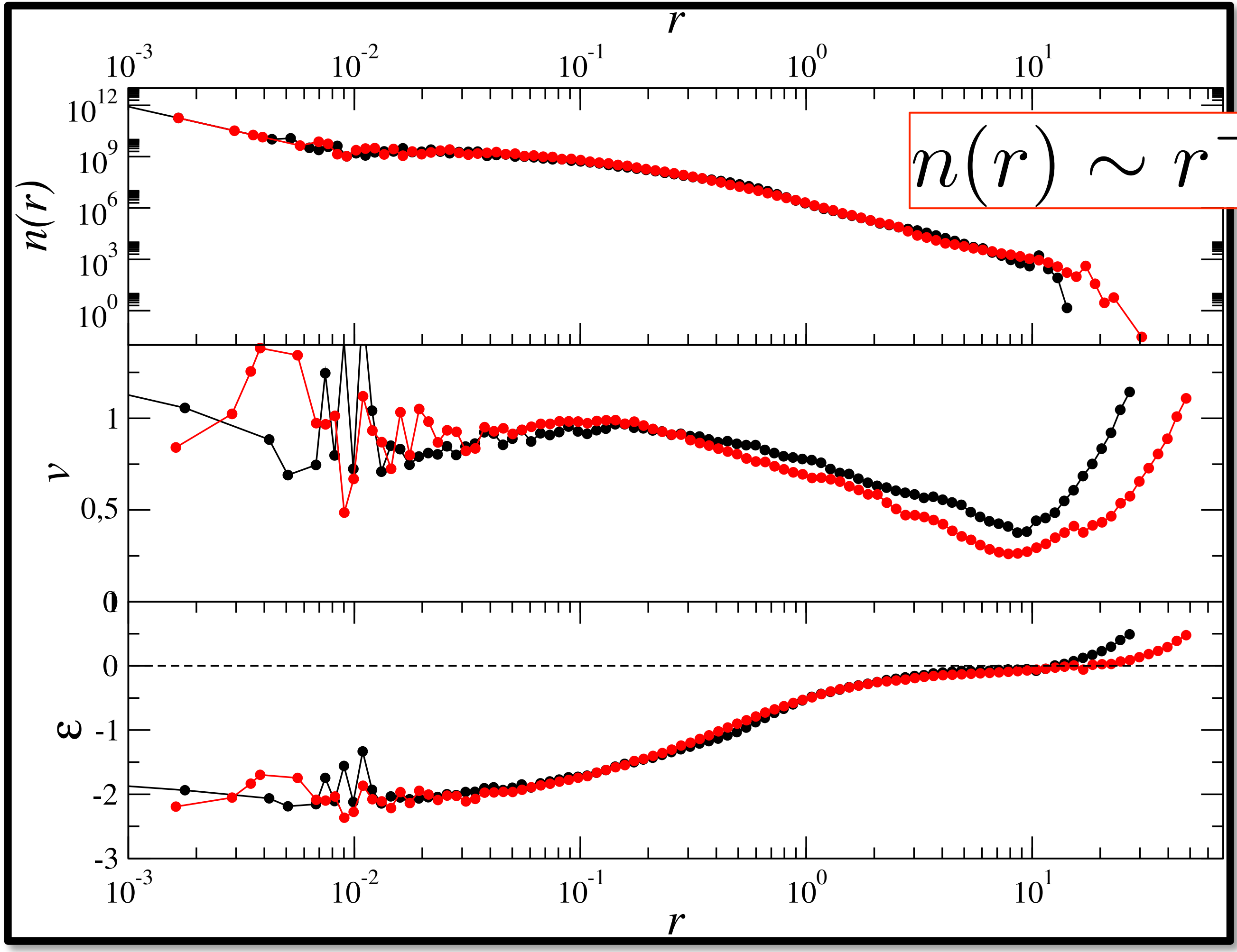

r
n(r)
v
ε
$n(r) \sim r^{-4}$

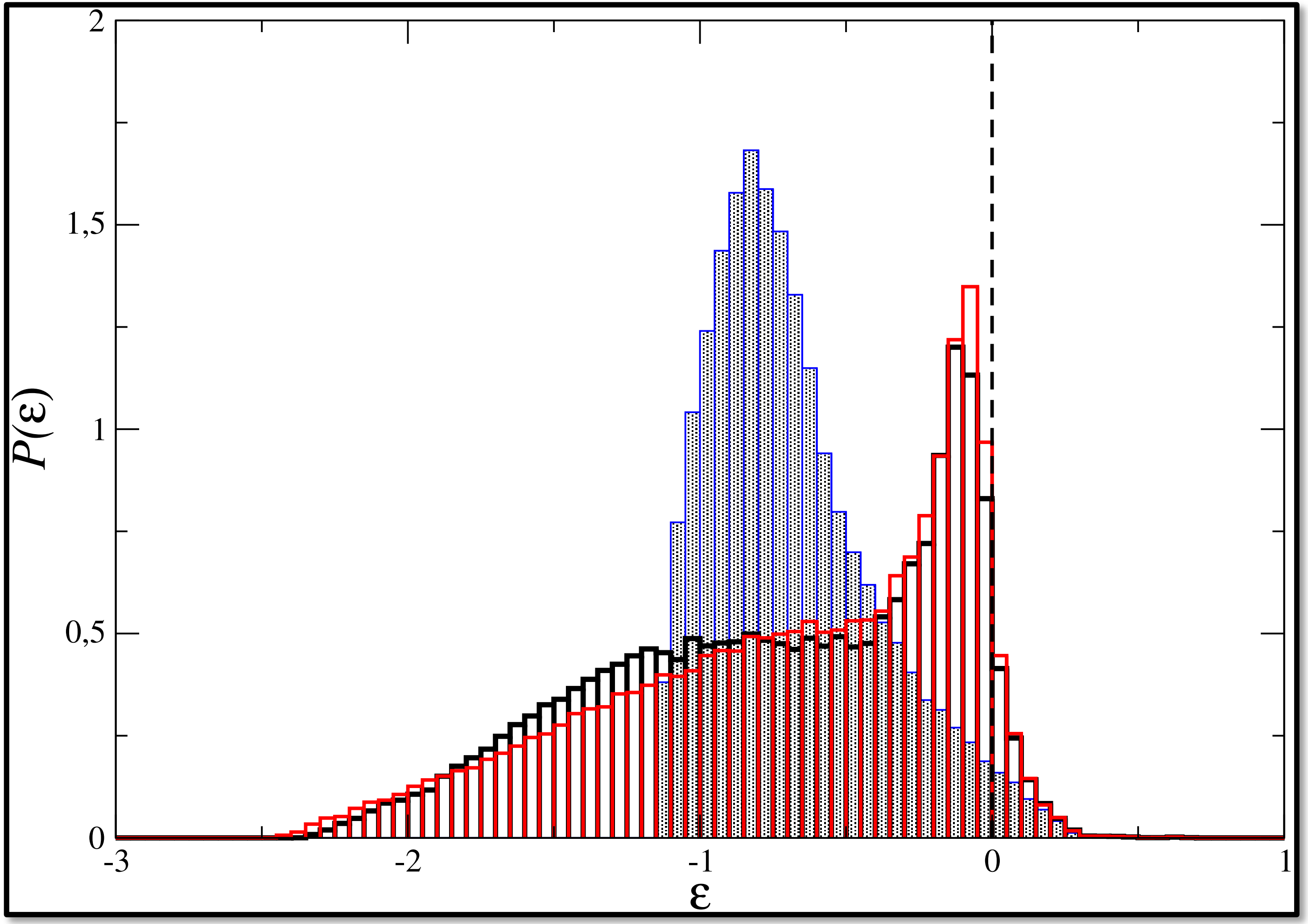

2
1,5
1
0,5
0
-3
-2
-1
0
1
$P(\varepsilon)$
ε

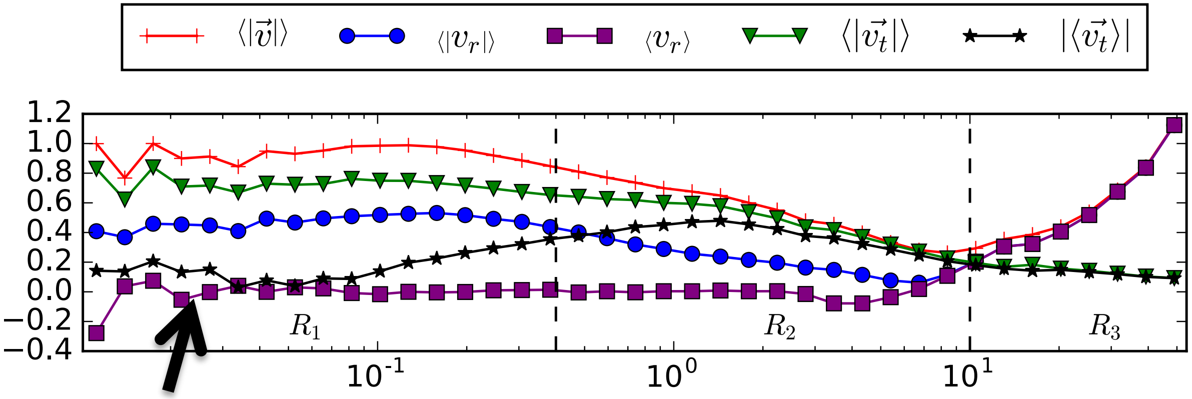

$$\left\{\begin{aligned} v_r &= \frac{\vec{r}\cdot\vec{v}}{r} \\ \vec{v}_t &= \frac{\vec{r}\times\vec{v}}{r} \end{aligned}\right.$$

$$\langle|\vec{v}_t|\rangle \gg |\langle\vec{v}_t\rangle|$$

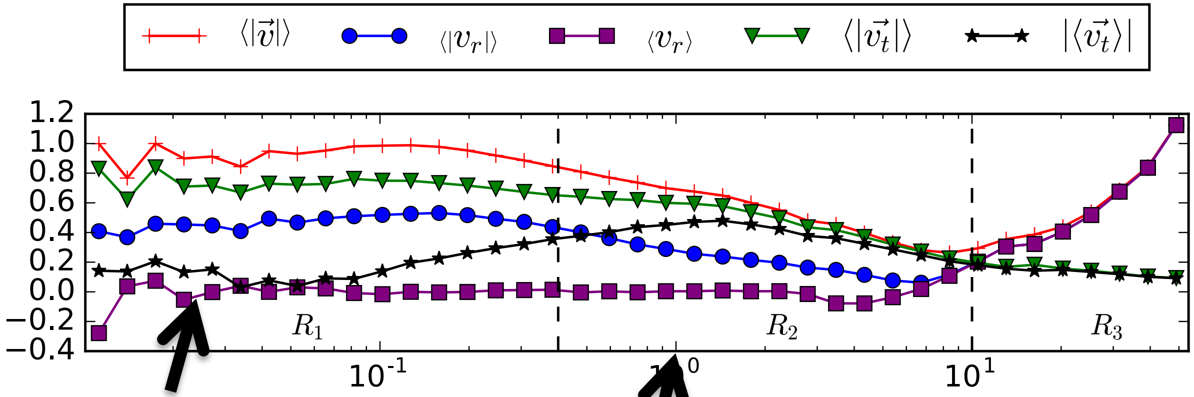

$$\left\{\begin{aligned} v_r &= \frac{\vec{r}\cdot\vec{v}}{r} \\ \vec{v}_t &= \frac{\vec{r}\times\vec{v}}{r} \end{aligned}\right.$$

$$\langle|\vec{v}_t|\rangle \gg |\langle\vec{v}_t\rangle|$$

$$\langle|\vec{v}_t|\rangle \approx |\langle\vec{v}_t\rangle| \gg \langle|v_r|\rangle$$

The maximum-disk hypothesis …

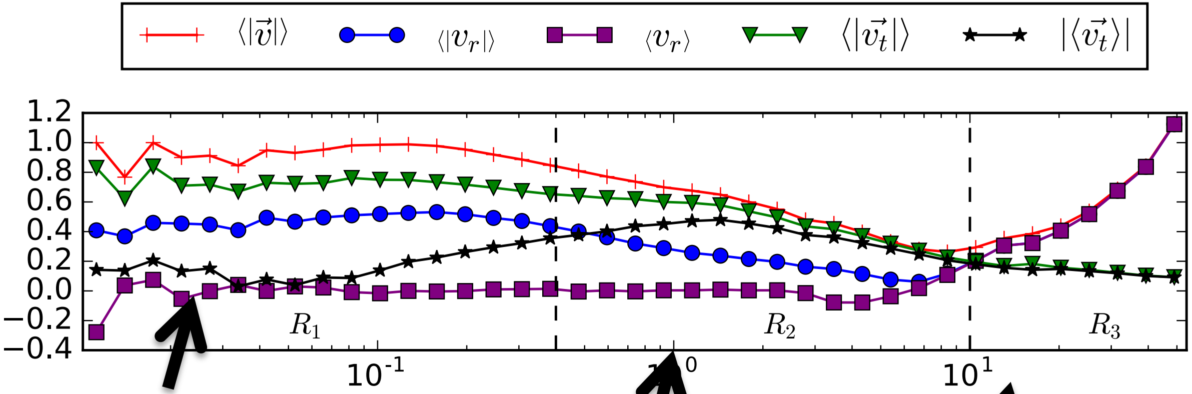

$$\left\{\begin{aligned} v_r &= \frac{\vec{r}\cdot\vec{v}}{r} \\ \vec{v}_t &= \frac{\vec{r}\times\vec{v}}{r} \end{aligned}\right.$$

$$\langle|\vec{v}_t|\rangle \gg |\langle\vec{v}_t\rangle|$$

$$\langle|\vec{v}_t|\rangle \approx |\langle\vec{v}_t\rangle| \gg \langle|v_r|\rangle$$

$$\langle|\vec{v}|\rangle \approx \langle|v_r|\rangle \approx |\langle v_r\rangle|$$

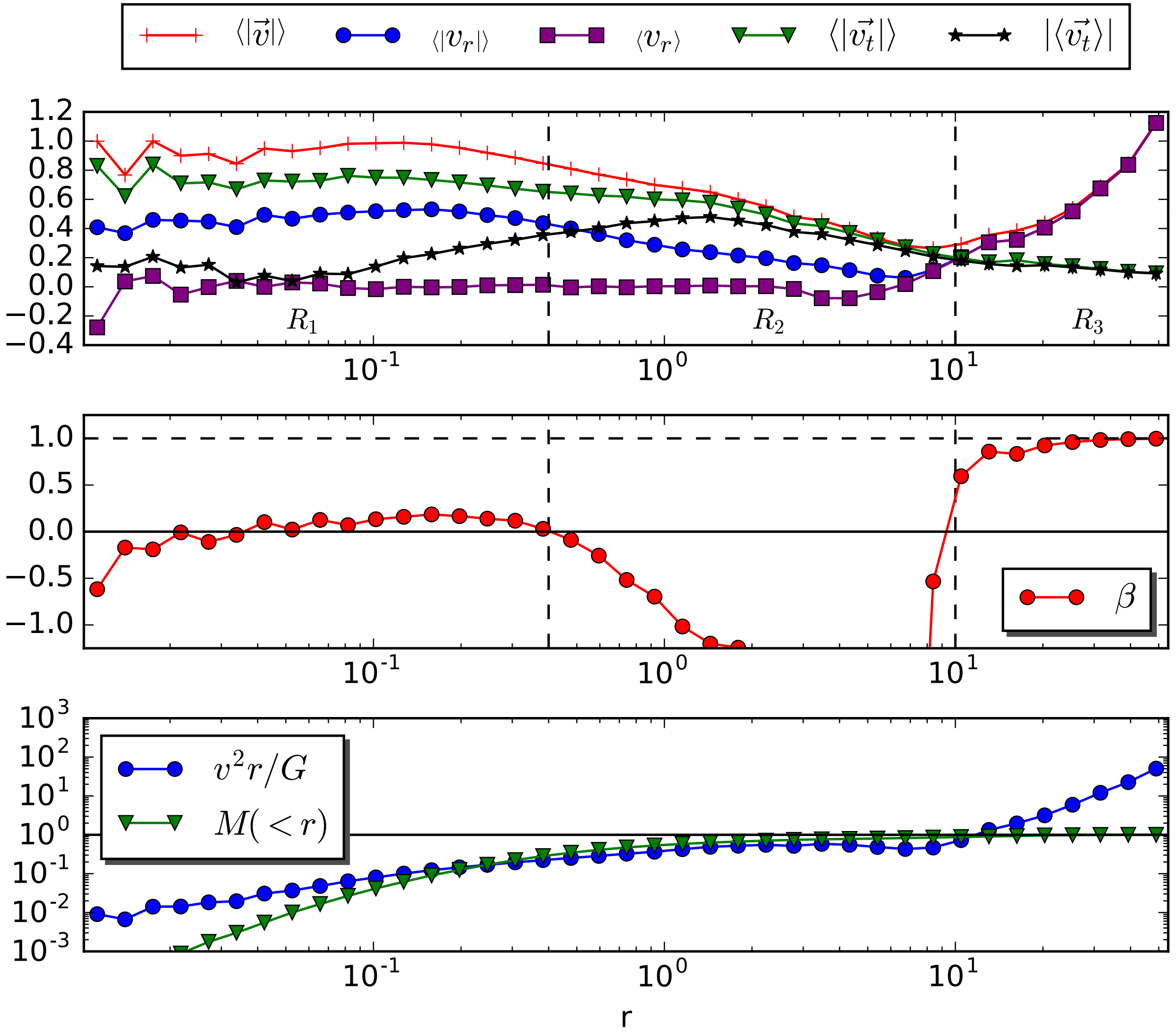

$$v_r = \frac{\vec{r} \cdot \vec{v}}{r}$$

$$\vec{v}_t = \frac{\vec{r} \times \vec{v}}{r}$$

$$\boxed{M_c = \frac{v^2 \cdot r}{G}}$$

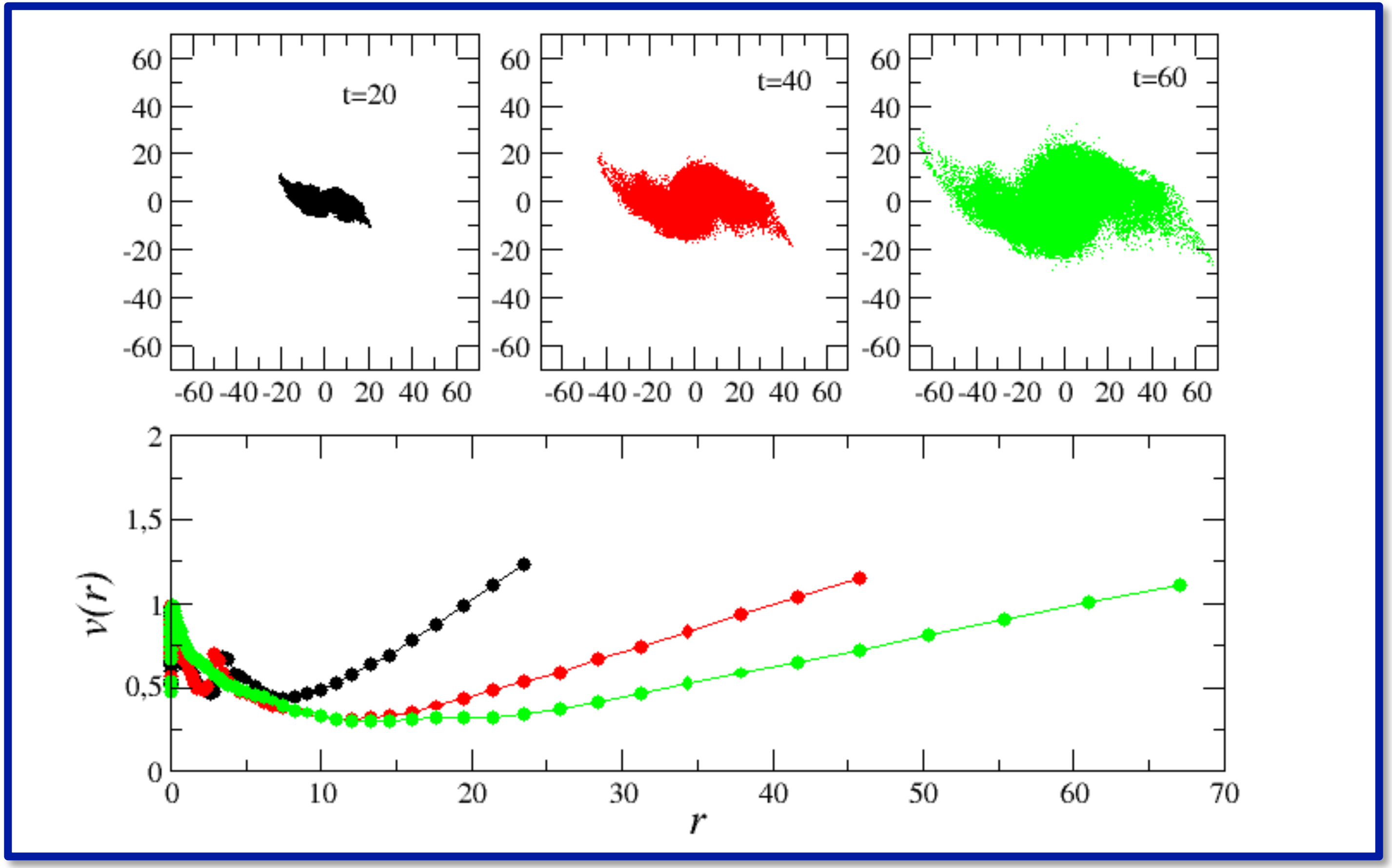

t=20
t=40
t=60
60
40
20
0
-20
-40
-60
-60 -40 -20 0 20 40 60
2
1,5
1
0,5
0
0 10 20 30 40 50 60 70
v(r)
r

$$\tau_d = \sqrt{\frac{\pi^2 a_3^3}{8GM}}$$

$$v_{200} = \frac{a_3/\tau_d}{200}\ \mathrm{km/sec}$$

$$\tau_d = \sqrt{\frac{\pi^2 a_3^3}{8GM}} \qquad\qquad v_{200} = \frac{a_3/\tau_d}{200}\ \mathrm{km/sec}$$

$$\left\{\begin{array}{l} a_3 \approx \left(\dfrac{200\, v_{200}}{n} \times t_{\mathrm{Gyr}}\right)\ \mathrm{kpc} \\ t_{\mathrm{Gyr}} \sim 1 \\ n \approx 50 \end{array}\right.$$

$$\tau_d = \sqrt{\frac{\pi^2 a_3^3}{8GM}}$$

$$v_{200} = \frac{a_3/\tau_d}{200}\ \mathrm{km/sec}$$

$$\left\{\begin{aligned} & a_3 \approx \left(\frac{200\, v_{200}}{n} \times t_{\mathrm{Gyr}}\right)\ \mathrm{kpc} \\ & t_{\mathrm{Gyr}} \sim 1 \\ & n \approx 50 \end{aligned}\right.$$

$$\boxed{\begin{aligned} & M = \frac{\pi^2 a_3^3}{8G\tau_d} \approx 10^{11} M_\odot \\ & R_2 \approx 50\ \ \mathrm{kpc} \\ & R_1 \approx 2\ \ \mathrm{kpc} \end{aligned}}$$

Comparison with observations of external Galaxies

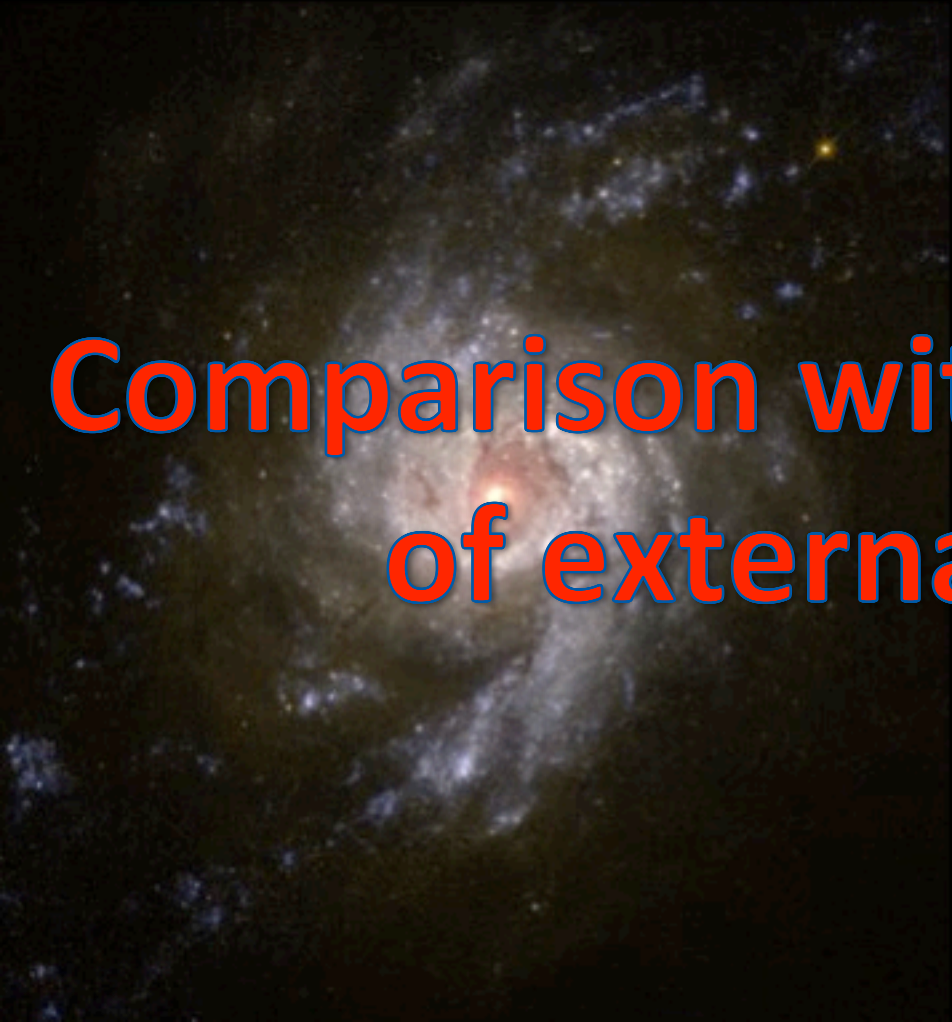

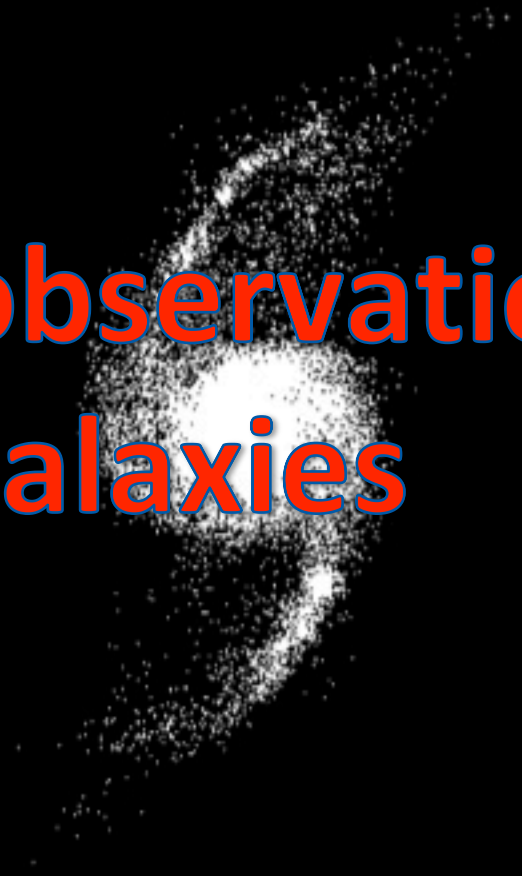

Erroz-Ferrier et al., MNRAS 451, 1004–1024 (2015)

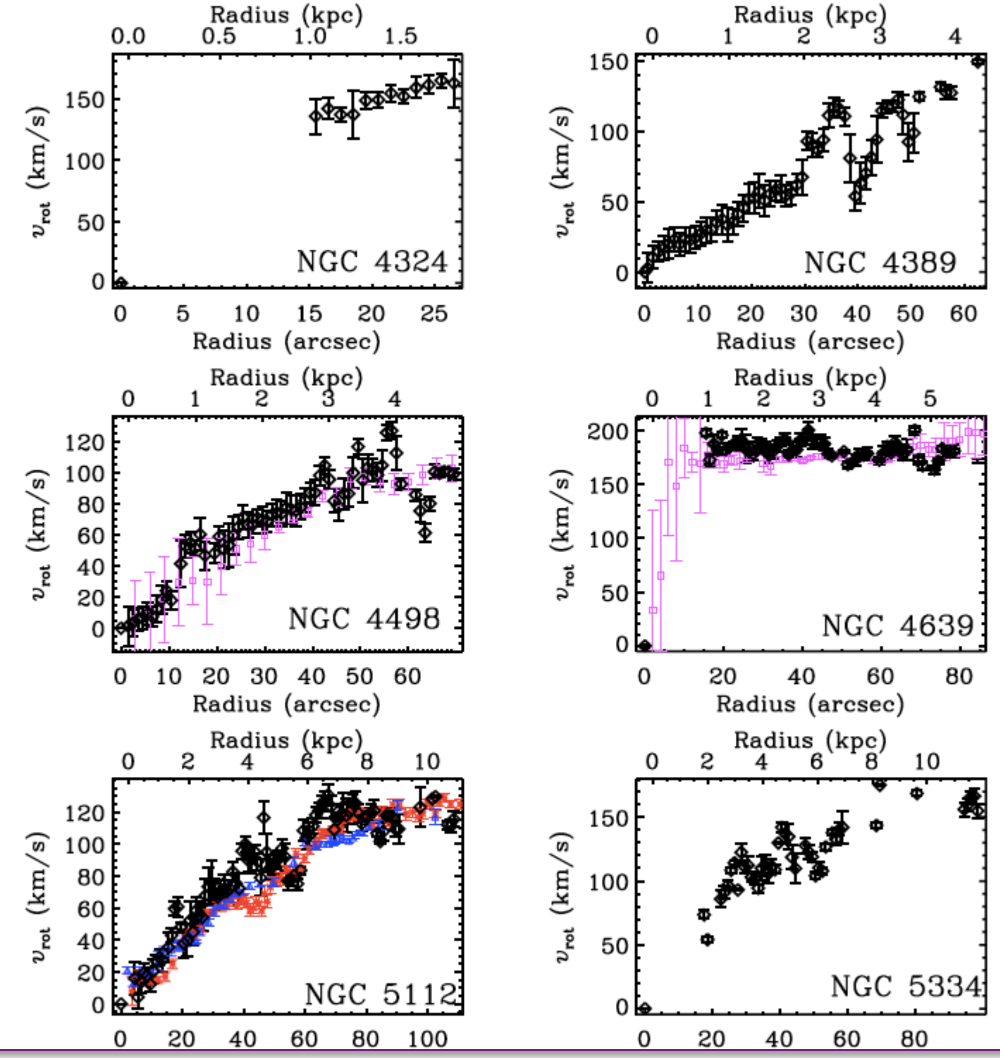

Erroz-Ferrier et al., MNRAS 451, 1004–1024 (2015)

NGC 2748

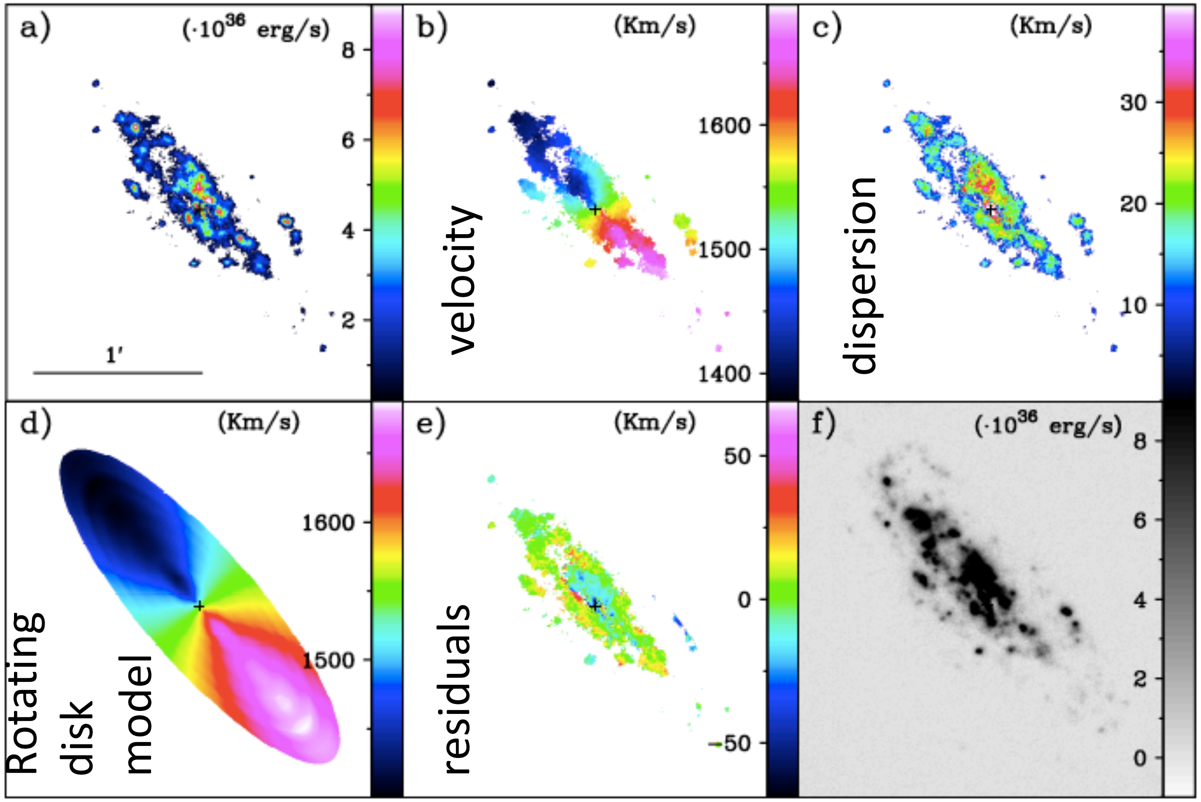

Figure A5. Same as Fig. A1 but for NGC 2712 (top) and NGC 2748 (bottom).

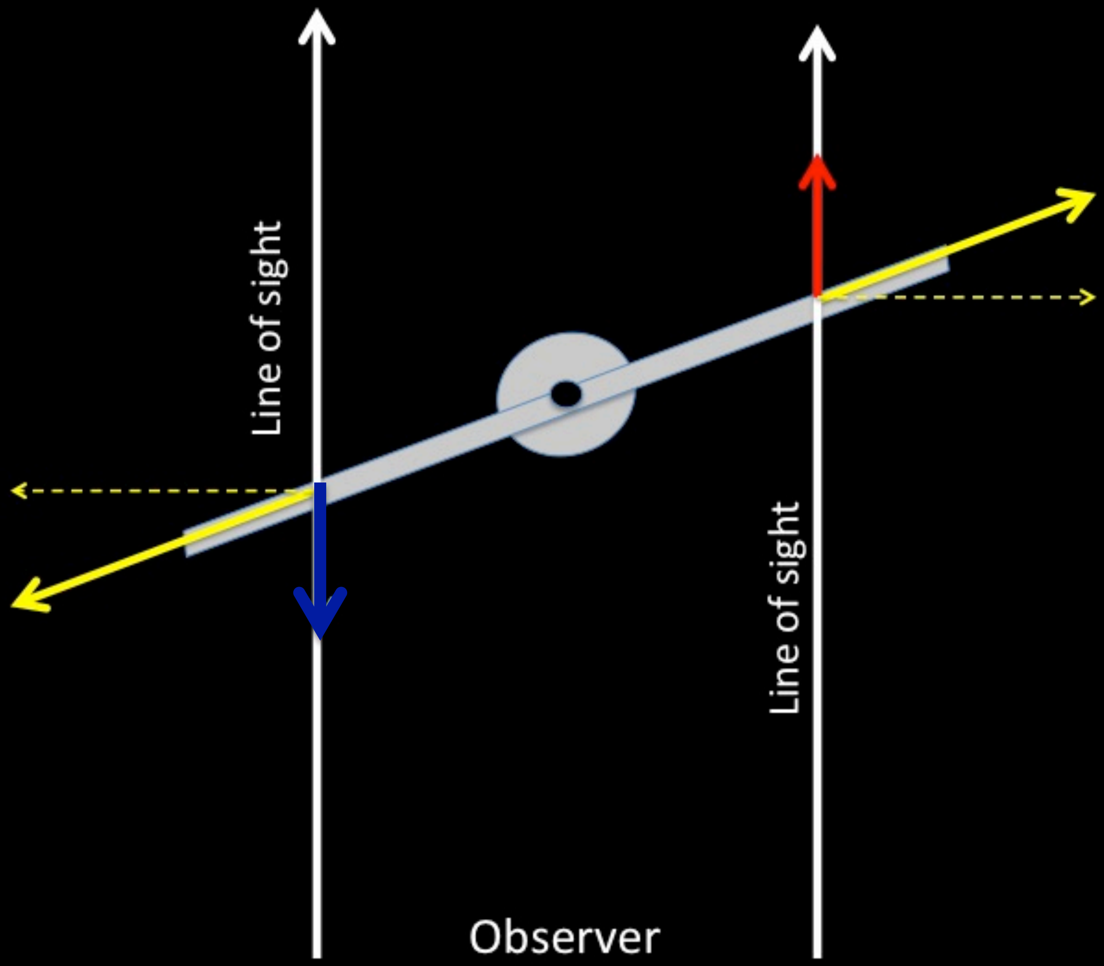

Line of sight
Line of sight
Observer

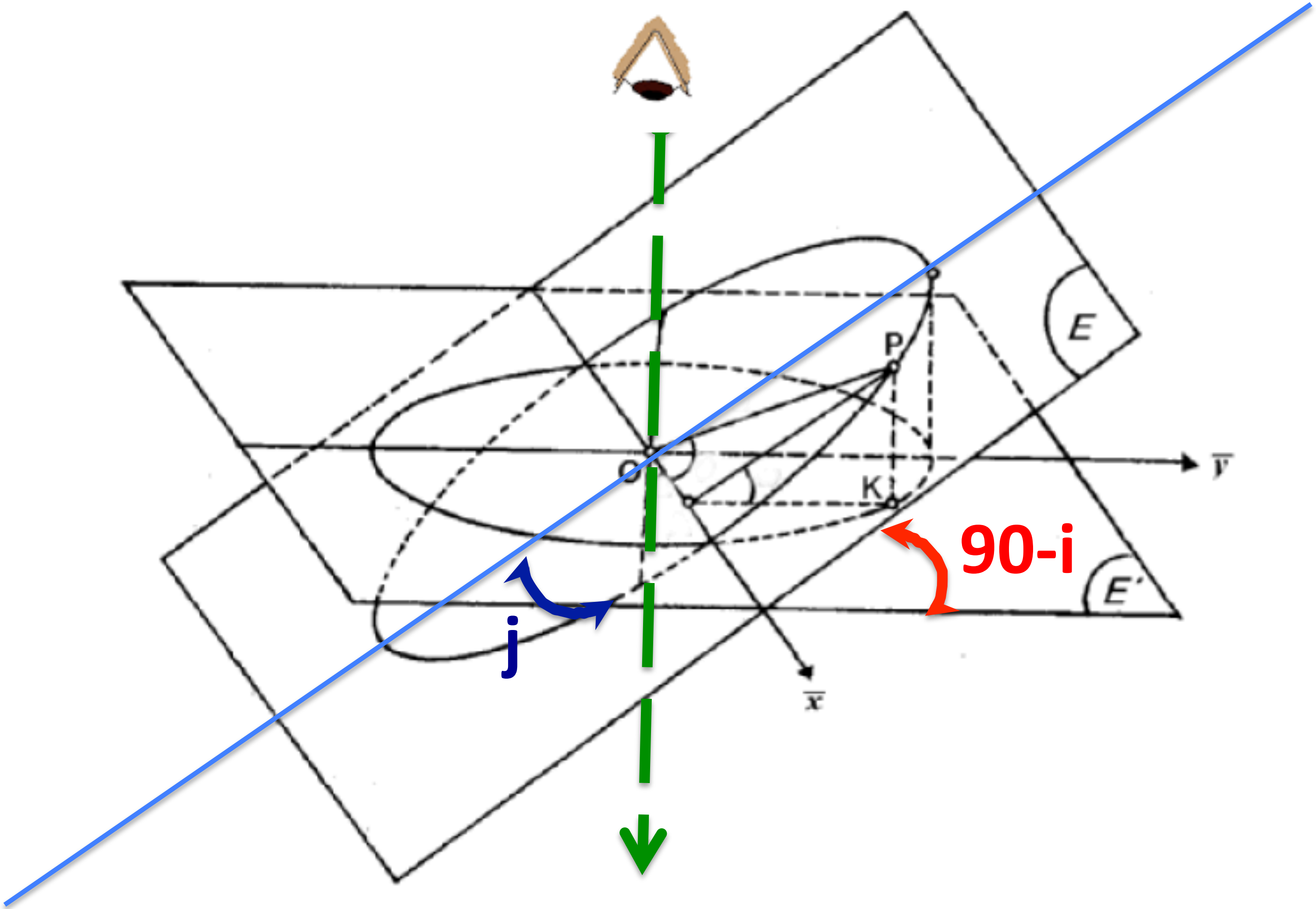

E
P
O
K
$\bar{y}$
$\bar{x}$
90-i
E'
j

Rotating disk

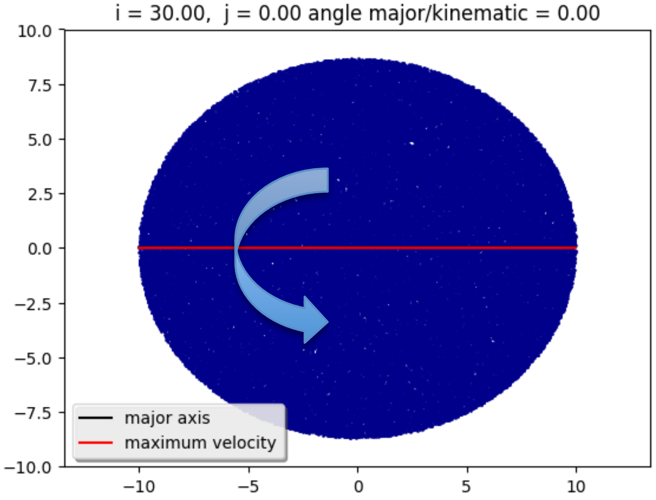

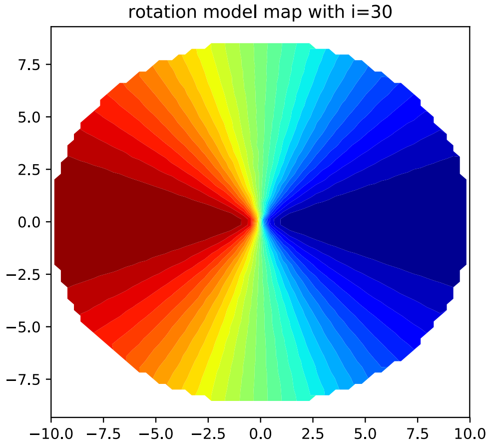

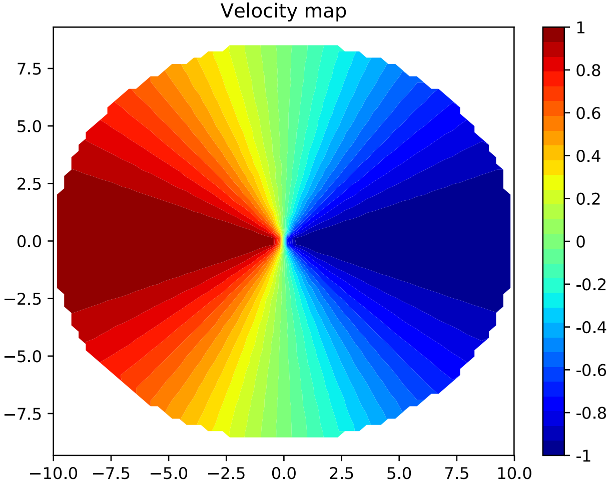

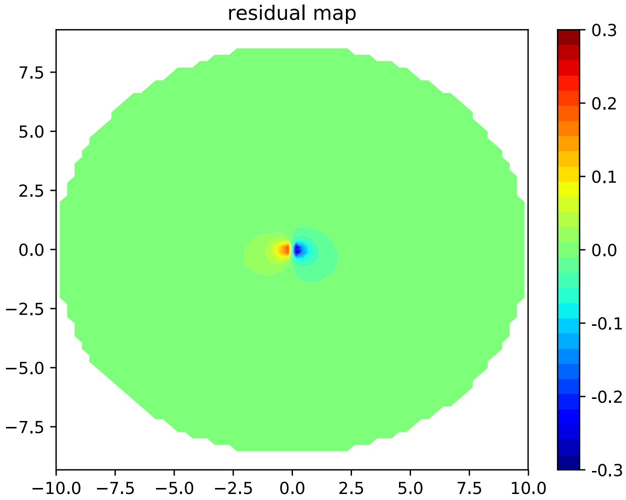

Rotating Disk

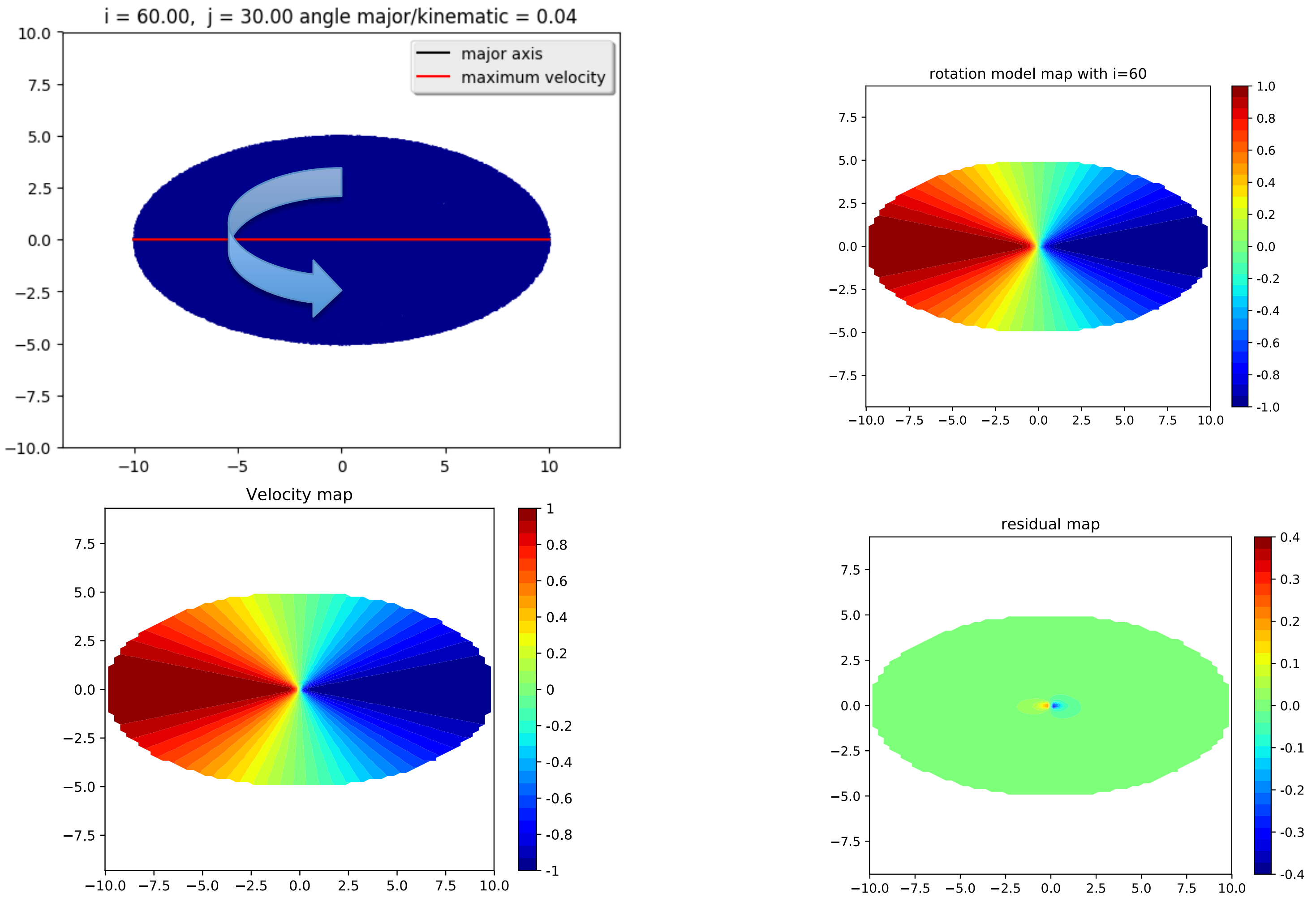

Radially expanding disk

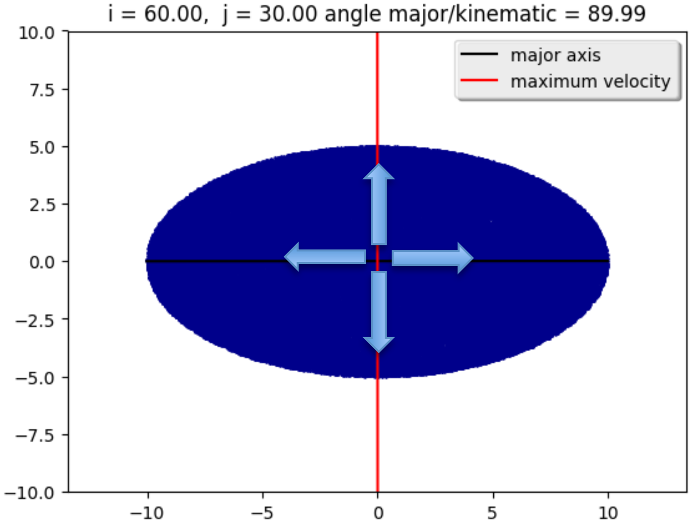

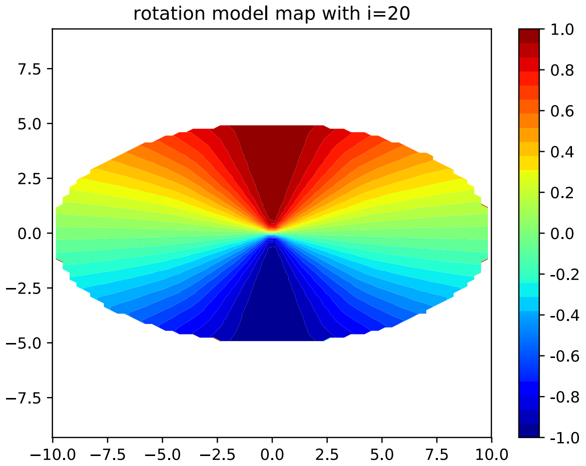

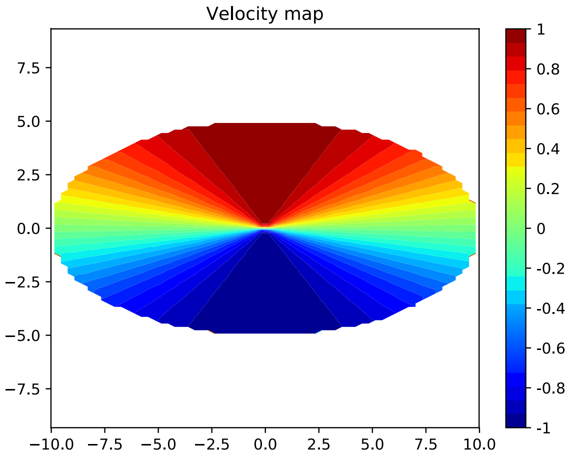

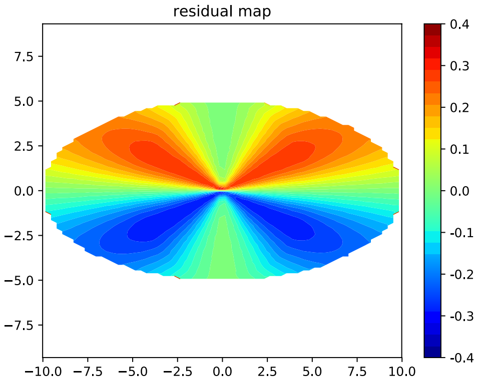

Rotating ellipse

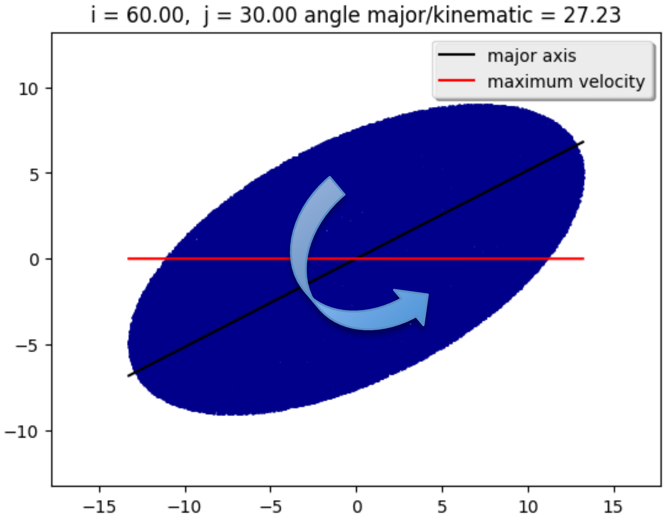

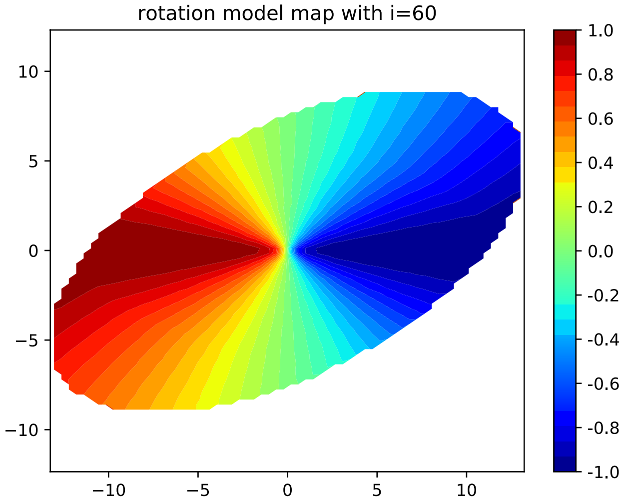

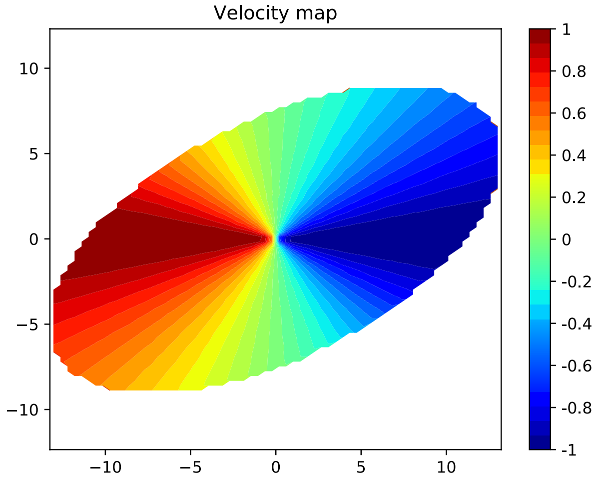

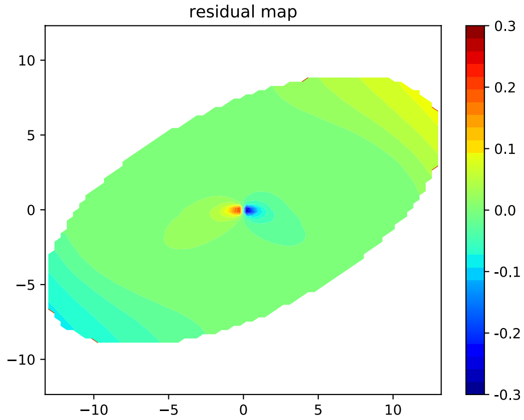

Radially expanding ellipse

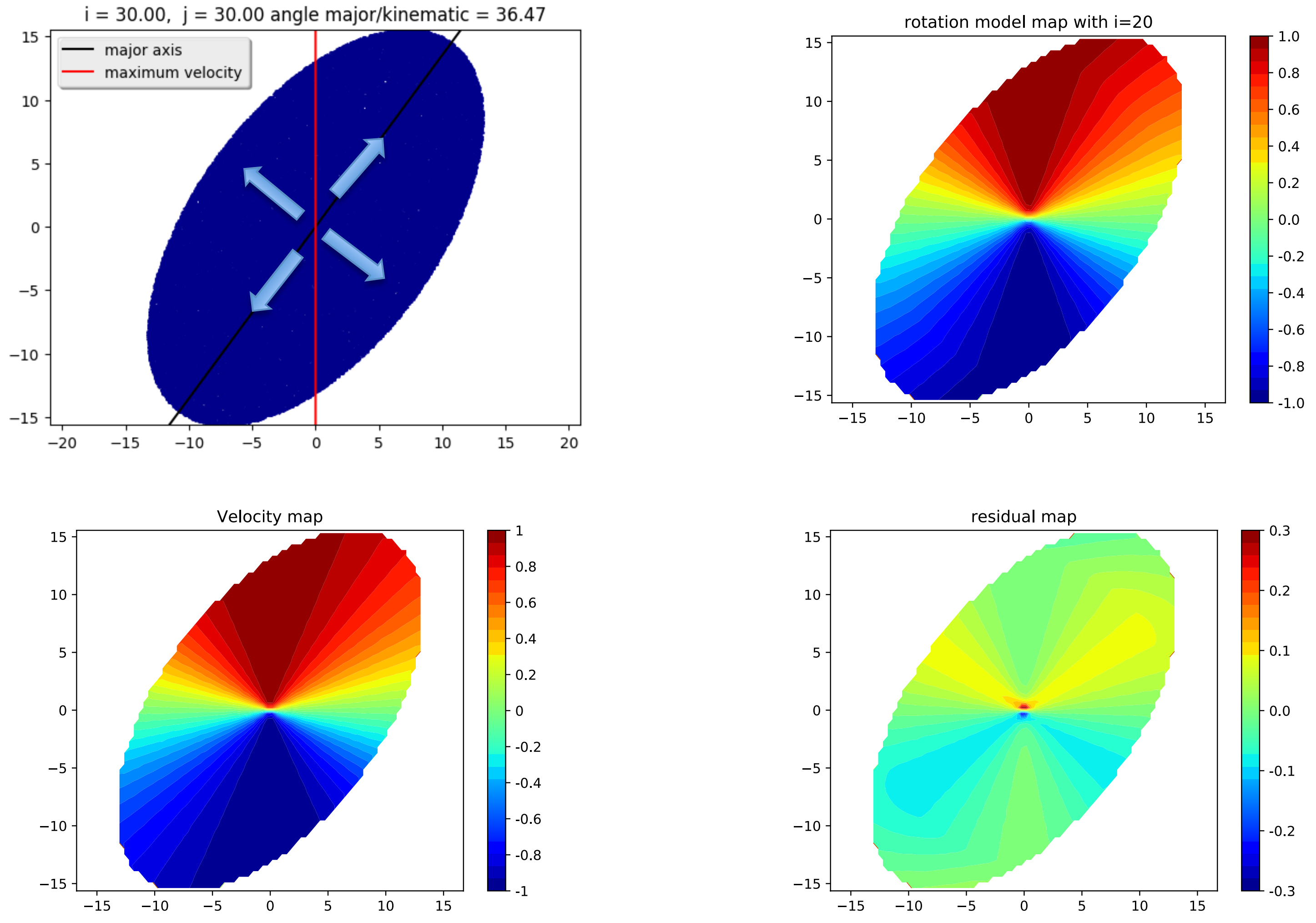

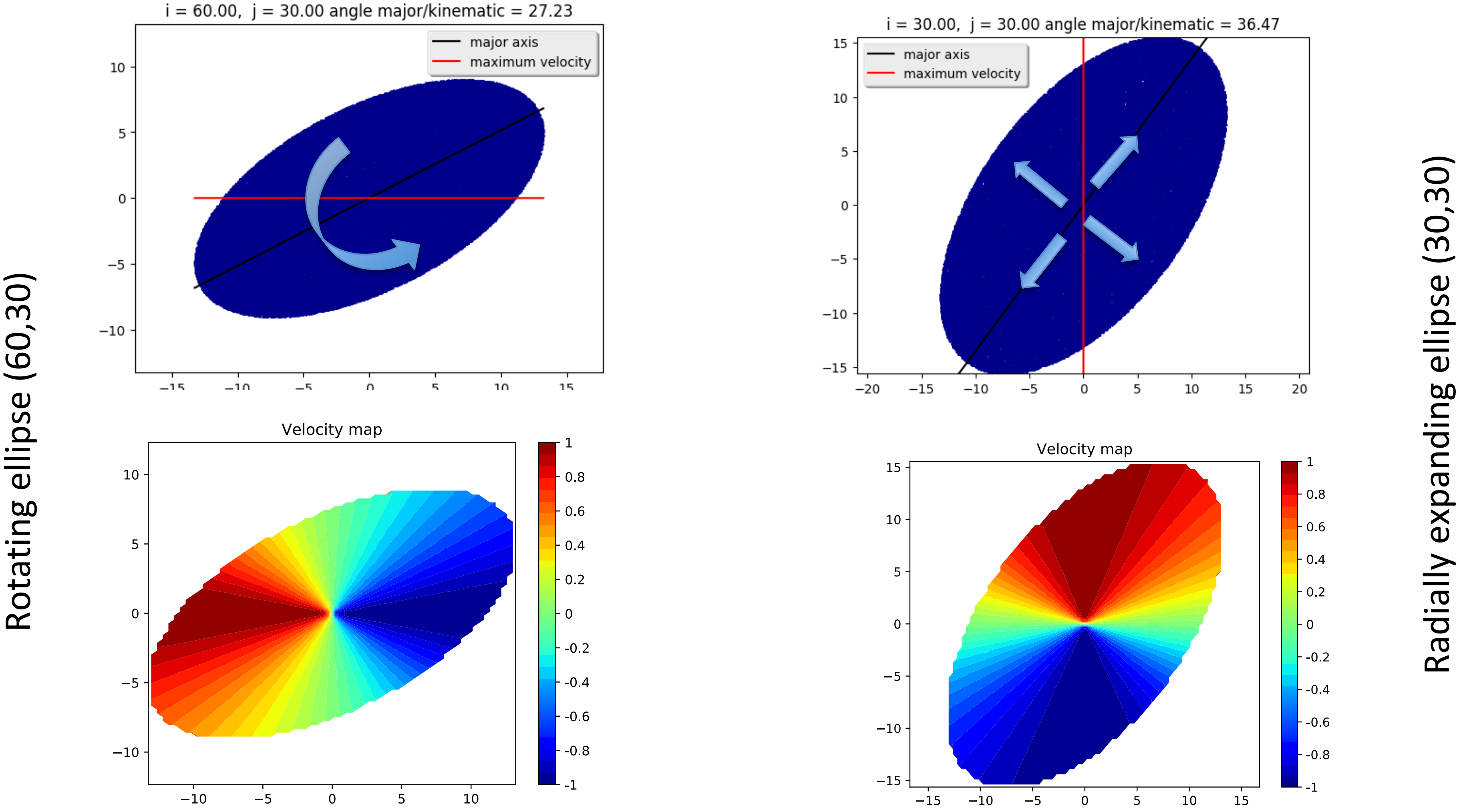
i = 60.00, j = 30.00 angle major/kinematic = 27.23
major axis
maximum velocity
Velocity map
Rotating ellipse (60,30)
i = 30.00, j = 30.00 angle major/kinematic = 36.47
major axis
maximum velocity
Velocity map
Radially expanding ellipse (30,30)

Rotating ellipse (60,30)

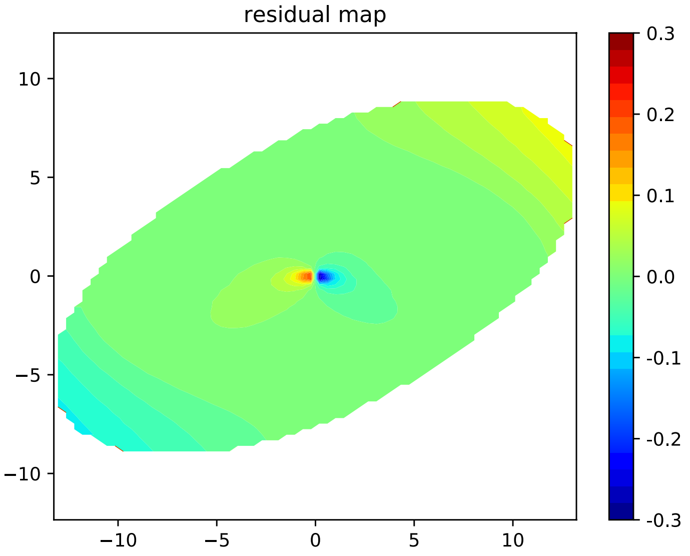

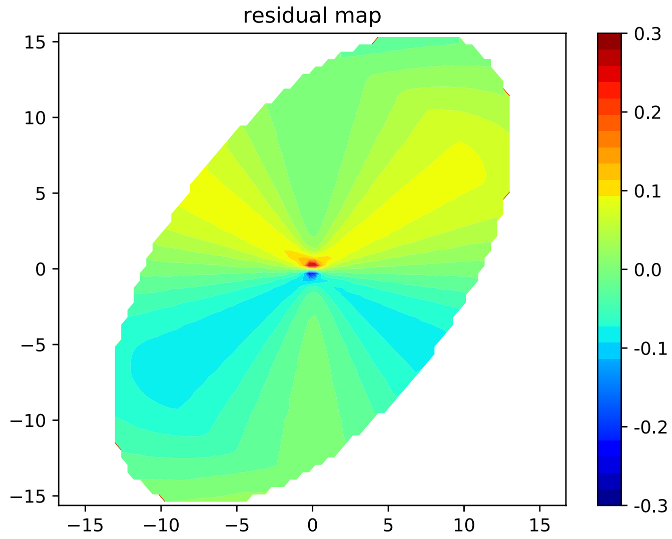

Radially expanding ellipse (30,30)

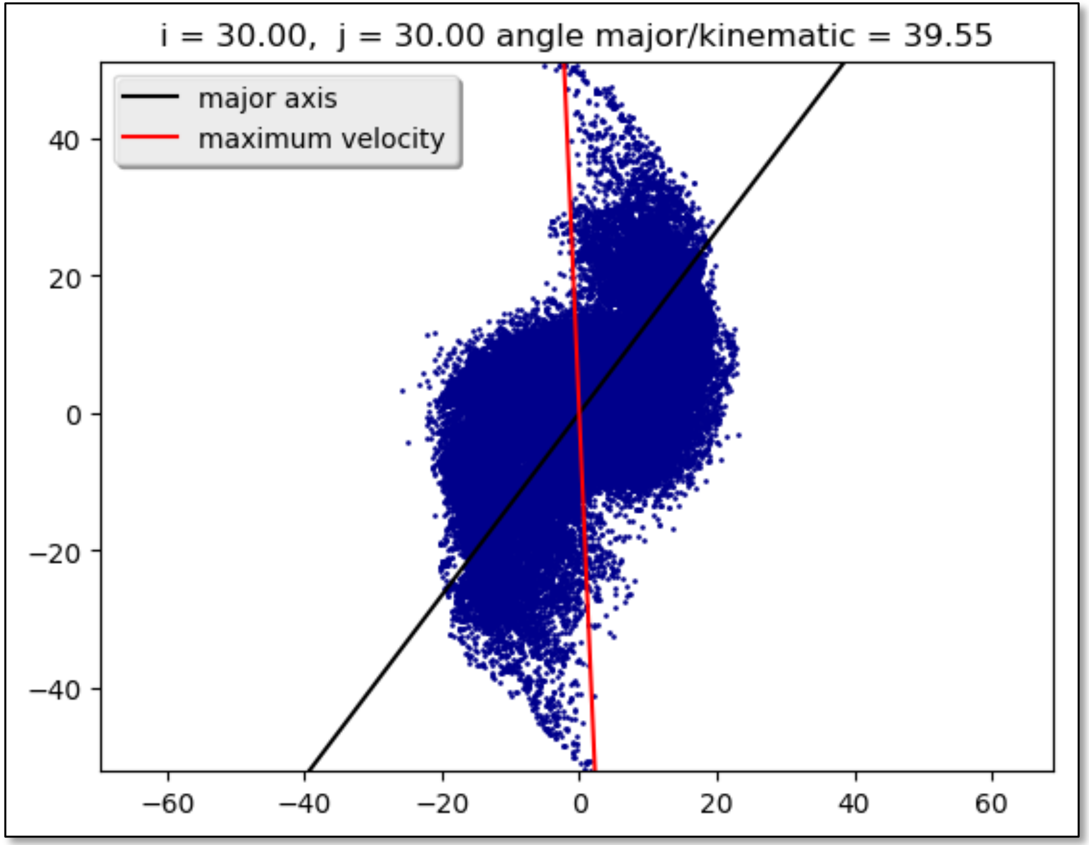
i = 30.00, j = 30.00 angle major/kinematic = 39.55
major axis
maximum velocity
40
20
0
−20
−40
−60
−40
−20
0
20
40
60

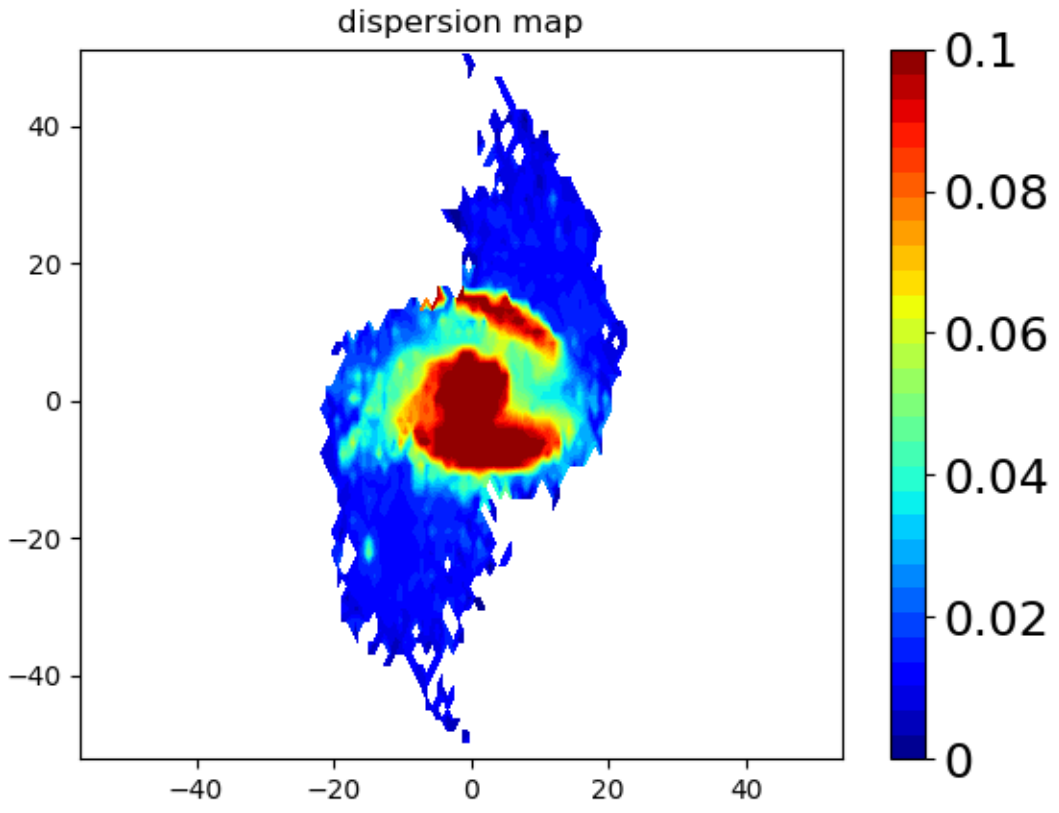
dispersion map
40
20
0
−20
−40
−40
−20
0
20
40
0.1
0.08
0.06
0.04
0.02
0

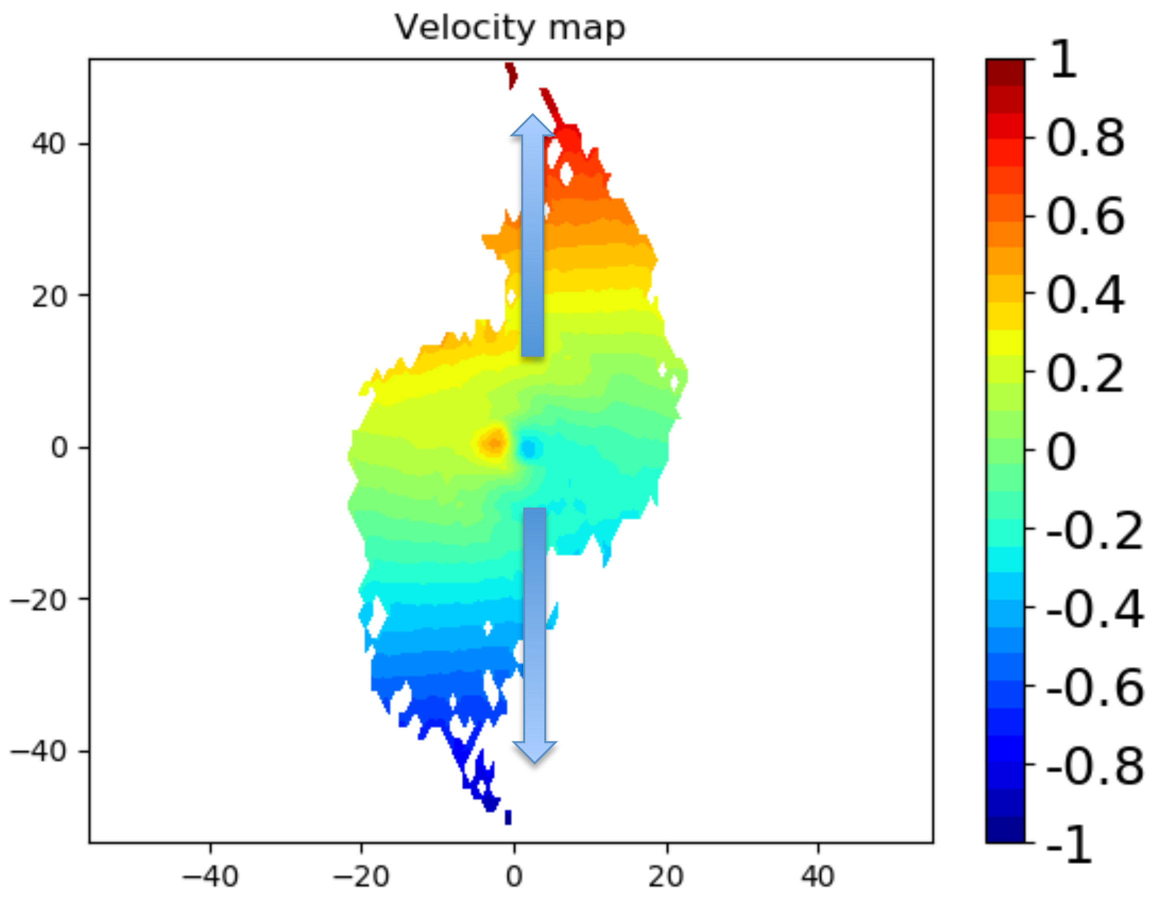
Velocity map
40
20
0
−20
−40
−40
−20
0
20
40
1
0.8
0.6
0.4
0.2
0
-0.2
-0.4
-0.6
-0.8
-1

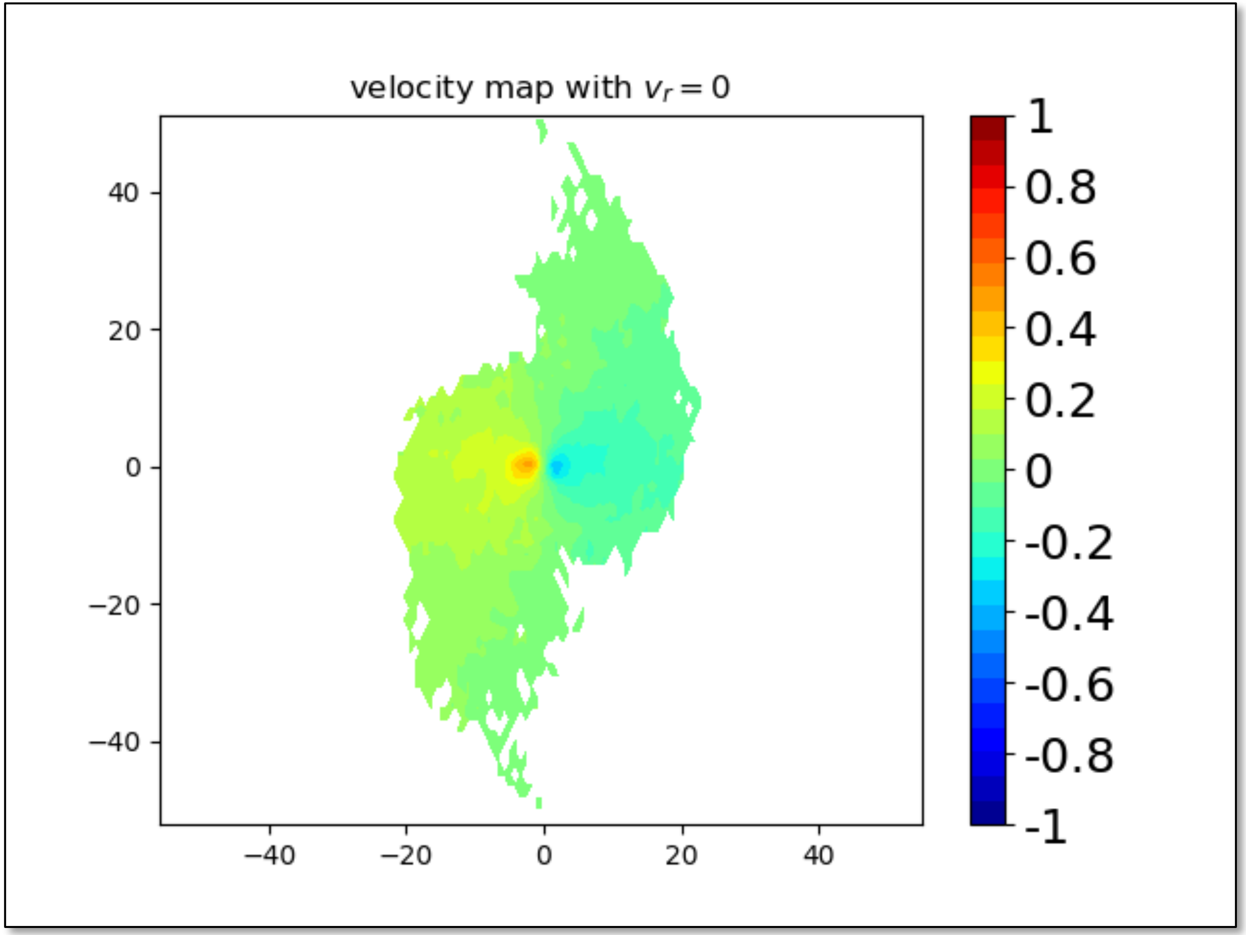

velocity map with $v_r = 0$
40
20
0
−20
−40
−40
−20
0
20
40
1
0.8
0.6
0.4
0.2
0
-0.2
-0.4
-0.6
-0.8
-1

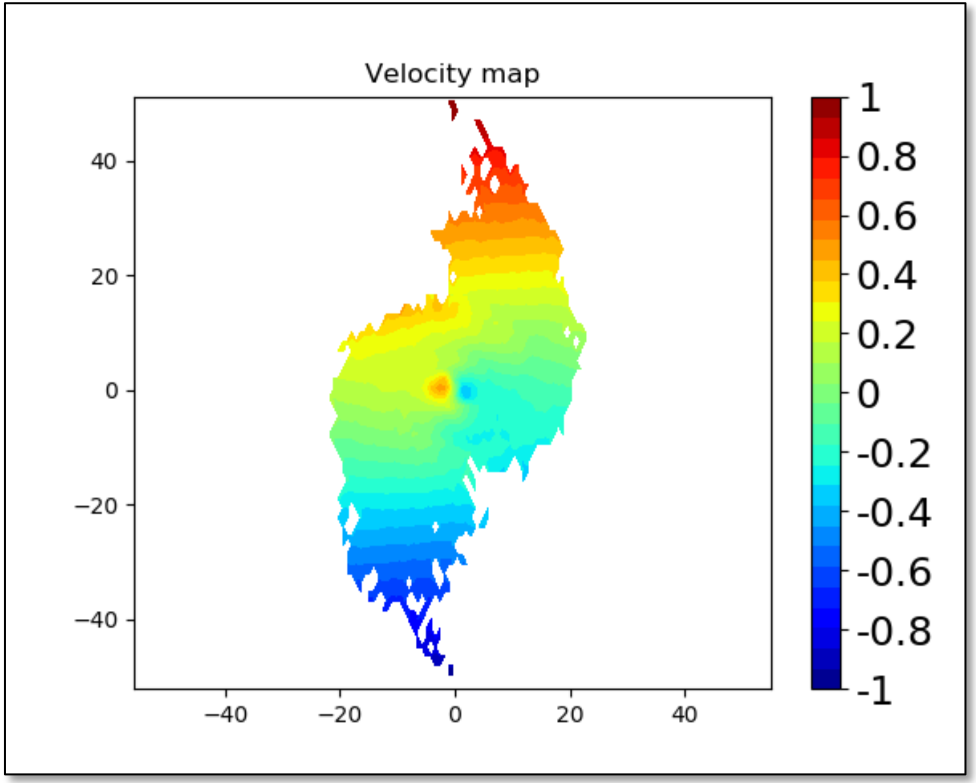
Velocity map
40
20
0
−20
−40
−40
−20
0
20
40
1
0.8
0.6
0.4
0.2
0
-0.2
-0.4
-0.6
-0.8
-1

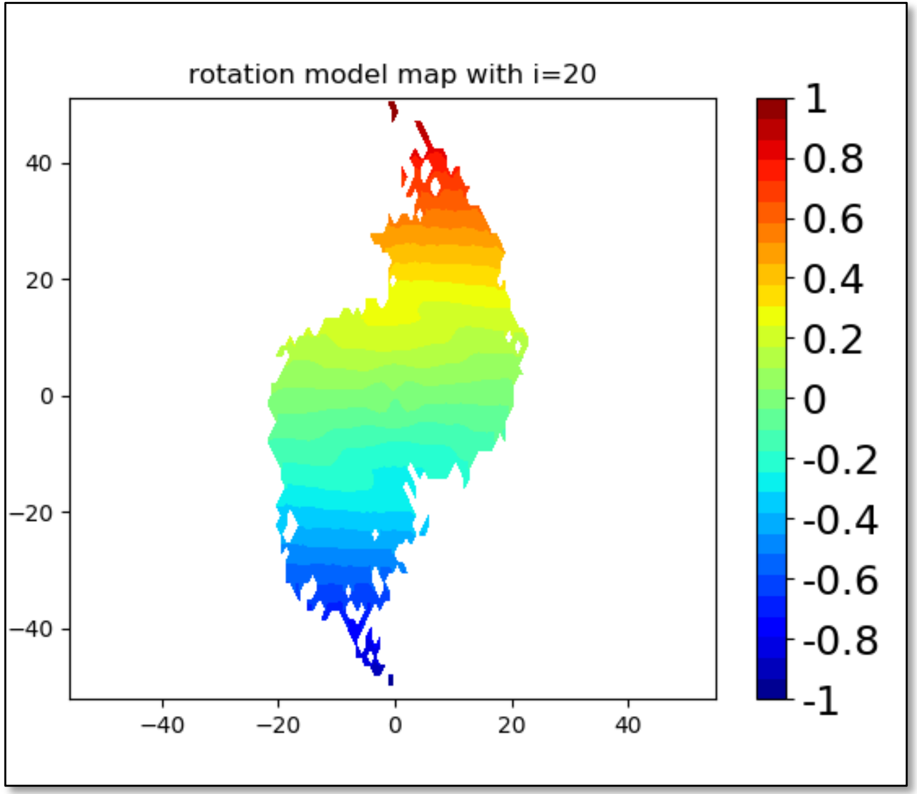
rotation model map with i=20
40
20
0
−20
−40
−40
−20
0
20
40
1
0.8
0.6
0.4
0.2
0
-0.2
-0.4
-0.6
-0.8
-1

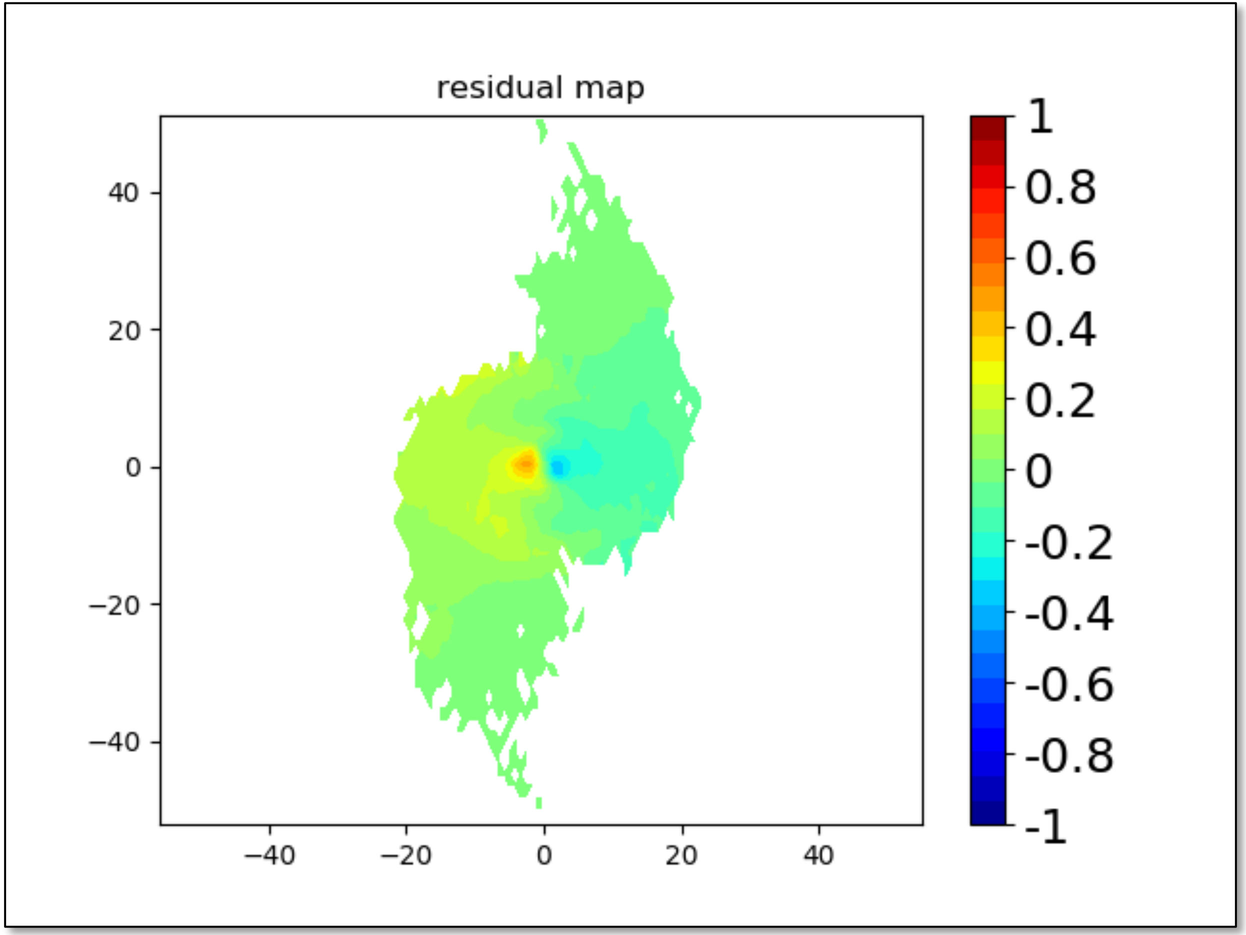
residual map
40
20
0
−20
−40
−40
−20
0
20
40
1
0.8
0.6
0.4
0.2
0
-0.2
-0.4
-0.6
-0.8
-1

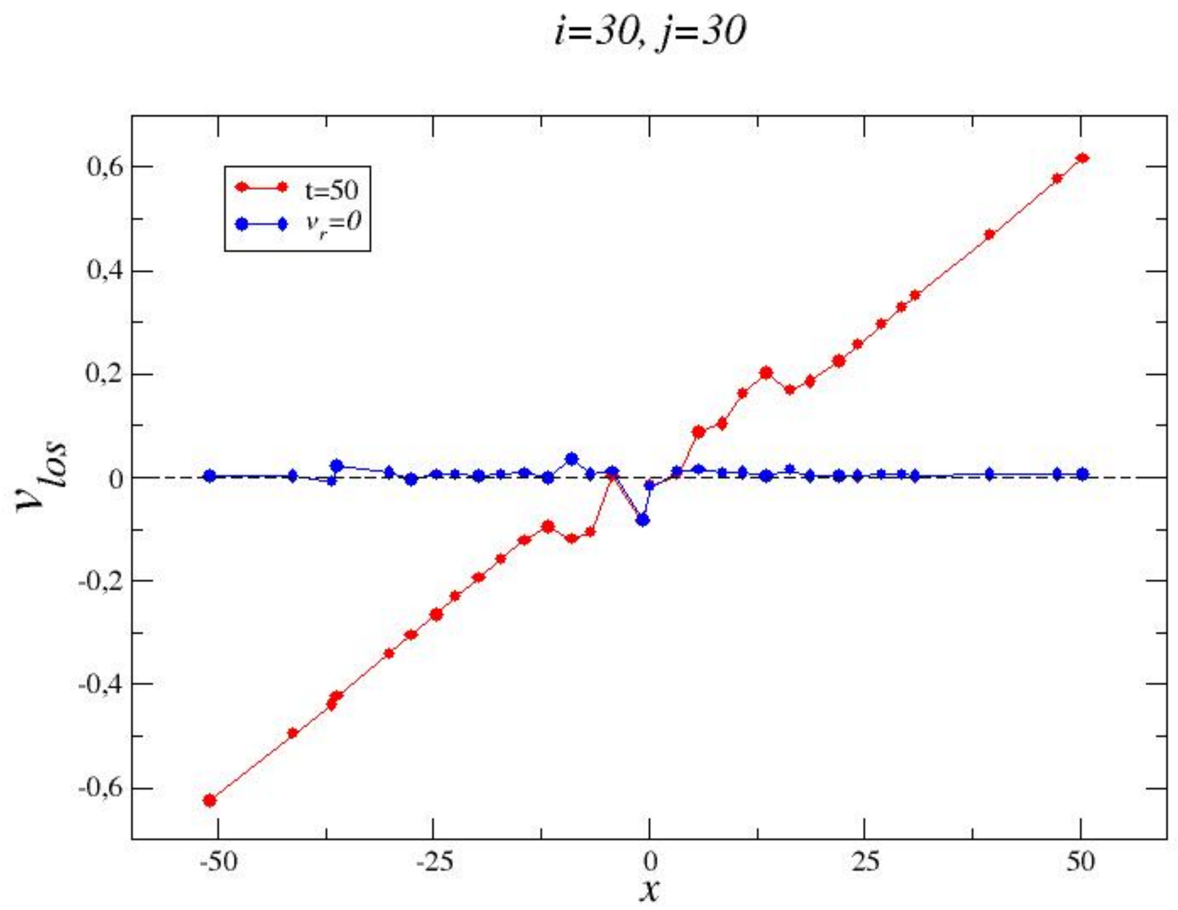

i=30, j=30
t=50
v_r=0
0,6
0,4
0,2
0
-0,2
-0,4
-0,6
v_{los}
-50
-25
0
25
50
x

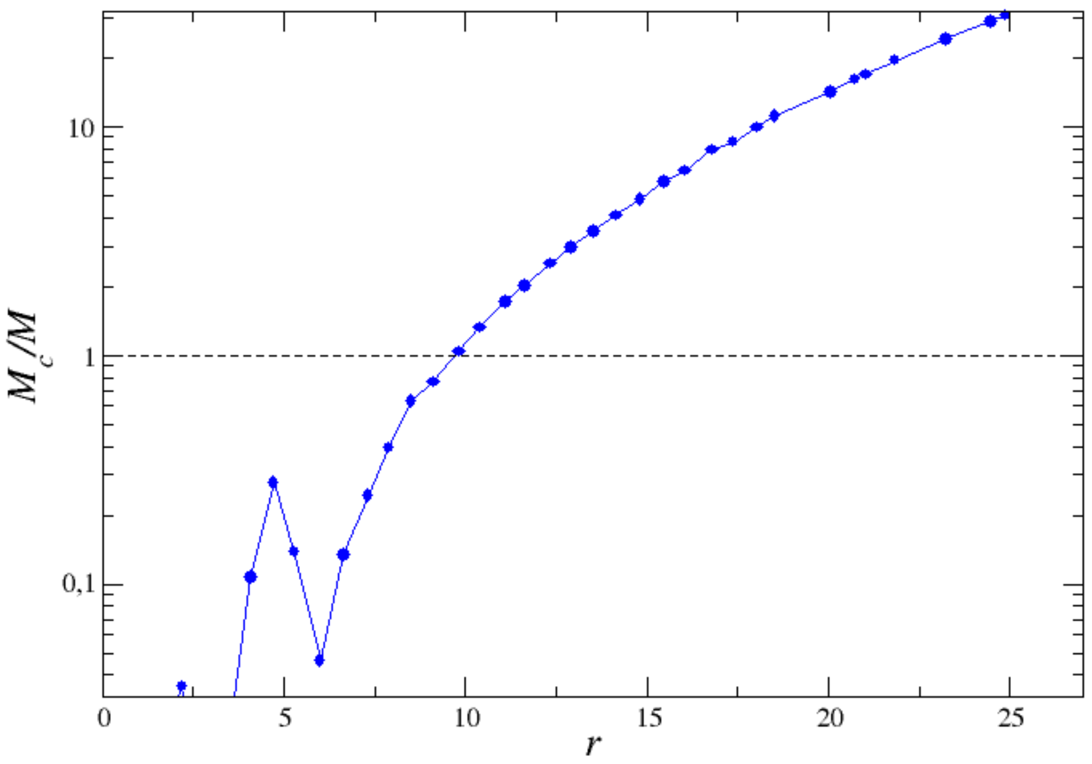

10
1
0,1
0
5
10
15
20
25
r
M_c /M

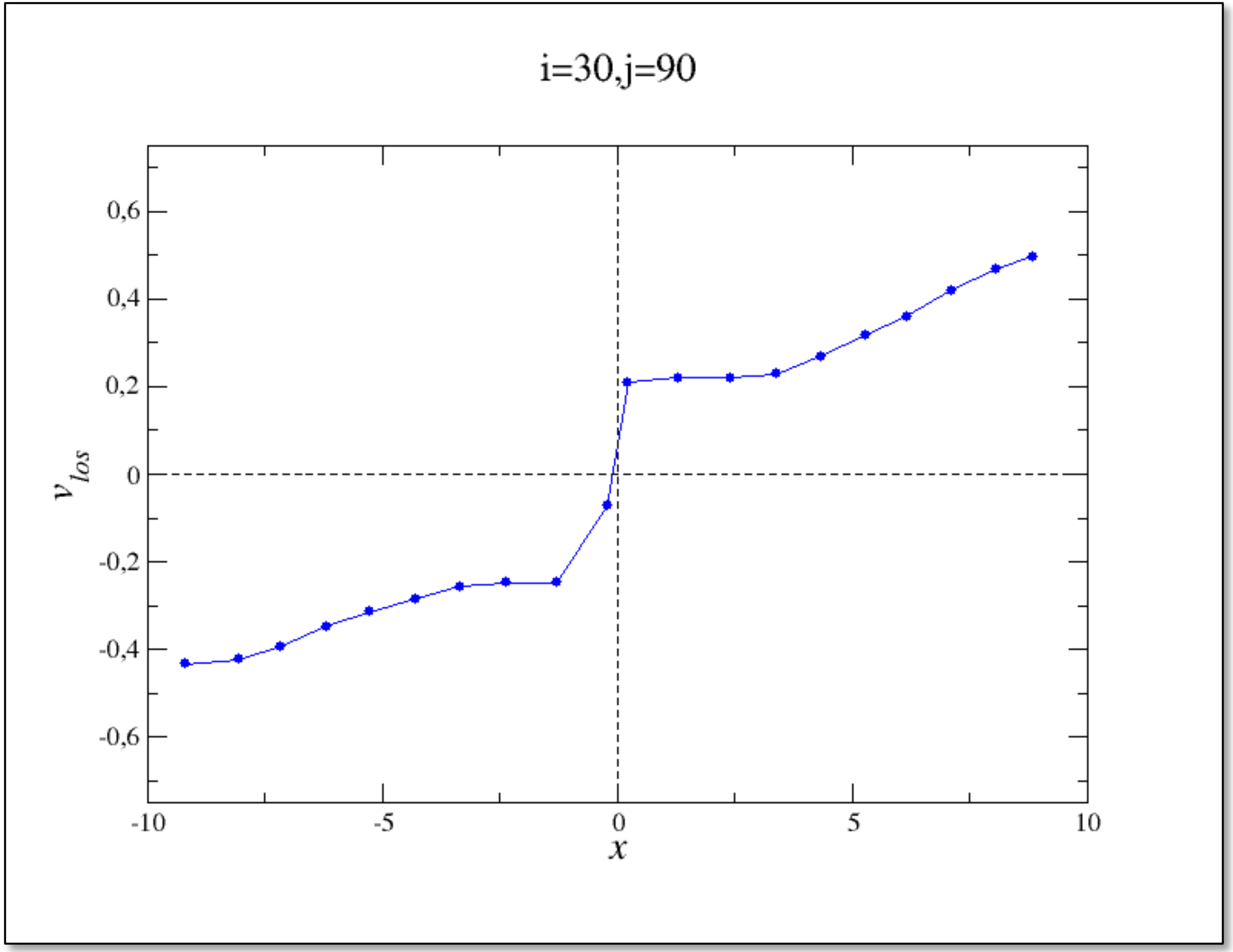

(no core-cusp problem …)

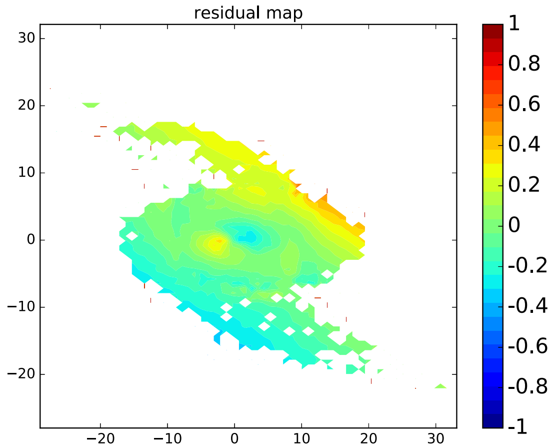
residual map
30
20
10
0
−10
−20
−20
−10
0
10
20
30
1
0.8
0.6
0.4
0.2
0
-0.2
-0.4
-0.6
-0.8
-1

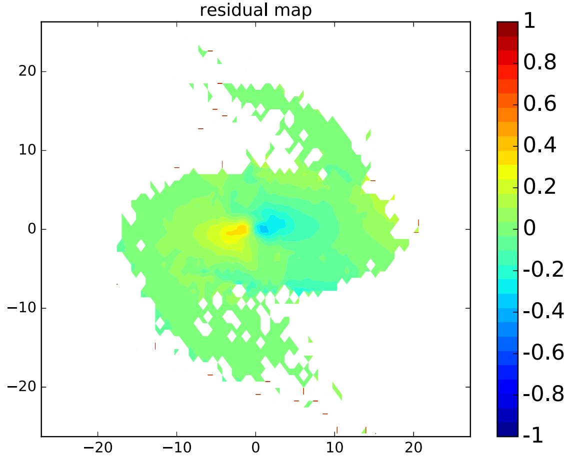
residual map
20
10
0
−10
−20
−20
−10
0
10
20
1
0.8
0.6
0.4
0.2
0
-0.2
-0.4
-0.6
-0.8
-1

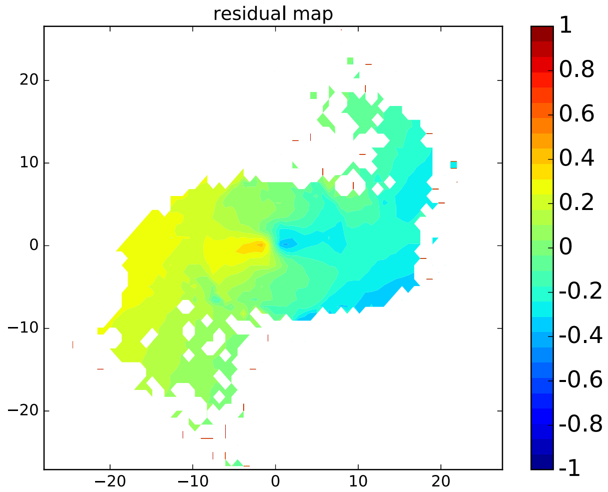
residual map
20
10
0
−10
−20
−20
−10
0
10
20
1
0.8
0.6
0.4
0.2
0
-0.2
-0.4
-0.6
-0.8
-1

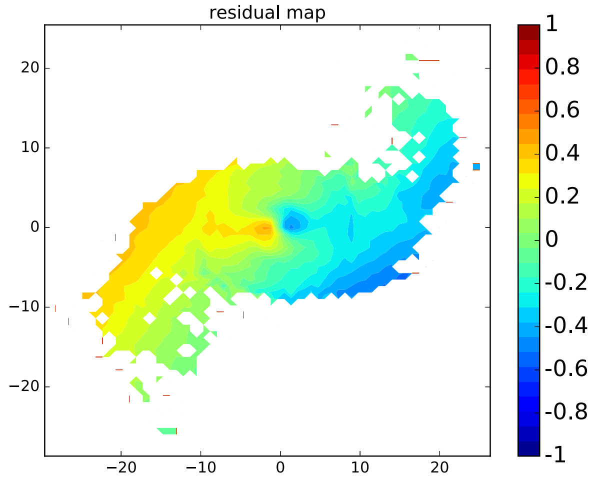
residual map
20
10
0
−10
−20
−20
−10
0
10
20
1
0.8
0.6
0.4
0.2
0
-0.2
-0.4
-0.6
-0.8
-1

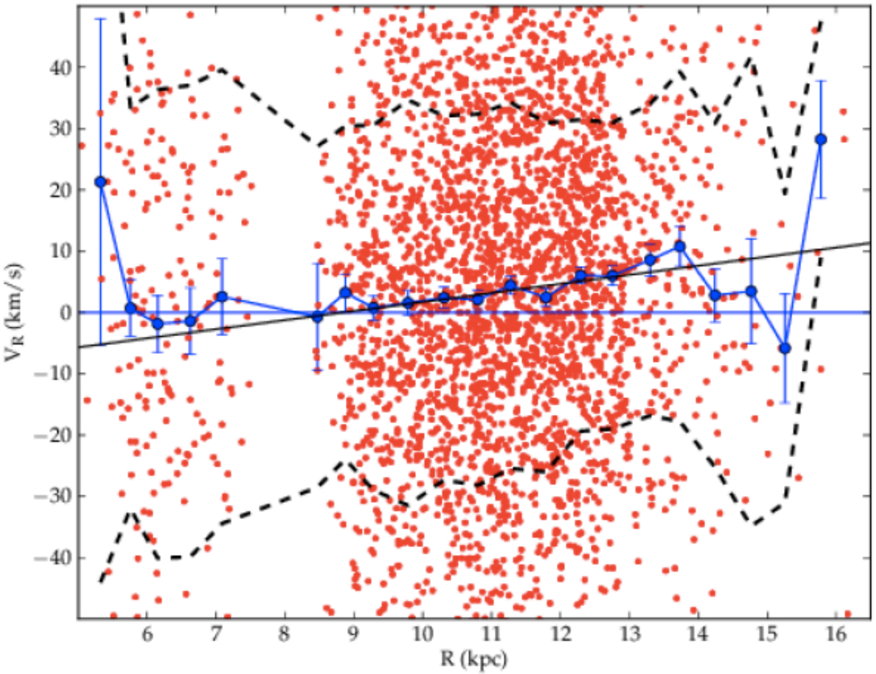

Figure 2. Radial galactocentric velocity derived from Eq. (4) with radial heliocentric velocities from APOGEE for RCG sources within a region close to the Galactic center-Sun line. The blue line and its error bars represent the average within bins of $\Delta R = 0.5$ kpc. The region between both dashed lines is the zone within one rms of dispersion of the points.

GAIA

determines the position, parallax, and annual proper motion of 1 billion stars with an accuracy of about 20 microarcseconds at 15 mag, and 200 μas at 20 mag.

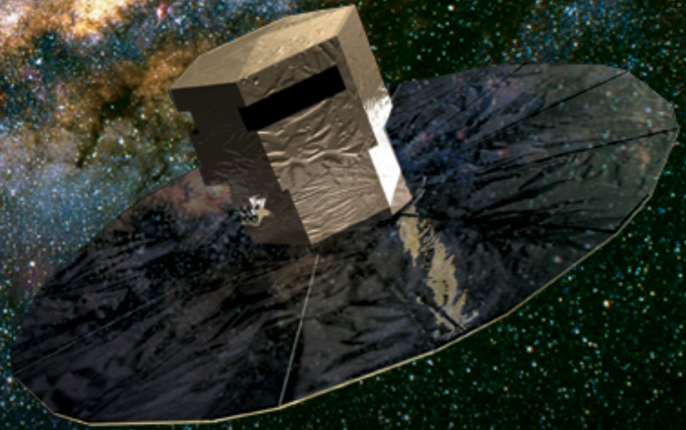

Thanks to . . ..

David Benhaiem

PostDoc at the Institute for Complex Systems of the Italian National Research Council in Rome (Italy)

Michael Joyce

Professor of Physics at the Université Pierre et Marie Curie – Paris VI (France)

Tirawut Worrakitpoonpon

Staff member at the Rajamangala University of Technology Suvarnabhumi (Bangkok, Thailand)

Istituto Nazionale di Fisica Nucleare

DYNSYSMATH

DYNamical systems and non equilibrium states of complex SYStems: MATHematical methods and physical concepts

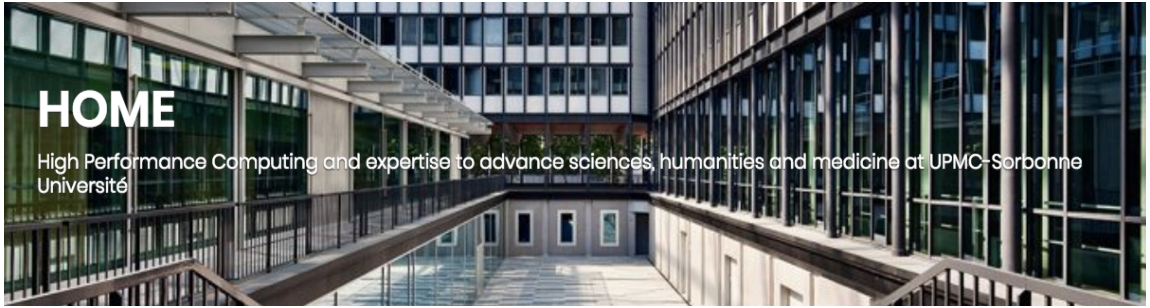

HPC resources of The Institute for scientific Computing and Simulation financed by Region Ile de France and the project Equip@Meso